# REPORT DOCUMENTATION PAGE

Form Approved
OMB No 0704-0188

| | |
|---|---|
| 1a REPORT SECURITY CLASSIFICATION<br>UNCLASSIFIED | 1b RESTRICTIVE MARKINGS |
| 2a SECURITY CLASSIFICATION AUTHORITY | 3 DISTRIBUTION / AVAILABILITY OF REPORT<br>Approved for public release; distribution is unlimited. |
| 2b DECLASSIFICATION / DOWNGRADING SCHEDULE | |
| 4 PERFORMING ORGANIZATION REPORT NUMBER(S) | 5 MONITORING ORGANIZATION REPORT NUMBER(S) |
| 6a NAME OF PERFORMING ORGANIZATION<br>Naval Postgraduate School<br>6b OFFICE SYMBOL (If applicable)<br>EC | 7a NAME OF MONITORING ORGANIZATION<br>Naval Postgraduate School |
| 6c ADDRESS (City, State, and ZIP Code)<br>Monterey, CA 93943-5000 | 7b ADDRESS (City, State, and ZIP Code)<br>Monterey, CA 93943-5000 |
| 8a NAME OF FUNDING / SPONSORING ORGANIZATION<br>8b OFFICE SYMBOL (If applicable) | 9 PROCUREMENT INSTRUMENT IDENTIFICATION NUMBER |
| 8c ADDRESS (City, State, and ZIP Code) | 10 SOURCE OF FUNDING NUMBERS<br>PROGRAM ELEMENT NO / PROJECT NO / TASK NO / WORK UNIT ACCESSION NO |

11 TITLE (Include Security Classification)

AN INTRODUCTION TO DOPPLER EFFECT AND FADING IN MOBILE COMMUNICATION

12 PERSONAL AUTHOR(S)

De Paula, Abdon B.

| 13a TYPE OF REPORT | 13b TIME COVERED | 14 DATE OF REPORT (Year, Month, Day) | 15 PAGE COUNT |
|---|---|---|---|
| Master's Thesis | FROM Jan 92 TO Dec 92 | December 1992 | 98 |

16 SUPPLEMENTARY NOTATION

The views expressed in this thesis are those of the author and do not reflect the official policy or position of the Department of Defense or the U.S. Government.

| 17 COSATI CODES | | | 18 SUBJECT TERMS (Continue on reverse if necessary and identify by block number) |
|---|---|---|---|
| FIELD | GROUP | SUB-GROUP | Mobile communications with Doppler effect, fading channels |
| | | | |
| | | | |

19 ABSTRACT (Continue on reverse if necessary and identify by block number)

In this research we present an introductory analysis of a complex aspect of mobile communications: Doppler effect is evaluated in both Ricean and Rayleigh channels. A noncoherent 2-FSK scheme is selected to evaluate the behavior of the system under very strong fading channel conditions. The analysis is conducted for the binary case due to the possibility of developing closed form solutions. Therefore, the approach is simplified avoiding long lasting simulations that may obscure the concepts. The probability of bit error for the 2-FSK case can also be used as an initial bound for a M-FSK scheme. Diversity is evaluated as a means of combating fading and Doppler effects. Error correcting codes, in the form of a convolutional codes, are also used and applied to both effects.

| 20 DISTRIBUTION / AVAILABILITY OF ABSTRACT | 21 ABSTRACT SECURITY CLASSIFICATION | |
|---|---|---|
| ☒ UNCLASSIFIED/UNLIMITED ☐ SAME AS RPT ☐ DTIC USERS | UNCLASSIFIED | |
| 22a NAME OF RESPONSIBLE INDIVIDUAL<br>Tri Ha | 22b TELEPHONE (Include Area Code)<br>(408) 656-2788 | 22c OFFICE SYMBOL<br>EC-HA |

DD Form 1473, JUN 86 *Previous editions are obsolete*

S/N 0102-LF-014-6603

SECURITY CLASSIFICATION OF THIS PAGE



UNCLASSIFIED

Approved for public release; distribution is unlimited

# An Introduction to Doppler Effect and Fading in Mobile Communication

by

Abdon B. de Paula
Lieutenant Commander, Engineer Corps, Brazilian Navy
B. S., Brazilian Naval Academy
B. S., São Paulo University

Submitted in partial fulfillment of the
requirements for the degree of

MASTER OF SCIENCE IN ELECTRICAL ENGINEERING

from the

NAVAL POSTGRADUATE SCHOOL

December 1992

# ABSTRACT

In this research we present an introductory analysis of a complex aspect of mobile communications: Doppler effect is evaluated in both Ricean and Rayleigh fading channels. A noncoherent 2-FSK scheme is selected to evaluate the behavior of the system under very strong fading channel conditions. The analysis is conducted for the binary case due to the possibility of developing closed form solutions. Therefore, the approach is simplified avoiding long lasting simulations that may obscure the concepts. The probability of bit error for the 2-FSK case can also be used as an initial bound for a M-FSK scheme. Diversity is evaluated as a means of combating fading and Doppler effects. Error correcting codes, in the form of convolutional algorithms, are also used and applied to both effects.

# TABLE OF CONTENTS

# LIST OF FIGURES

# ACKNOWLEDGMENT

The author would like to express his appreciation to Professor Tri Ha at the Naval Postgraduate School for the knowledge transmitted in various courses. Appreciation is also due to Professor Ralph Hippenstiel for his comments on the present work.

Gratitude is also due to LT Janet Stevens, his friend and partner in several research projects, for reviewing the material and text corrections.

To Jim Allen for his editing and typesetting work.

To Bel, his lovely wife, for the continuous support and understanding with his career.

[THIS PAGE INTENTIONALLY LEFT BLANK]

# I. INTRODUCTION

The term "mobile communication" is used to describe the radio communication link between two terminals of which one or both are in motion.

In urban areas, we observe the growth of cellular terrestrial mobile communication systems. Such systems are also employed where base stations can be located relatively close to mobile users. However, in rural or remote areas, with low population density, cellular systems are not economically feasible.

Satellite technology has reached the ability to bridge the gap of communications between mobile elements, complementing the existing cellular systems. Mobile satellite systems are not restricted to land coverage. They include aeronautical and maritime services as well.

Mobile land communication is greatly affected not only by the losses encountered in atmospheric propagation, but also by the general topography of the terrain. The texture and roughness of the terrain tend to dissipate propagated energy, reducing the received signal strength at both mobile and fixed units. Shadowing caused by trees and other natural or man made obstacles also affects the strength of the received signal.

In addition, there is multipath fading, which is caused by the reflecting of various types of signal scatterers. The effects of multipath phenomena are more significant in terrestrial communications than in air-to-base station or satellite-to-earth station communications.

In this thesis, we assume that there are multiple propagation paths in the model of the mobile link. A propagation delay and an attenuation factor are associated with each path.

The fading phenomenon is basically a result of time variations in the phase of signals in each path. Sometimes, the components from the paths add constructively so that the received signal is large. Other times, they add destructively, resulting in a very small or practically zero signal. Thus, fading, the amplitude variation in the received signal, is due to the time-variant multipath characteristic of the channel [1].

To generalize the model for the practical cases of mobile communications, we also consider the presence of a direct component of the signal. We define a direct-to-diffuse ratio $r = \alpha^2/2\sigma^2$ using the channel parameters. Physical interpretations can be given to those parameters: $\alpha^2$ is associated with the strength of the direct component and $2\sigma^2$ is associated with the diffuse component.

Therefore, we consider a Ricean fading channel which is general enough to allow us to solve the following types of problems:

a) Non-fading channel,

b) Rayleigh fading channel,

c) Ricean fading channel.

Another major concern in mobile communications is the Doppler effect. It is well known that this effect occurs due to the relative speed between the elements in the communication system. The effect of the Doppler is directly proportional to the magnitude of the relative speed. Therefore, this effect can only be considered significant when high speeds apply, i.e., in airplanes.

The Doppler effect is modeled here as a contribution to the carrier frequency. This contribution will be either positive or negative, according to the direction of the relative movement between the communications elements.

Both fading and Doppler effects can impair the reception of the transmitted signal. The error rate, as shown in [1], is only inversely proportional to the SNR in a Rayleigh fading channel, in contrast with the exponential decrease in AWGN.

Diversity, as stated by Proakis [1], is an effective way of improving error rate performance in fading channels. By supplying to the receiver several replicas of the same information bit over independently fading channels, the probability that the signals will fade at the same time is considerably reduced.

We only use time diversity in the form of signal repetition or in an equivalent form of sampling the same bit several times at a rate greater than the bit rate.

To further improve the reception of a Doppler affected signal, we no longer use matched filters, but use bandpass filters instead. We will verify that time diversity, can be used to combat the fading characteristics of the channel and the Doppler effect.

Finally, we consider the use of a convolutional code as a way of providing error corrections. A convolutional code is generated by passing the information sequence through a linear finite-state shift register. The input data is shifted into the shift registers $\ell$ bits at a time. As an output, we obtain $n$ bits for each set of $\ell$ input bits. Thus, the code rate is defined as $R_c = \ell/n$.

Observing the tree that is generated by the convolutional encoder, we notice that the structure repeats itself after the $\nu^{\text{th}}$ stage, where $\nu$ is the code constraint length.

The distance properties and the error rate performance of a convolutional code can be obtained from its state diagram. The same diagram is used to compute the code transfer function. From there, we obtain the minimum distance, $d_f$, and bounds for the probability of error rate.

Proakis has already shown that a convolutional code can be viewed as a type of repetition scheme [1]. Thus, it is equivalent to time diversity. We will apply this characteristic of the convolutional code over Doppler effect.

Due to the strong fading nature of the channels we want to analyze, we have selected a non-coherent signaling scheme in which it is not required to estimate the phase of the received signal. Nor will we be estimating the channel parameters. Under these assumptions, our system can be simplified and has very robust characteristics.

In our analysis, we consider a constant Doppler, i.e., we develop a bit error probability for Ricean fading channels conditioned on the Doppler effect coefficient. In our approach, we obtain closed form solutions that may bring some insight and avoid long lasting simulations.

The binary frequency shift keying (2-FSK) schemes proposed is well-suited for further development of the initial base for future M-ary frequency shift keying (M-FSK) base extension or to obtain M-FSK error performance bounds.

In Figure 1 we present the basic system on which we conduct our analysis. It shows two energy detectors followed by a possible (non-coherent) average. The two upper branches are responsible for the detection of the first signal of the binary scheme and the two lower branches take care of the second signal. In our analysis we will assume that the signal corresponding to the frequency $f_0$ is sent. Therefore the two upper branches will have the signal present and the two lower branches will only have noise.

In Chapter II, we develop the probability of bit error for a square law detector, 2-FSK scheme, with diversity $L$, under Rayleigh and Ricean fading, and without Doppler shifts. In Chapter III, the Doppler effect is added to the previous result in the form of a Doppler effect coefficient.

In Chapter IV, we extend the already developed conditional probability by accounting for the convolutional error correcting code.

Finally, in Chapter V, we present verifications of the equations with some numerical results, including some special cases, and compare them with results in the literature. We evaluate the influence of the diversity size over the performance of error rate. Also, we verify the performance of $R_c = 1/2$ and $R_c = 2/3$ convolutional codes under the same conditions. In addition, we confirm the influence of the code constraint length on the performance.

[THIS PAGE INTENTIONALLY LEFT BLANK]

# II. DIVERSITY AND FADING CHANNELS

In this chapter we derive the error rate performance of binary FSK over a frequency-nonselective, slowly fading Ricean channel. We assume that each diversity signal fades independently. The signal can be considered as the sum of two components, a nonfaded (direct) component and a Rayleigh-faded (diffuse) component, hence the amplitude of the signal is a Ricean random variable.

We will analyze the bit error probability of the proposed system in Figure 1. The Doppler effect will not be taken into consideration in this chapter but it will be considered in Chapter 3.

For mathematical convenience we adopt the complex envelope notation for a real signal. Therefore, the summer outputs are (under signal $f_0$ present condition):

$$Y_0 = \sum_{k=1}^{L} |X_k + n_{c_0 k} + j n_{s_0 k}|^2 \ , \tag{2.1a}$$

$$Y_1 = \sum_{k=1}^{L} |n_{c_1 k} + j n_{s_1 k}|^2 \ , \tag{2.1b}$$

where $X_k$, assuming a Doppler shift of $w_d$, is given by

$$X_k = \frac{A_k}{\sqrt{2}} \int_{(k-1)T}^{k} e^{j w_d t} dt \ , \tag{2.2}$$

and all the quadrature noise samples $n_{cik}$, $n_{sik}$ are independent and identically distributed (i.i.d.) zero-mean Gaussian random variables (RV) with variance $N_0 T/2$. Each amplitude $A_k$ of the signal is assumed to fade independently for each bit duration $T$.

Since $Y_1$ is the sum of squares of $2L$ i.i.d. Gaussian RVs with zero-mean and variance $\sigma_k^2 = N_o T/2$, $Y_1$ is chi-square distributed with the following probability

density function (pdf) [1]

$$f_{Y_1}(y_1) = \frac{1}{(L-1)!2^L\sigma_k^{2L}} y_1^{L-1} e^{-y_1/2\sigma_k^2} , \quad y_1 \geq 0 . \tag{2.3}$$

On the other hand, $Y_0$ is the sum of squares of $L$ independent Gaussian RVs with variance $\sigma_k^2$ and mean $\mathcal{R}\mathrm{e}\,[X_k]$, and $L$ independent Gaussian RVs with variance $\sigma_k^2$ but with mean $\mathcal{I}\mathrm{m}\,[X_k]$. Thus $Y_0$ is non-central chi-square distributed with the following conditional pdf [1]

$$f_{Y_0}(y_0/v) = \frac{1}{2\sigma_k^2}\left(\frac{y_0}{v}\right)^{(L-1)/2} e^{-(y_0+v)/2\sigma_k^2} I_{L-1}\left(\frac{\sqrt{vy_0}}{\sigma_k^2}\right) , \quad y_0 \geq 0 , \tag{2.4}$$

where $I_{L-1}(\cdot)$ is the $(L-1)^{\text{th}}$ order modified Bessel function of the first kind and $v$ is the value assumed by the random variable $V$ defined as

$$V = \sum_{k=1}^{L} |X_k|^2 . \tag{2.5}$$

The conditional probability of error is given by

$$\mathcal{P}_b(v) = P_r\{Y_1 \geq y_0 | v\} = \int_0^\infty \int_{y_0}^\infty f_{Y_1}(y_1/v) f_{Y_0}(y_0|v) dy_1 dy_0 . \tag{2.6}$$

The inner integral can be evaluated as follows (see Appendix A)

$$\int_{y_0}^\infty f_{Y_1}(y_1) dy_1 = e^{-y_0/2\sigma^2} \sum_{k=0}^{L-1} \left(\frac{y_0}{2\sigma^2}\right)^k \frac{1}{k!} . \tag{2.7}$$

Substituting (2.4) and (2.7) into (2.6) we obtain (see Appendix C)

$$\mathcal{P}_b(z) = \frac{e^{-z/2}}{2^L} \sum_{k=0}^{L-1} \frac{1}{2^k} \sum_{m=0}^{k} \binom{k+L-1}{m+L-1} \frac{\left(\frac{z}{2}\right)^m}{m!} , \tag{2.8}$$

where the random variable $Z$ is defined as:

$$Z = \frac{T^2}{4\sigma^2} \sum_{k=1}^{L} A_k^2 = \beta \sum_{k=1}^{L} A_k^2 , \tag{2.9}$$

where $\beta = T^2/4\sigma_k^2$.

Equation (2.8) has been derived in [2] for the case of fixed amplitude $A_k = A$. For such cases equation (2.9) reduces to

$$Z = \frac{T^2}{4\sigma_k^2} L A^2 = L\left(\frac{A^2T^2}{4\frac{N_0T}{2}}\right) = L\left(\frac{A^2T}{2N_0}\right) = L\left(\frac{E}{N_0}\right) , \tag{2.10}$$

where $E/N_0$ is the signal energy-to-noise density ratio and $E = A^2T/2$.

For the Ricean channel the signal amplitude $A_k$ is Ricean-distributed with pdf

$$f_{A_k}(a_k) = \frac{a_k}{\sigma_k^2} e^{-(a_k^2+\alpha_k^2)/2\sigma_k^2} I_0\left(\frac{a_k\alpha_k}{\sigma_k^2}\right) , \quad a_k \geq 0 , \tag{2.11}$$

where $\alpha_k^2$ is the average power of the nonfaded (direct) component of the signal and $2\sigma_k^2$ is the average power of the Rayleigh-faded (diffuse) component of the signal.

The total average received power in the interval $(k-1)T \leq t \leq kT$ is

$$E\left\{\frac{A_k^2}{2}\right\} = \frac{(\alpha_k^2 + 2\sigma_k^2)}{2} , \tag{2.12}$$

and it is assumed to be constant for any integer $k$, $1 \leq k \leq L$.

Note that if $\alpha_k^2 = 0$, the channel is a Rayleigh fading model and if $2\sigma_k^2 = 0$ there is no fading.

The random variable $W$ defined below

$$W = \sum_{k=1}^{L} A_k^2 \tag{2.13}$$

has a noncentral chi-square pdf given by [1]

$$f_W(w/p) = \frac{1}{2\sigma_k^2}\left(\frac{w}{p}\right)^{(L-1)/2} e^{-(w+p)/2\sigma_k^2} I_{L-1}\left(\frac{\sqrt{pw}}{\sigma_k^2}\right) , \quad w \geq 0 , \tag{2.14}$$

where

$$p = \sum_{k=1}^{L} \alpha_k^2 . \tag{2.15}$$

Consequently, the pdf of the random variable $Z = \beta W$ in (2.9) is

$$f_Z(z) = \frac{1}{2\beta\sigma_k^2}\left(\frac{z}{\beta p}\right)^{(L-1)/2} e^{-(z+\beta p)/2\beta\sigma_k^2} I_{L-1}\left(\frac{\sqrt{\beta p z}}{\beta\sigma_k^2}\right), \quad z \geq 0 \tag{2.16}$$

Taking the expected value of $\mathcal{P}_b(z)$ in (2.8) (see Appendix D) by using (2.16) we obtain

$$\begin{aligned} P_b(\beta) &= \frac{1}{2^L}\frac{e^{-(p/2\sigma_k^2)[1-1/(1+\beta\sigma_k^2)]}}{(1+\beta\sigma_k^2)^L}\sum_{k=0}^{L-1}\frac{1}{2^k}\sum_{m=0}^{k}\binom{k+L-1}{m+L-1}\left(\frac{\beta\sigma_k^2}{1+\beta\sigma_k^2}\right)^m \\ &\quad \times \sum_{i=0}^{m}\binom{m+L-1}{i+L-1}\left(\frac{p}{2\sigma_k^2(1+\beta\sigma_k^2)}\right)^i \frac{1}{i!}. \end{aligned} \tag{2.17}$$

Let

$$\bar{E} = \frac{T}{2}(\alpha_k^2 + 2\sigma_k^2) \tag{2.18}$$

be the average signal energy with the assumption that $\alpha_k^2$ and $2\sigma_k^2$ are constant for any $1 \leq k \leq L$ (hereafter we drop the $\beta$ argument of $P_b(\beta)$ to simplify the notation). Also let the ratio $r$ of the direct component power to the diffuse component power during a bit time be defined as follows:

$$r = \frac{\alpha_k^2}{2\sigma_k^2}. \tag{2.19}$$

Combining (2.10), (2.18), and (2.19) we obtain

$$\beta\sigma_k^2 = \frac{\dfrac{\bar{E}}{N_0}}{2(r+1)}. \tag{2.20}$$

Substituting (2.15), (2.19), and (2.20) into (2.17) we get the average bit error probability (zero Doppler) as follows:

$$\begin{aligned} P_b &= \frac{1}{2^L} \times \frac{e^{-Lr[1-(1+(\bar{E}/N_0)/2(r+1))^{-1}]}}{\left[1+\dfrac{\bar{E}/N_0}{2(r+1)}\right]^L} L \times \sum_{k=0}^{L-1}\frac{1}{2^k}\sum_{m=0}^{k}\binom{k+L-1}{m+L-1} \\ &\quad \times \left(\frac{1}{1+\dfrac{2(r+1)}{\bar{E}/N_0}}\right)^m \times \sum_{i=0}^{m}\binom{m+L-1}{i+L-1} \times \left(\frac{Lr}{1+\dfrac{\bar{E}/N_0}{2(r+1)}}\right)^i \frac{1}{i!} \end{aligned} \tag{2.21}$$

As a check we observe that when $L = 1$ and $r = \infty$ (no fading condition) equation (2.21) reduces to [1]

$$P_b = \frac{1}{2} e^{-\bar{E}/N_0/2} . \tag{2.22}$$

For a non-fading channel with diversity $L$, equation (2.21) can be reduced to the next equation. Even though a similar equation is found in [2] we also developed it in Appendix C. By replacing the value of $Z$ given by (2.10) leads to:

$$P_b = \frac{e^{-(L/2)(\bar{E}/N_0)}}{2^L} \sum_{k=0}^{L-1} \frac{1}{2^k} \sum_{m=0}^{k} \binom{k+L-1}{k-m} \frac{\left(\frac{L\bar{E}/N_0}{2}\right)^m}{m!} . \tag{2.23}$$

For a Rayleigh fading channel ($r = 0$) and assuming $L = 1$ we get the result of [1]:

$$P_b = \frac{1}{2 + \bar{E}/N_0} . \tag{2.24}$$

For a Ricean fading channel and assuming $L = 1$ we obtain the result

$$P_b = \frac{r+1}{2(r+1) + \bar{E}/N_0} e^{-r[1-2(r+1)/(2(r+1)+\bar{E}/N_0)]} . \tag{2.25}$$

Also for a Rayleigh fading channel and diversity $L$, equation (2.21) reduces to the result obtained in [1, 4, 5]:

$$P_b = \left(\frac{1}{2 + \bar{E}/N_0}\right)^L \sum_{k=0}^{L-1} \frac{1}{2^k} \sum_{m=0}^{k} \binom{k+L-1}{m+L-1} \left(\frac{\bar{E}/N_0}{2 + \bar{E}/N_0}\right)^m . \tag{2.26}$$

[THIS PAGE INTENTIONALLY LEFT BLANK]

# III. THE PROBABILITY OF BIT ERROR CONDITIONED ON THE DOPPLER EFFECT IN A RICEAN FADING CHANNEL

In a real mobile communication system, the signal may be distorted by Doppler, which can seriously increase the bit error probability. In this chapter, we investigate the system performance when Doppler is present.

The received signal affected by the Doppler in a fading channel with diversity, at time $k$, can be represented as follows:

$$r_k(t) = A_k \cos(2\pi f_i t + 2\pi f_d t + \theta_i) \ , \quad i = 0, 1 \ , \tag{3.1}$$

where $f_d$ is the Doppler frequency and $\theta_i$ is the signal phase.

Equation (3.1) can be manipulated as follows:

$$r_k(t) = A_k \cos(2\pi[f_i + f_d]t + \theta_i) \ , \quad i = 0, 1 \ . \tag{3.2}$$

The orthogonality condition for 2-FSK (no Doppler shift) requires:

$$\Delta f = f_1 - f_0 = \frac{1}{T} \qquad \text{(minimum frequency spacing)} \tag{3.3}$$

and

$$f_1 + f_0 = \frac{k}{T} \ , \qquad k \text{ is a positive integer} \ . \tag{3.4}$$

In practice we may use an approximation to orthogonality condition by imposing that

$$f_1 + f_0 \gg \frac{1}{T} \ . \tag{3.5}$$

To study the Doppler effect, we assume a wideband 2-FSK, that is, $\Delta f \gg 1/T$. This ensures that the orthogonality condition is almost satisfied, and we can analyze the performance as if we have an ideal orthogonal 2-FSK.

Returning now to the complex envelope notation, we see that equations (2.1) and (2.2) remain the same with $X_k$ given below:

$$X_k = \frac{A_k}{\sqrt{2}} \int_{(k-1)T}^{kT} e^{jw_d t} dt \ . \tag{3.6}$$

Equation (2.5) will give us (see Appendix E):

$$\begin{aligned} V &= \sum_{k=1}^{L} |X_k|^2 \\ &= \frac{T^2}{2} \left\{ \frac{\sin(\pi f_d T)}{(\pi f_d T)} \right\}^2 \sum_{k=1}^{L} A_k^2 \ . \end{aligned} \tag{3.7}$$

The definition of equation (2.9) remains the same but now the value of $\beta$ is given by:

$$\beta = \left( \frac{T^2}{4\sigma^2} \right) \times \left[ \frac{\sin \pi f_d T}{\pi f_d T} \right]^2 = \left( \frac{T^2}{4\sigma^2} \right) \ \mathrm{sinc}^2(fdt) \ , \tag{3.8}$$

where sinc $(x) = \dfrac{\sin(\pi x)}{\pi x}$.

Thus equation (2.10) is transformed to:

$$Z = L \left( \frac{\bar{E}}{N_0} \right) \times \mathrm{sinc}^2(f_d T) \ . \tag{3.9}$$

Equation (2.17) is still valid and if we use the value of $\beta\sigma_k^2$ given below:

$$\beta\sigma_k^2 = \frac{\dfrac{\bar{E}}{N_0}}{2(r+1)} \ \mathrm{sinc}^2(f_d T) \ . \tag{3.10}$$

We get the average bit error probability conditioned on a given Doppler shift $f_d$:

$$P_b = \frac{1}{2^L} \frac{e^{-Lr\left[1-(1+(\bar{E}/N_0)\ \mathrm{sinc}^2(f_dT)/2(r+1))^{-1}\right]}}{\left[1+\dfrac{\left(\dfrac{\bar{E}}{N_0}\right)\mathrm{sinc}^2(f_dT)}{2(r+1)}\right]^L} \sum_{k=0}^{L-1} \frac{1}{2^k}$$

$$\times \sum_{m=0}^{k} \binom{k+L-1}{m+L-1} \left[\frac{1}{1+\dfrac{2(r+1)}{\left(\dfrac{\bar{E}}{N_0}\right)\mathrm{sinc}^2(f_dT)}}\right]^m$$

$$\times \sum_{i=0}^{m} \binom{m+L-1}{i+L-1} \left[\frac{Lr}{1+\dfrac{(\bar{E}/N_0)\ \mathrm{sinc}^2(f_dT)}{2(r+1)}}\right]^i \frac{1}{i!} . \qquad (3.11)$$

Again we may now obtain from equation (3.11) the equation corresponding to (2.23) with the Doppler shift accounted for:

$$P_b = \frac{e^{-(L/2)(\bar{E}/N_0)\ \mathrm{sinc}^2(f_dT)}}{2^L} \times \sum_{k=0}^{L-1} \frac{1}{2^k} \sum_{m=0}^{k} \binom{k+L-1}{m+L-1} \frac{\left[\dfrac{L}{2}\left(\dfrac{\bar{E}}{N_0}\right)\mathrm{sinc}^2(f_dT)\right]^m}{m!} . \qquad (3.12)$$

For a Rayleigh fading channel ($r = 0$) and an $L$ of 1, we get the following equation which corresponds to (2.24)

$$P_b = \frac{1}{2 + (\bar{E}/N_0)\ \mathrm{sinc}^2(f_dT)} . \qquad (3.13)$$

For a Ricean fading channel and an $L$ of 1, we obtain the following equations which corresponds to (2.25)

$$P_b = \frac{r+1}{2(r+1) + (\bar{E}/N_0)\ \mathrm{sinc}^2(f_dT)} e^{-r(1-2(r+1)/(2(r+1)+(\bar{E}/N_0)\ \mathrm{sinc}^2(f_dT)))} . \qquad (3.14)$$

For a Rayleigh fading channel and diversity $L$ we get the following equation which corresponds to (2.26)

$$P_b = \left(\frac{1}{2 + (\bar{E}/N_0)\ \mathrm{sinc}^2(f_d T)}\right)^L \sum_{k=0}^{L-1} \frac{1}{2^k} \sum_{m=0}^{k} \binom{k+L-1}{m+L-1} \left(\frac{(\bar{E}/N_0)\ \mathrm{sinc}^2(f_d t)}{2 + (\bar{E}/N_0)\ \mathrm{sinc}^2(f_d T)}\right)^m . \tag{3.15}$$

Again, as a fast check we observe that for $L = 1$, $r = \infty$ and $f_d T = 0$ (no Doppler effect) in equation (3.11), we obtain (2.22).

For a Rayleigh fading channel ($r = 0$), $L = 1$, and $f_d T = 0$ we obtain (2.23).

For a Ricean fading channel, $L = 1$ and $f_d T = 0$, we obtain (2.25).

Also from (3.11) we observe that the Doppler effect reduces the signal-to-noise ratio (SNR) by a factor equal to $\mathrm{sinc}^2(f_d T)$. SNR is defined to be $\bar{E}/N_0$. For example, when the Doppler frequency $f_d$ is an integer multiple of $1/T$, then $\mathrm{sinc}^2(f_d T) = 0$.

Therefore, when the Doppler frequency is large the receiver should sample the signal faster than the bit time $T$ to reduce the Doppler perturbation. Such an adaptive change in the sampling rate is equivalent to changing the diversity number of the system. The receiver would modify the system resultant diversity.

We can also combine the diversity that we obtain by sending $L$ replicas of the signal with the diversity we obtain by sampling at a rate faster than the bit rate. In other words, letting $T'$ be the sampling interval (where $T' = T/N$ and $N$ is a positive integer) and replacing the receiver of Figure 1 with a receiver whose integration time (and sampling time) is $T'$ and whose diversity is $NL$.

Letting $\bar{E}'$ be $\bar{E}/N$, using equation (3.11) with $L$, $\bar{E}$, and $T$ replaced by $NL$, $\bar{E}'$ and $T'$, respectively, we get:

$$P_b = \frac{1}{2^{NL}} \frac{e^{-NLr\left[1-(1+((\bar{E}/NN_0)\ \mathrm{sinc}^2(f_dT/N))/2(r+1))^{-1}\right]}}{\left[1+\dfrac{\left(\dfrac{\bar{E}}{NN_0}\right)\ \mathrm{sinc}^2\left(f_d\dfrac{T}{N}\right)}{2(r+1)}\right]^{NL}} \cdot \sum_{k=0}^{NL-1} \frac{1}{2^k}$$

$$\times \sum_{m=0}^{k} \binom{k+NL-1}{m+NL-1} \left[\frac{1}{1+\dfrac{1}{\dfrac{\left(\dfrac{\bar{E}}{NN_0}\right)\ \mathrm{sinc}^2\left(f_d\dfrac{T}{N}\right)}{2(r+1)}}}\right]^m$$

$$\times \sum_{i=0}^{m} \binom{m+NL-1}{i+NL-1} \left[\frac{NLr}{1+\dfrac{\left(\dfrac{\bar{E}}{NN_0}\right)\ \mathrm{sinc}^2\left(f_d\dfrac{T}{N}\right)}{2(r+1)}}\right]^i \times \frac{1}{i!} \ . \quad (3.16)$$

Using again the same interpretation as before, we obtain the counterpart to equation (3.12) for a non-fading channel with Doppler perturbation:

$$P_b = \frac{e^{-(L/2)(\bar{E}/N_0)\ \mathrm{sinc}^2(f_dT/N)}}{2^{NL}} \sum_{k=0}^{NL-1} \frac{1}{2^k} \sum_{m=0}^{k} \binom{k+NL-1}{m+NL-1} \frac{\left[\dfrac{L}{2}\left(\dfrac{\bar{E}}{N_0}\right)\ \mathrm{sinc}^2\left(f_d\dfrac{T}{n}\right)\right]^m}{m!} \ . \quad (3.17)$$

In that case we have:

$$Z = NL\left(\frac{\bar{E}}{NN_0}\right)\ \mathrm{sinc}^2\left(f_d\frac{T}{N}\right) = L\left(\frac{\bar{E}}{N_0}\right)\ \mathrm{sinc}^2\left(f_d\frac{T}{N}\right) \ . \quad (3.18)$$

We can see in equation (3.18) the influence of increasing the sampling rate (i.e., increasing $N$). Sampling at rate faster than the bit rate reduces the argument of the sinc function. Therefore, the value of the sinc function is increased.

[THIS PAGE INTENTIONALLY LEFT BLANK]

# IV. CODED PERFORMANCE

In this chapter the performance of the L-fold diversity receiver with error correction code is investigated. Specifically we consider convolutional codes with Viterbi soft decision decoding.

For a rate $\ell/n$ code the bit error probability $P_b$ is upper bounded by the following union bound [1, 6, 7]:

$$P_b < \frac{1}{\ell} \sum_{d=df}^{\infty} a_d P_d \ , \tag{4.1}$$

where $df$ is the fine distance of the code, $a_d$ is the information weight of a code path of weight $d$, and $P_d$ is the probability the all-zero path is eliminated by a path of weight $d$ merging with it on the code trellis.

We observe that $P_d$ is exactly the probability that the sum of $d$ samples of $Y_1$ is greater than the sum of $d$ samples of $Y_0$ in Figure 1, that is, $P_d$ is the probability of error for noncoherent combining of $d$ transmissions where each transmission has L-fold diversity.

Thus the expansion for $P_d$ is exactly the same as $P_d$ in (3.11) with $dL$ replacing $L$, $(\ell/n)\bar{E}/N_0$ replacing $\bar{E}/N_0$ and $\ell T/n$ replacing $T$, that is

$$P_d = \frac{1}{2^{dL}} \frac{e^{-dLr\left[1-(1+(\ell/n)(\bar{E}/N_0)\ \mathrm{sinc}^2((\ell/n)\, f_d T)/2(r+1))^{-1}\right]}}{\left[1+\dfrac{\left(\dfrac{\ell}{n}\right)\dfrac{\bar{E}}{N_0}\ \mathrm{sinc}^2\left(\dfrac{\ell}{n} f_d T\right)}{2(r+1)}\right]^{dL}}$$

$$\times \sum_{k=0}^{dL-1} \frac{1}{2^k} \sum_{m=0}^{k} \binom{k+dL-1}{m+dL-1} \left[\frac{1}{1+\dfrac{2(r+1)}{\left(\dfrac{\ell}{n}\right)\dfrac{\bar{E}}{N_0}\ \mathrm{sinc}^2\left(\dfrac{\ell}{n} f_d T\right)}}\right]^{m}$$

$$\times \sum_{i=0}^{m} \binom{m+dL-1}{i+dL-1} \left[\frac{dLr}{1+\dfrac{\left(\dfrac{\ell}{n}\right)\dfrac{\bar{E}}{N_0}\ \mathrm{sinc}^2\left(\dfrac{\ell}{n} f_d T\right)}{2(r+1)}}\right]^{i} \frac{1}{i!} \,. \qquad (4.2)$$

# V. ANALYSIS OF RESULTS

In this chapter, we analyze the performance (probability of bit error, $P_b$) for the 2-FSK, square law detector system of Figure 1. We assume that the signal is transmitted $L$ times. We recall that by sampling faster than the bit rate we may produce an equivalent diversity to sending the signal $L$ times.

In Figure 2, the results for an additive white Gaussian noise (AWGN) channel are presented. The curve for a 2-FSK signal, $L = 1$ and no Doppler perturbation is shown as a reference. This plot provides us with a numerical check of the results presented in Proakis [1].

Varying the diversity size has proven to be an efficient way to improve the performance in the presence of Doppler. The curves we have obtained by setting $L = 1$ to $L = 10$, show worse performance than the mentioned 2-FSK curve.

Sending the signal twice (i.e., $L = 2$) provides a $P_b = 0.10$ at an SNR of 10. We can see an improvement when comparing this value to $P_b = 0.50$ which is the bit error probability for an $L$ of 1 (i.e., no diversity).

Note that a larger $L$ may give poorer performance at low SNR than a smaller $L$ would provide. On the other hand, at high SNR, increasing $L$ gives better performance. Hence, there are crossovers among the various diversity rates in an AWGN channel, as illustrated in Figure 2, for $L = 3$ and $L = 4$.

In addition, we notice that the best relative improvement occurs when we increase diversity from $L = 1$ to $L = 2$. The next best improvement is obtained by increasing $L$ from 2 to 3, representing a 2 dB gain at large SNR.

At large SNR, we can see that the improvement is less than 0.50 dB when going from $L = 4$ to $L = 10$ in a non-fading channel.

In Figure 3, the bit error probability for a Rayleigh fading channel ($r = 0$) is presented. Again we plot the 2-FSK, no Doppler perturbation curve, in order to provide a numerical check with the results of [1].

Now, we can see that increasing diversity will result in even better performance than the mentioned 2-FSK reference curve ($L = 1$ and no Doppler effect).

Again, the best improvement occurs when we change from $L = 1$ to $L = 2$. The next best improvement is obtained by changing from $L = 2$ to $L = 3$ (i.e., about 4 dB at a large SNR).

Moving from $L = 3$ to $L = 4$ and from $L = 4$ to $L = 10$ gives us approximately a gain of 2 dB at a large SNR.

In Figures 4 through 11, the probability of bit error as a function of diversity size is presented. We show the results for two cases: zero Doppler and $f_dT = 0.5$. Also, we present four plots in each figure: SNR = 3, 10, 30, 100.[1]

The same kind of behavior that we see in a Rayleigh fading channel [1] occurs in a Ricean fading channel, i.e., for low SNR there is a point of minimum $P_b$.

Besides, we notice that the Doppler perturbation reduces the value of $L$ where the minimum appears. This is consistent with the fact that the Doppler coefficient is a factor that reduces the SNR.

Therefore, increasing the diversity at low SNR may result in a reduction in performance in a Rayleigh or Ricean fading channel.

By sampling the received signal at a rate faster than the bit rate we may reduce the influence of the Doppler perturbation. We note that increasing the diversity order results into an increased value of $L$ where the minimum $P_b$ is located.

[1]Those values are in linear units and allow easy comparison with [1, 2, 7, 9].

The behavior of the curves in a Ricean fading channel tends to resemble the behavior of a non-fading channel as we increase the $r$ value. This effect is presented in Figures 12 through 15.

Figures 15 and 16 allow us a quick numerical verification of equation (4.2) with the results of [1] and [7]. We have used $f_d T = 0$, which means the Doppler coefficient (i.e., sinc part of equation (3.16)) equals to 1. By using $r = 10,000$ we approach the AWGN channel. Therefore, the uncoded signal represents a 2-FSK in an AWGN channel. Also, both figures present the comparison of the performance of the system without convolutional code ('uncoded signal') and the rate 1/2, $\nu = 2$, $d_f = 5$ convolutional code. The systems have the same $L$. For the initial verification we used $L = 1$, and no Doppler effect. Figure 16 provides a comparison for a Rayleigh fading channel. By inspecting the values of $P_b$ from Figures 15 and 16 we notice that diversity does not improve performance in AWGN channel, thus confirming Proakis' observations [1]. The results obtained for both the coded and uncoded signal agree with the one presented by [7].

At large SNR we obtain a gain of about 2.5 dB over the uncoded signal in an AWGN channel.[2] We recall Doppler has not been considered yet.

Thereafter, we consider the maximum reduction, due to Doppler (i.e., Doppler coefficient equals zero). In our approach, we identify an effective and efficient way of combating Doppler and fading. We compared sending $L$ copies of the same information bit (or sampling the received signal at a rate faster than the bit rate) or the use of error correcting code (we also tried some combinations of diversity and coding).

We propose to use the information about the minimum $P_b$ (see Figures 4–11) to select candidate convolutional codes so as not to mae the system diversity large.

[2]The gain is a bound due to equation (4.1).

The comparisons that follow are between a coded system and an uncoded system. Of course, both systems have the same energy, SNR, and diversity $L$. We want to verify how much improvement we may obtain by using a code over the existent system that contains diversity only.

We evaluate two types of convolutional code: rate $1/2$, $\nu = 2$, and rate $2/3$, $\nu = 2$.

As we have seen before, the minimum values for $P_b$ occur for diversity value between 5 and 20. Choosing the rate $1/2$, $\nu = 2$, convolutional code, we obtain $d_f = 5$ [7]. We use $L = 2$. Therefore, observing equation (4.2) we verify a reduction to $1/4$ of the original Doppler frequency in this case.

Figure 17 presents the results for zero Doppler. This result agrees with the one presented in [7].

Figure 18 presents the details mentioned above in a Rayleigh fading channel ($r = 0$). At low SNR we see a possible loss. Since the code rate is $1/2$ we have expanded the system bandwidth two times over the bandwidth of the uncoded system.

Figure 19 shows that for a Ricean fading channel ($r = 10$) the bound on the gain is very much reduced in comparison with the one obtained in the Rayleigh case. There is still a chance of loss at low SNR. Figures 19 and 21 show that an increase in diversity size improves the performance of the uncoded system more than the one of the coded system in a Ricean fading channel with $r = 10$ (which is getting close to a practical AWGN channel). For Rayleigh fading, the improvement is about the same as for Ricean fading.

Figure 22 provides a numerical check with the literature [1, 7] for the rate $2/3$, $\nu = 2$, convolutional code. The same type of performance improvement using diversity is also observed in this code (Figures 23 to 26).

We analyze two other convolutional codes that are more suitable for practical use (due to the fact that they have larger value for $d_f$): rate $1/2$, $\nu = 6$ with $d_f = 10$ and rate $2/3$, $\nu = 6$ with $d_f = 6$.

We consider a Rayleigh fading ($r = 0$) and Ricean fading channels for some values of $L$. The results are presented in Figures 27 to 42.

The gains we obtain here are much greater than the ones obtained before. We point out that such selected codes have greater free distance than the previous ones.

The coding gains are greater in a Rayleigh fading channel than in a Ricean fading channel, confirming what we have seen in the other codes. $P_b$ can be reduced by increasing the system diversity $L$ and the direct-to-diffuse ratio $r$, but the relative gain is reduced as $r$ increases, i.e., as the channel tends to an AWGN channel.

The rate $1/2$ codes presented here perform better than the rate $2/3$ codes, although the gain per bandwidth expansion ratio in the rate $2/3$ code is greater than the rate $1/2$ code.

Finally, we notice that there are crossovers among the various uncoded and coded schemes. This is illustrated in Figures 15 through 41.

[THIS PAGE INTENTIONALLY LEFT BLANK]

# VI. CONCLUSION

A closed form expression for the probability of bit error was independently derived for 2-FSK, square law detector, conditioned on Doppler in a Ricean fading channel. We have shown how to obtain the Rayleigh fading channel and AWGN cases (with Doppler) from that expression. The equations agree with the ones presented in the literature for the zero Doppler cases.

The equation can also be used in a Jensen's inequality [9] to obtain a lower bound if the Doppler frequency is assumed to be a random variable. In this situation, it may also be used to estimate $P_b$ by some statistical simulation method.

The probability density function that was developed can be used to get an expression for a $P_b$ in a M-FSK scheme. We can directly apply the equation for $P_b$ for the binary case in a bound for the M-ary case [1].

In addition, we have demonstrated the use of convolutional codes to address both fading and Doppler effects. We have verified that a bandwidth expansion, due to coding rate, is the price that we pay for obtaining the SNR gains.

Finally, we suggest the use of non-linear schemes, similar to Trellis Coded Modulation, to keep the SNR gain and provide a savings in terms of bandwidth expansion.

In addition, it seems a natural extension of the present research is to study the application of a dual-k convolutional code [1, 7] coupled with a noncoherent detection M-FSK scheme.

[THIS PAGE INTENTIONALLY LEFT BLANK]

# APPENDIX A

## EVALUATION OF THE INNER INTEGRAL OF EQUATION 2.6

Evaluation of the inner integral of Equation (2.6):

$$\int_{y_0}^{\infty} f_{Y_1}(y_1)dy_1 = \int_{y_0}^{\infty} \frac{1}{(L-1)!2^L\sigma^{2L}} y_1^{L-1} e^{-y_1/2\sigma^2} dy_1$$

$$= \int_{y_0}^{\infty} \frac{\left(\frac{y_1}{2\sigma^2}\right)^{L-1}}{2\sigma^2(L-1)!} e^{-(y_1/2\sigma^2)} dy_1 = \int_{y_0}^{\infty} \frac{\left(\frac{y_1}{2\sigma^2}\right)^{L-1}}{(L-1)!} e^{-(y_1/2\sigma^2)} \left(\frac{dy_1}{2\sigma^2}\right) \tag{A.1}$$

Changing variables in (A.1):

$$x = \frac{y_1}{2\sigma^2} \tag{A.2}$$

$$x_0 = \frac{y_0}{2\sigma^2} \tag{A.3}$$

$$dx = \frac{1}{2\sigma^2} dy_1 = \left(\frac{dy_1}{2\sigma^2}\right) \tag{A.4}$$

$$= \int_{x_0}^{\infty} \frac{x^{L-1}}{(L-1)!} e^{-x} dx = \frac{e^{-x}}{-1} \left(\sum_{k=0}^{L-1} \frac{x^k}{k!}\right) \Bigg]_{x_0}^{\infty}$$

$$= \lim_{x_0 \to \infty} \left[\frac{e^{-x}}{-1} \left(\sum_{k=0}^{L-1} \frac{x^k}{k!}\right)\right] - \left[\frac{e^{-x_0}}{-1} \left(\sum_{k=0}^{L-1} \frac{x_0^k}{k!}\right)\right] = e^{-x_0} \sum_{k=0}^{L-1} \frac{x_0^k}{k!} \tag{A.5}$$

Substituting (A.3) in (A.5):

$$\int_{y_0}^{\infty} f_{Y_1}(y_1)dy_1 = e^{-y_0/2\sigma^2} \sum_{k=0}^{L-1} \frac{\left(\frac{y_0}{2\sigma^2}\right)^k}{k!} \tag{A.6}$$

[THIS PAGE INTENTIONALLY LEFT BLANK]

# APPENDIX B

## BESSEL FUNCTION PROPERTIES

$$\int_0^\infty x^{m+\nu/2} e^{\gamma x} J_\nu \left(2\beta\sqrt{x}\right) dx \tag{B.1}$$

$$= m!\beta^\nu e^{-\beta^2/\gamma}\gamma^{-m-\nu-1} L_m^\nu \left(\frac{\beta^2}{\gamma}\right) \qquad [m+\nu > -1] \tag{B.2}$$

where

$$L_m^\nu(b) = \sum_{n=0}^{m}(-1)^n \left( \begin{array}{c} n+\nu \\ n-m \end{array} \right) \frac{b^n}{n!} \tag{B.3}$$

$$I_\nu(x) = j^{-n} J_\nu(jx) \tag{B.4}$$

$$\beta = j\alpha \tag{B.5}$$

$$J_\nu \left(2\beta\sqrt{x}\right) = J_\nu \left(j2\alpha\sqrt{x}\right) = \frac{1}{j^{-\nu}} I_\nu \left(2\alpha\sqrt{x}\right) \tag{B.6}$$

Substituting (B.6) in (B.1)

$$\int_0^\infty x^{m+\nu/2} e^{-\gamma x} J_\nu \left(j2\alpha\sqrt{x}\right) dx = \int_0^\infty x^{m+\nu/2} e^{-\gamma x} j^\nu I_\nu \left(2\alpha\sqrt{x}\right) dx$$

$$= j^\nu \int_0^\infty x^{m+\nu/2} e^{-\gamma x} I_\nu \left(2\alpha\sqrt{x}\right) dx = m! j^\nu \alpha^\nu e^{\alpha^2/\gamma}\gamma^{-m-\nu-1} L_m^\nu \left(\frac{-\alpha^2}{\gamma}\right) \tag{B.7}$$

Thus:

$$\int_0^\infty x^{m+\nu/2} e^{-\gamma x} I_\nu \left(2\alpha\sqrt{x}\right) dx = m!\alpha^\nu e^{\alpha^2/\gamma}\gamma^{-1-\nu-1} L_m^\nu \left(\frac{-\alpha^2}{\gamma}\right) \tag{B.8}$$

where

$$L_m^{\nu}\left(\frac{-\alpha^2}{\gamma}\right) = \sum_{n=0}^{m}(-1)^n \begin{pmatrix} n+\nu \\ n-m \end{pmatrix} \frac{1}{n!}\left(\frac{-\alpha^2}{\gamma}\right)^n$$

$$= \sum_{n=0}^{m}(-1)^n \begin{pmatrix} n+\nu \\ n-m \end{pmatrix} \frac{1}{n!}\left(\frac{\alpha^2}{\gamma}\right)^n (-1)^n = \sum_{n=0}^{m} \begin{pmatrix} n+\nu \\ n-m \end{pmatrix} \frac{\left(\frac{\alpha^2}{\gamma}\right)^n}{n!} \tag{B.9}$$

Substituting (B.9) in (B.8)

$$\int_0^{\infty} x^{m+\nu/2} e^{-\gamma x} I_{\nu}\left(2\alpha\sqrt{x}\right) dx = m!\alpha^{\nu} e^{\alpha^2/\gamma} \gamma^{-m-\nu-1} \sum_{n=0}^{m} \begin{pmatrix} n+\nu \\ n-m \end{pmatrix} \frac{\left(\frac{\alpha^2}{\gamma}\right)^n}{n!} \tag{B.10}$$

# APPENDIX C

## DEVELOPMENT OF $P_b$ EQUATION

Substituting Equation (A.4) and Equation (A.6) of Appendix A in Equation (2.6) of Chapter 2:

$$\mathcal{P}_b = \int_0^\infty e^{-y_0/2\sigma^2} \sum_{k=0}^{L-1} \frac{1}{k!} \left(\frac{y_0}{2\sigma^2}\right)^k \left\{ \frac{1}{2\sigma^2} \left(\frac{y_0}{v}\right)^{(L-2)/2} e^{-(y_0+v)/2\sigma^2} I_{L-1}\left(\frac{\sqrt{vy_0}}{\sigma^2}\right) \right\} dy_0 \tag{C.1}$$

Let

$$x = \frac{y_0}{2\sigma^2} , \qquad dx = \frac{1}{2\sigma^2} dy_0 .$$

$$\mathcal{P}_b = \int_0^\infty e^{-x} \sum_{k=0}^{L-1} \frac{1}{k!} x^k \left(\frac{x}{v/2\sigma^2}\right)^{(L-1)/2} e^{-(x+v/2\sigma^2)} I_{L-1}\left(2\sqrt{\frac{v}{2\sigma^2}x}\right) dx$$

$$= \int_0^\infty e^{-x} \sum_{k=0}^{L-1} \frac{1}{k!} x^k \left(\frac{x}{z}\right)^{(L-1)/2} e^{-(x+z)} I_{L-1}\left(2\sqrt{zx}\right) dx$$

$$= \frac{e^{-z}}{z^{(L-1)/2}} \sum_{k=0}^{L-1} \frac{1}{k!} \int_0^\infty x^{((L-1)/2+k)} e^{-2v} I_{L-1}\left(2\sqrt{zx}\right) dx . \tag{C.2}$$

Using Equation (A.10) of Appendix A, let

$$\nu = L-1 ,$$

$$n = k ,$$

$$\gamma = 2 ,$$

$$\alpha = \sqrt{z} .$$

$$\mathcal{P}_b = \frac{e^{-z}}{z^{(L-1)/2}} \sum_{k=0}^{L-1} \frac{1}{k!} \left\{ k! z^{(L-1)/2} e^{z/2} 2^{-k-L} \right\}$$

$$\times \sum_{m=0}^{k} (-1)^m \begin{pmatrix} k+L-1 \\ k-m \end{pmatrix} \frac{1}{m!} (-1)^m \left(\frac{z}{2}\right)^m \tag{C.3}$$

$$\mathcal{P}_b = \frac{e^{-z/2}}{2^L} \sum_{k=0}^{L-1} \frac{1}{2^k} \sum_{m=0}^{k} \begin{pmatrix} k+L-1 \\ k-m \end{pmatrix} \frac{(z/2)^m}{m!} \tag{C.4}$$

$$\mathcal{P}_b = \frac{e^{-z/2}}{2^L} \sum_{k=0}^{L-1} \frac{1}{2^k} \sum_{m=0}^{k} \begin{pmatrix} k+L-1 \\ m+L-1 \end{pmatrix} \frac{(z/2)^m}{m!} \,. \tag{C.5}$$

Equations (C.4) and (C.5) agree with the results presented in [2] and [7].

# APPENDIX D

## AVERAGE BIT ERROR PROBABILITY FOR A NON-COHERENT 2-FSK IN A RICEAN FADING CHANNEL

$$P_b = \int_{-\infty}^{\infty} \mathcal{P}_b(z,\beta) f_Z(z) dz = \int_0^{\infty} \mathcal{P}_b(z,\beta) f_Z(z) dz \tag{D.1}$$

$$P_b(\beta) = \int_0^{\infty} \frac{e^{-z/2}}{2^L} \sum_{k=0}^{L-1} \frac{1}{2^k} \sum_{m=0}^{k} \binom{k+L-1}{m+L-1} \frac{\left(\frac{z}{2}\right)^m}{m!} \frac{1}{2\beta\sigma_k^2} \left(\frac{z}{\beta p}\right)^{(L-1)/2} e^{(z+\beta p)/2\beta\sigma_k^2}$$

$$\times I_{L-1}\left(\frac{\sqrt{\beta p z}}{\beta\sigma_k^2}\right) dz$$

$$= \frac{1}{2^L} \sum_{k=0}^{L-1} \frac{1}{2^k} \sum_{n=0}^{k} \binom{k+L-1}{m+L-1} \frac{1}{m!(2\beta\sigma_k^2)(\beta p)^{(L-1)/2} 2^m}$$

$$\int_0^{\infty} z^{m+(L-1)/2} e^{-(\beta\sigma_k^2+1)z/2\beta\sigma_k^2} e^{-\beta p/2\beta\sigma_k^2} I_{L-1}\left(\frac{\sqrt{\beta p z}}{\beta\sigma_k^2}\right) dz$$

$$= \frac{1}{2^L} \sum_{k=0}^{L-1} \frac{1}{2^k} \sum_{m=0}^{k} \binom{k+L-1}{m+L-1} \frac{e^{-p/2\sigma_k^2}}{m!(2\beta\sigma_k^2)(\beta p)^{(L-1)/2^m}} \times F(z) \tag{D.2}$$

$$F(z) = \int_0^{\infty} z^{m+(L-1)/2} e^{-(1/2+1/2\beta\sigma_k^2)z} I_{L-1}\left(\frac{\sqrt{\beta p}}{\beta\sigma_k^2} \cdot \sqrt{z}\right) dz \tag{D3}$$

Using Equation (B.8) of Appendix B and making the following change of variables:

$$\nu = L-1$$

$$\gamma = \frac{1}{2} + \frac{1}{2\beta\sigma_k^2}$$

$$\alpha = \frac{\sqrt{\beta p}}{2\beta\sigma_k^2}$$

we get:

$$F(z) = m! \left[\frac{\sqrt{\beta p}}{2\beta\sigma_k^2}\right]^{L-1} e^{-p/2\sigma_k^2[1+\beta\sigma_k^2]} \left[\frac{1}{2} + \frac{1}{2\beta\sigma_k^2}\right]^{-m-(L-1)-1} L_m^{\nu}\left(-\frac{p}{2\sigma_k^2[1+\beta\sigma_k^2]}\right) \tag{D.4}$$

Further applying (B.10) of Appendix B to (D.4):

$$F(z) = m! \frac{(\beta p)^{(L-1)/2}}{(2\beta\sigma_k^2)^{L-1}} e^{-p/2\sigma_k^2[1+\beta\sigma_k^2]} \left[\frac{1}{2} + \frac{1}{2\beta\sigma_k^2}\right]^{-m-L} \sum_{i=0}^{m} \binom{m+\nu}{m-i} \left(\frac{p}{2\sigma_k^2[1+\beta\sigma_k^2]}\right)^i \frac{1}{i!} \tag{D.5}$$

Substituting (D.5) in (D.2):

$$P_b(\beta) = \frac{1}{2^L} \sum_{k=0}^{L-1} \frac{1}{2^k} \sum_{m=0}^{k} \binom{k+k-1}{m+L-1} \frac{e^{-p/2\sigma_k^2}}{m!(2\beta\sigma_k^2)(\beta p)^{L-1/2}2^m} m! \frac{(\beta p)^{(L-1)/2)}}{(2\beta\sigma_k^2)^{L-1}} e^{-p/2\sigma_k^2[1+\beta\sigma_k^2]}$$

$$\times \left[\frac{1}{2} - \frac{1}{2\beta\sigma_k^2}\right]^{-m-L} \sum_{i=0}^{m} \binom{m+\nu}{m-i} \frac{\left(\frac{p}{2\sigma_k^2[1+\beta\sigma_k^2]}\right)^i}{i!} \tag{D.6}$$

$$P_b(\beta) = \frac{1}{2^L} \frac{e^{-(p/2\sigma_k^2)[1+1/[1+\beta\sigma_k^2]]}}{(2\beta\sigma_k^2)^L} \sum_{k=0}^{L-1} \frac{1}{2^k} \sum_{m=0}^{k} \binom{k+L-1}{m+L-1} \left[\frac{1}{2} + \frac{1}{2\beta\sigma_k^2}\right]^{-m-L}$$

$$\times \frac{1}{2^m} \sum_{i=0}^{m} \binom{m+L-1}{m-i} \frac{1}{i!} \left(\frac{p}{2\sigma_k^2[1+\beta\sigma_k^2]}\right)^i$$

$$= \frac{1}{2^L} e^{-(p/2\sigma_k^2)[1+(1+\beta\sigma_k^2)^{-1}]} \sum_{k=0}^{L-1} \frac{1}{2^k} \sum_{m=0}^{k} \binom{k+L-1}{m+L-1} [1+\beta\sigma_k^2]^{-m-L} \frac{(2\beta\sigma_k^2)^{m+L}}{2^m(2\beta\sigma_k^2)^L}$$

$$\times \sum_{i=0}^{m} \binom{m+L-1}{m-i} \frac{1}{i!} \left(\frac{p}{2\sigma_k^2[1+\beta\sigma_k^2]}\right)^i$$

$$= \frac{1}{2^L} \frac{e^{-(p/2\sigma_k^2)[1+(1+\beta\sigma_k^2)^{-1}]}}{[1+\beta\sigma_k^2]^L} \sum_{k=0}^{L-1} \frac{1}{2^k} \sum_{m=0}^{k} \begin{pmatrix} k+L-1 \\ m+L-1 \end{pmatrix} \left[\frac{\beta\sigma_k^2}{1+\beta\sigma_k^2}\right]^m$$

$$\times \sum_{i=0}^{m} \begin{pmatrix} m+L-1 \\ m-i \end{pmatrix} \frac{\left(\frac{p}{2\sigma_k^2[1+\beta\sigma_k^2]}\right)^i}{i!} \tag{D.7}$$

Note:

$$\begin{pmatrix} m+L-1 \\ m-i \end{pmatrix} = \frac{(m+L-1)!}{(m-i)!(i+L-1)!} = \frac{(m+L-1)!}{(i+L-1)!(m-i)!} = \begin{pmatrix} m+L-1 \\ i+L-1 \end{pmatrix} \tag{D.8}$$

Substituting (D.8) in (D.7):

$$P_b(\beta) = \frac{1}{2^L} \frac{e^{-(p/2\sigma_k^2)[1+(1+\beta\sigma_k^2)^{-1}]}}{(1+\beta\sigma_k^2)^L} \sum_{k=0}^{L-1} \frac{1}{2^k} \sum_{m=0}^{k} \begin{pmatrix} k+L-1 \\ m+L-1 \end{pmatrix} \left[\frac{\beta\sigma_k^2}{1+\beta\sigma_k^2}\right]^m$$

$$\times \sum_{i=0}^{m} \begin{pmatrix} m+L-1 \\ i+L-1 \end{pmatrix} \frac{\left(\frac{p}{2\sigma_k^2[1+\beta\sigma_k^2]}\right)^i}{i!} \tag{D.9}$$

[THIS PAGE INTENTIONALLY LEFT BLANK]

# APPENDIX E

## DOPPLER EFFECT COEFFICIENT

Doppler effect coefficient:[1]

$$X_k = \frac{A_k}{\sqrt{2}} \int_{(k-1)T}^{kT} e^{jw_d t} dt \tag{E.1}$$

$$V = \sum_{k=1}^{L} |X_k|^2 = \frac{1}{2} \sum_{k=1}^{L} A_k^2 \left| \int_{(k-1)T}^{kT} e^{jw_d t} dt \right|^2 \tag{E.2}$$

$$\int_{(k-1)T}^{kT} e^{jw_d t} dt = (-j) \frac{e^{jw_d kT} - e^{jw_d (k-1)T}}{w_d} \qquad (\text{for } w_d \neq 0)$$

$$= (-j) e^{jw_d (k-1)T} \left[ \frac{e^{jw_d T} - 1}{w_d} \right] \tag{E.3}$$

$$\left| \int_{(k-1)T}^{kT} e^{jw_d t} dt \right|^2 = \left| \frac{e^{jw_d T} - 1}{w_d} \right|^2 = T^2 \left| \frac{e^{jw_d T} - 1}{w_d T} \right|^2$$

$$= T^2 \left| \frac{\cos w_d T + j \sin w_d T - 1}{w_d T} \right|^2 = T^2 \left| \frac{(\cos w_d T - 1) + j \sin w_d T}{w_d T} \right|^2$$

$$= T^2 \left| \frac{\cos^2 w_d T + \sin^2 w_d T + 1 - 2 \cos w_d T}{(w_d T)^2} \right| = T^2 \left| \frac{2 - 2 \cos w_d T}{(w_d T)^2} \right|$$

$$= 2T^2 \left| \frac{2 \sin^2 \dfrac{w_d T}{2}}{(w_d T)^2} \right| = 4T^2 \left| \frac{2 \sin^2 \dfrac{w_d T}{2}}{(w_d T)^2} \right| = T^2 \left| \frac{\sin^2 \left( \dfrac{w_d T}{2} \right)}{\left( \dfrac{w_d T}{2} \right)^2} \right| = T^2 \left\{ \frac{\sin \left( \dfrac{w_d T}{2} \right)}{\left( \dfrac{w_d T}{2} \right)} \right\}^2 \tag{E.4}$$

[1]Note that here $w_d = 2\pi f_d$.

When $w_d = 0$:

$$\left| \int_{(k-1)T}^{kT} e^0 dt \right|^2 = T^2 \tag{E.5}$$

Taking the limit of (E.4) when $w_d \longrightarrow 0$:

$$\lim_{w \longrightarrow 0} T^2 \left\{ \frac{\sin\left(\frac{w_d T}{2}\right)}{\left(\frac{w_d T}{2}\right)} \right\}^2 = T^2 \tag{E.6}$$

Thus the expression (E.4) is valid also for $w_d = 0$.

Substituting (E.4) in (E.2):

$$V = \frac{T^2}{2} \left\{ \frac{\sin\left(\frac{w_d T}{2}\right)}{\left(\frac{w_d T}{2}\right)} \right\}^2 \sum_{k=1}^{L} A_k^2 \tag{E.7}$$

# APPENDIX F
## FIGURES

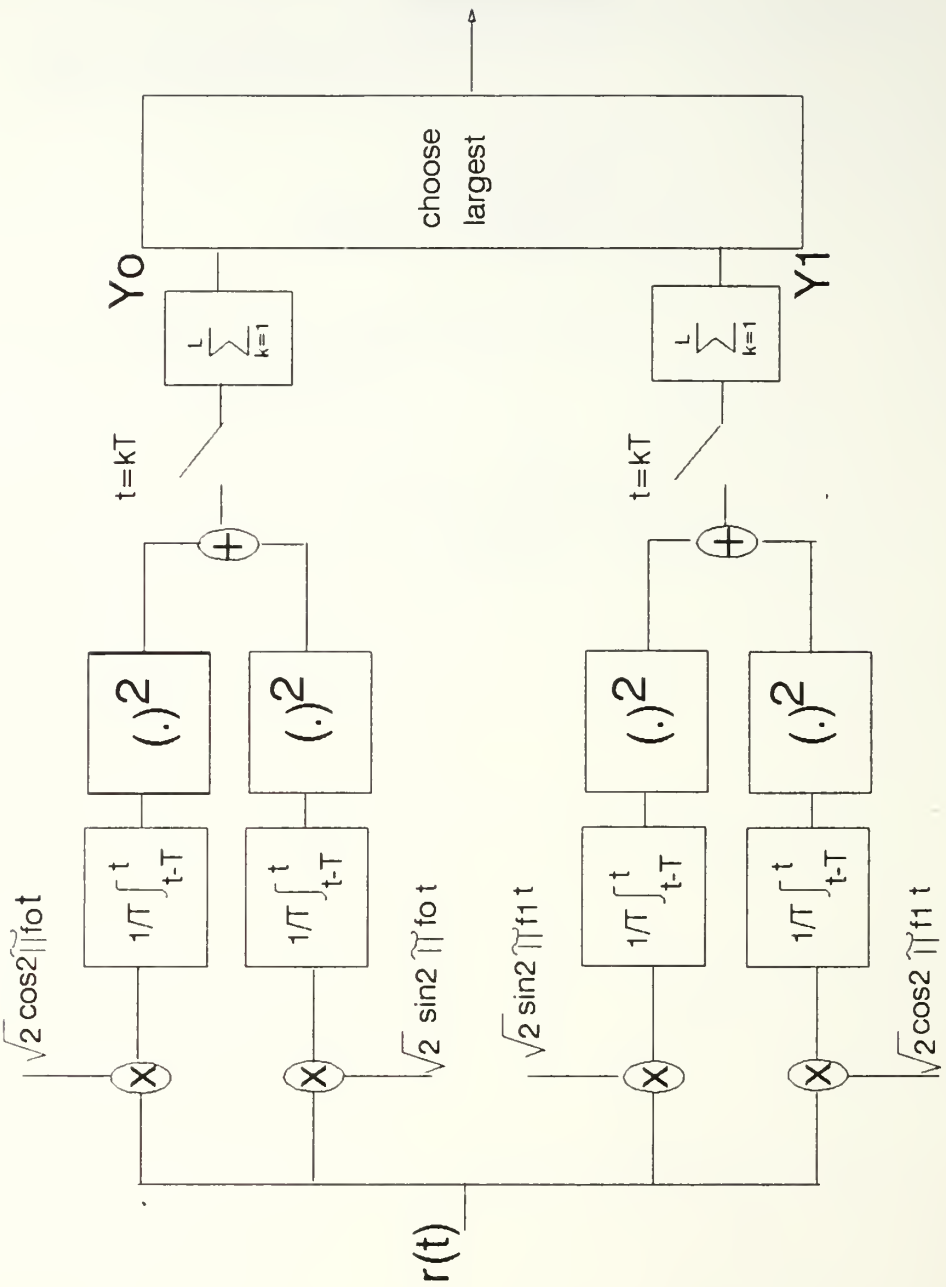


**Figure 1: An L-fold diversity 2-FSK receiver.**

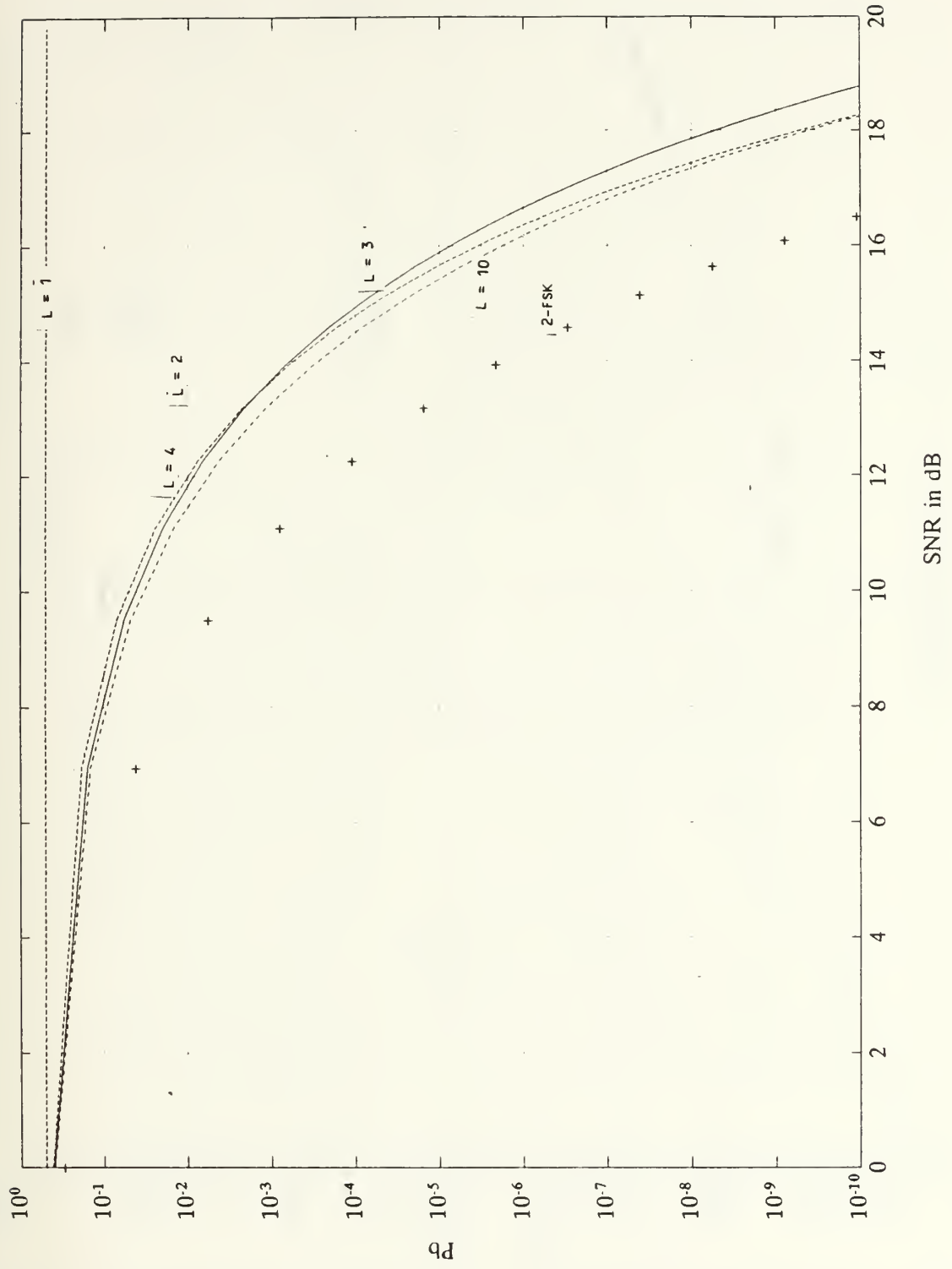


**Figure 2: Probability of bit error conditioned on the Doppler effect coefficient in an AWGN channel as a function of the system diversity.**

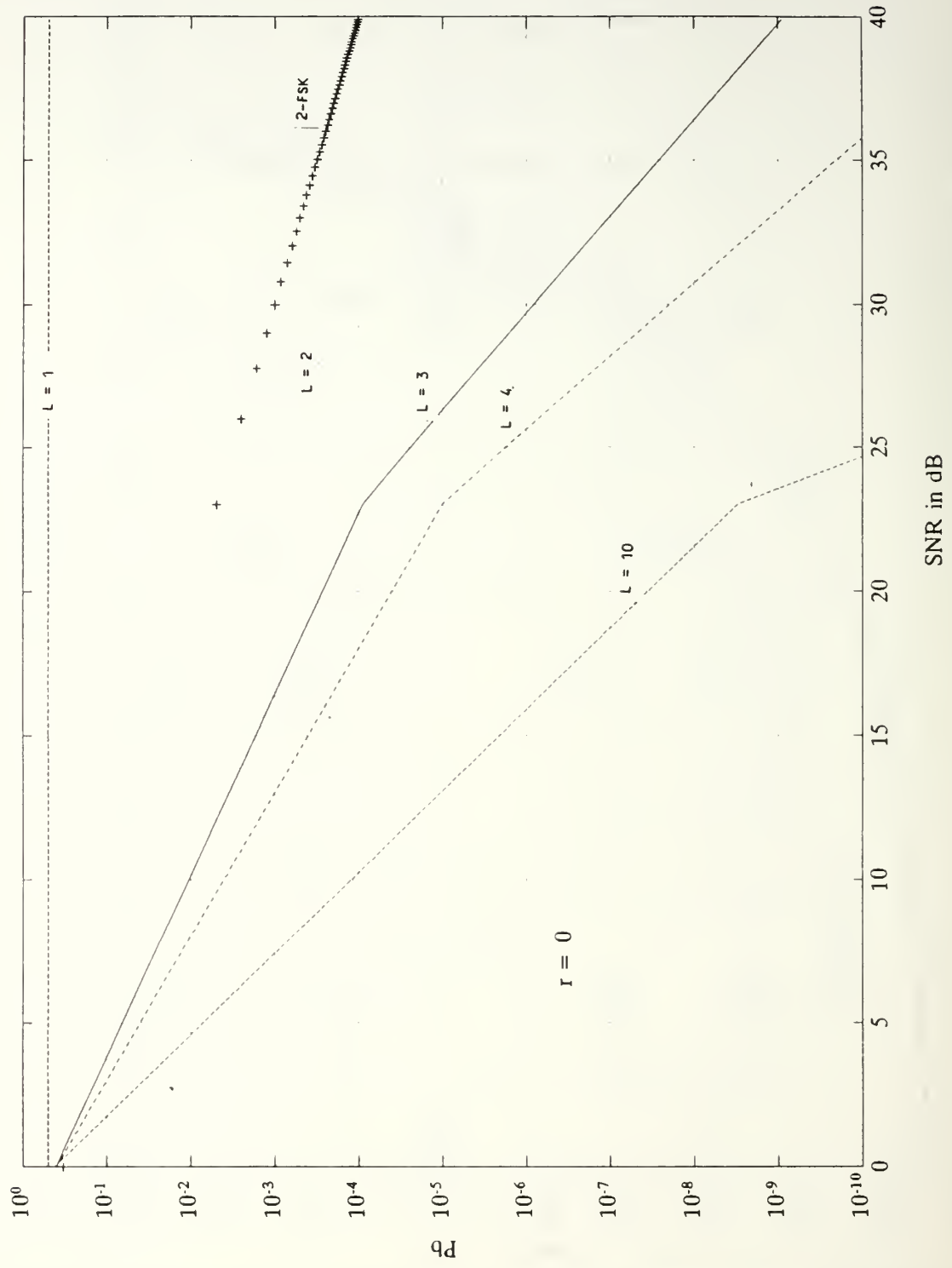


**Figure 3: Probability of bit error conditioned on the Doppler effect coefficient in a Rayleigh fading channel ($r = 0$) as a function of the system diversity.**

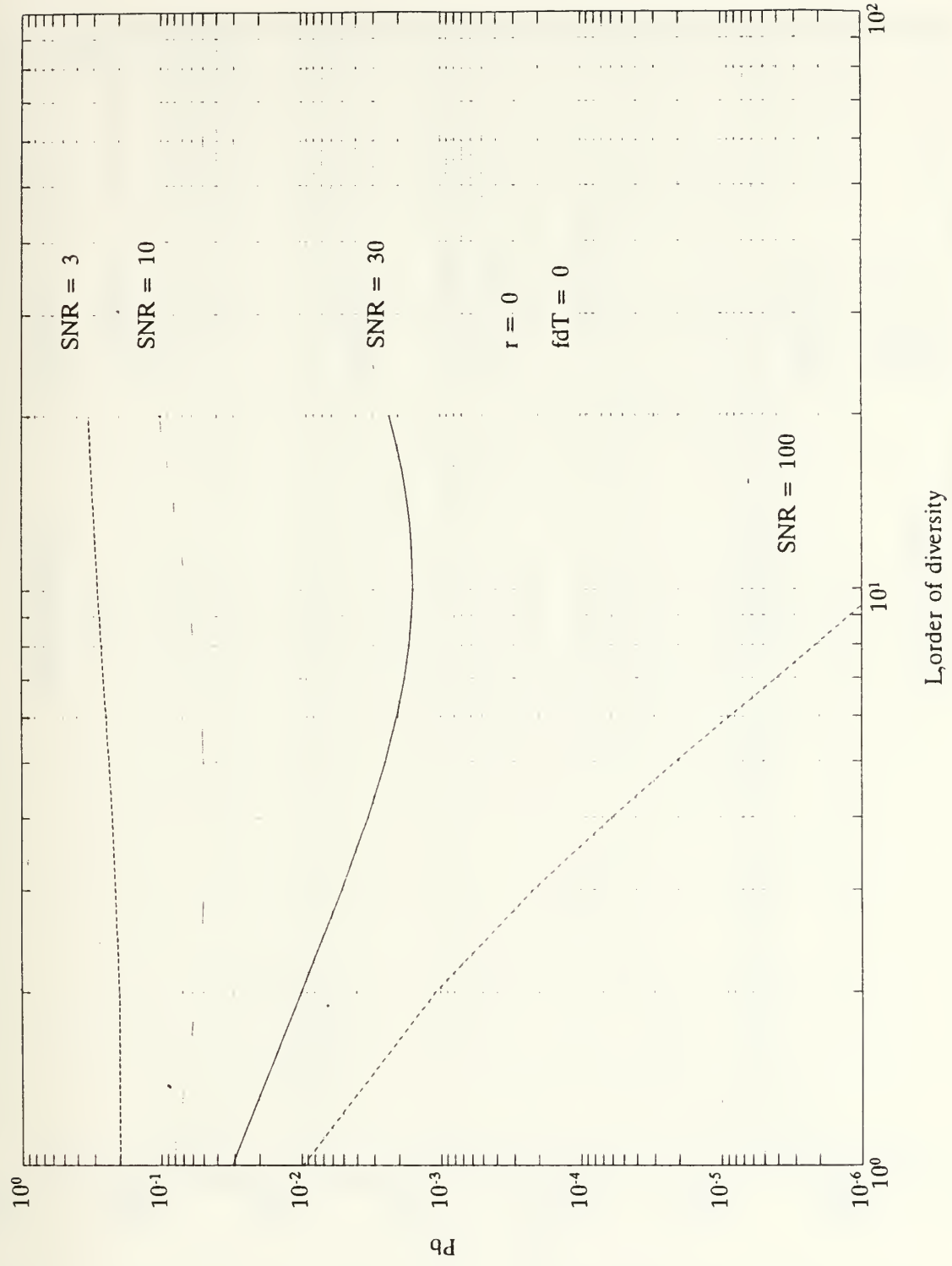


**Figure 4: Probability of bit error conditioned on the Doppler effect coefficient ($f_dT = 0$) in a Rayleigh fading channel ($r = 0$) as a function of the system diversity.**

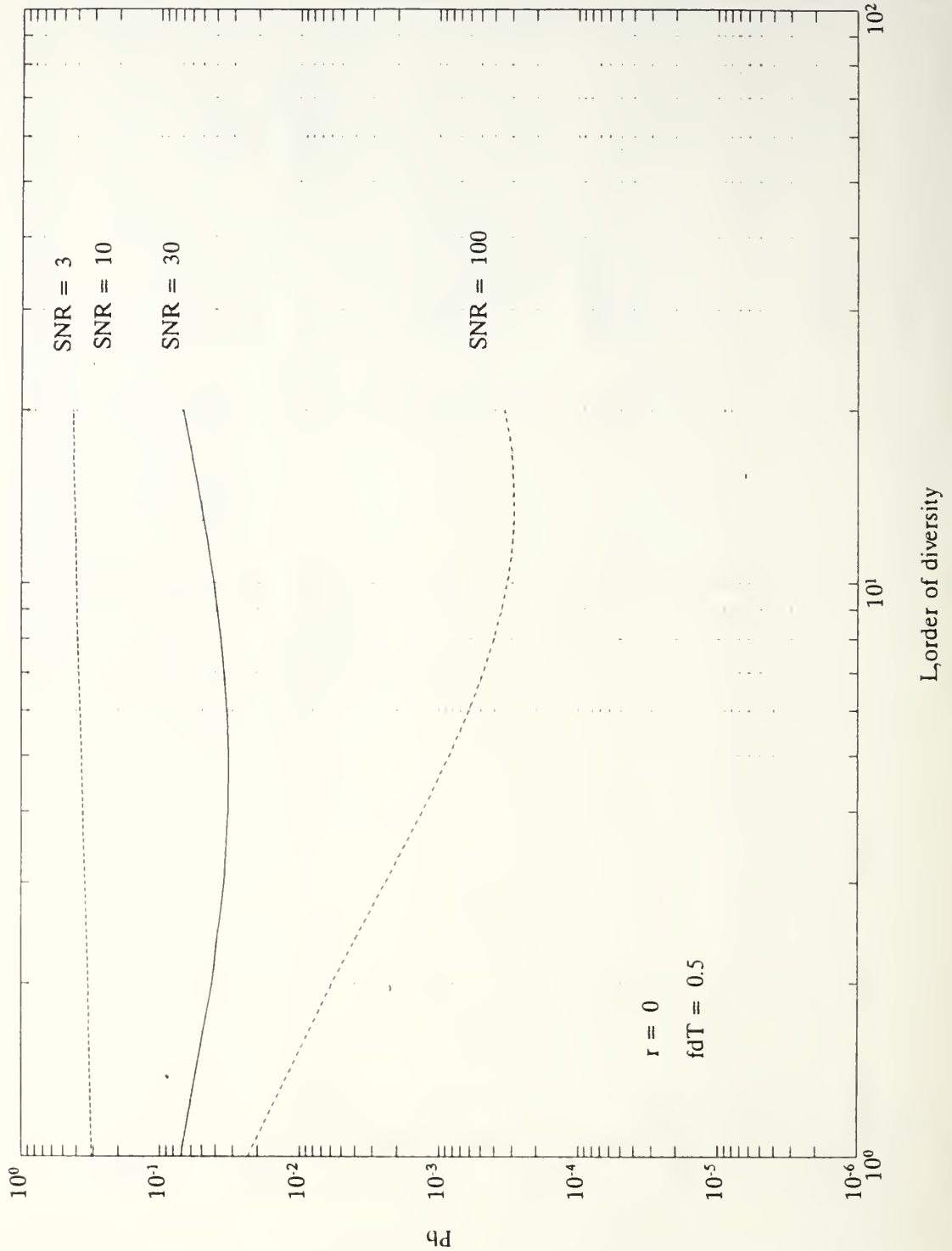


**Figure 5: Probability of bit error conditioned on the Doppler effect coefficient ($f_dT = 0.5$) in a Rayleigh fading channel ($r = 0$) as a function of the system diversity.**

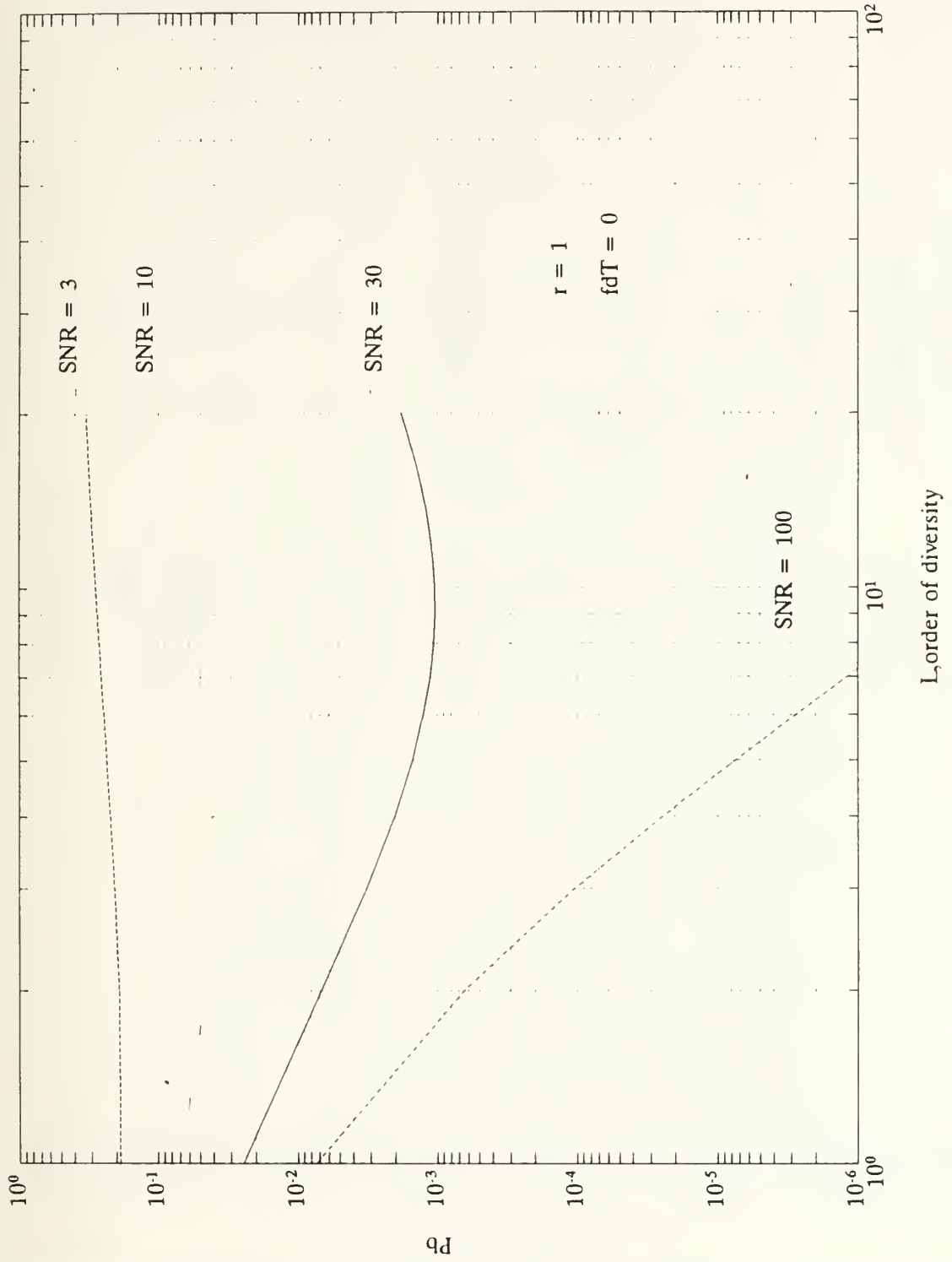


**Figure 6: Probability of bit error conditioned on the Doppler effect coefficient ($f_d T = 0$) in a Ricean fading channel ($r = 1$) as a function of the system diversity.**

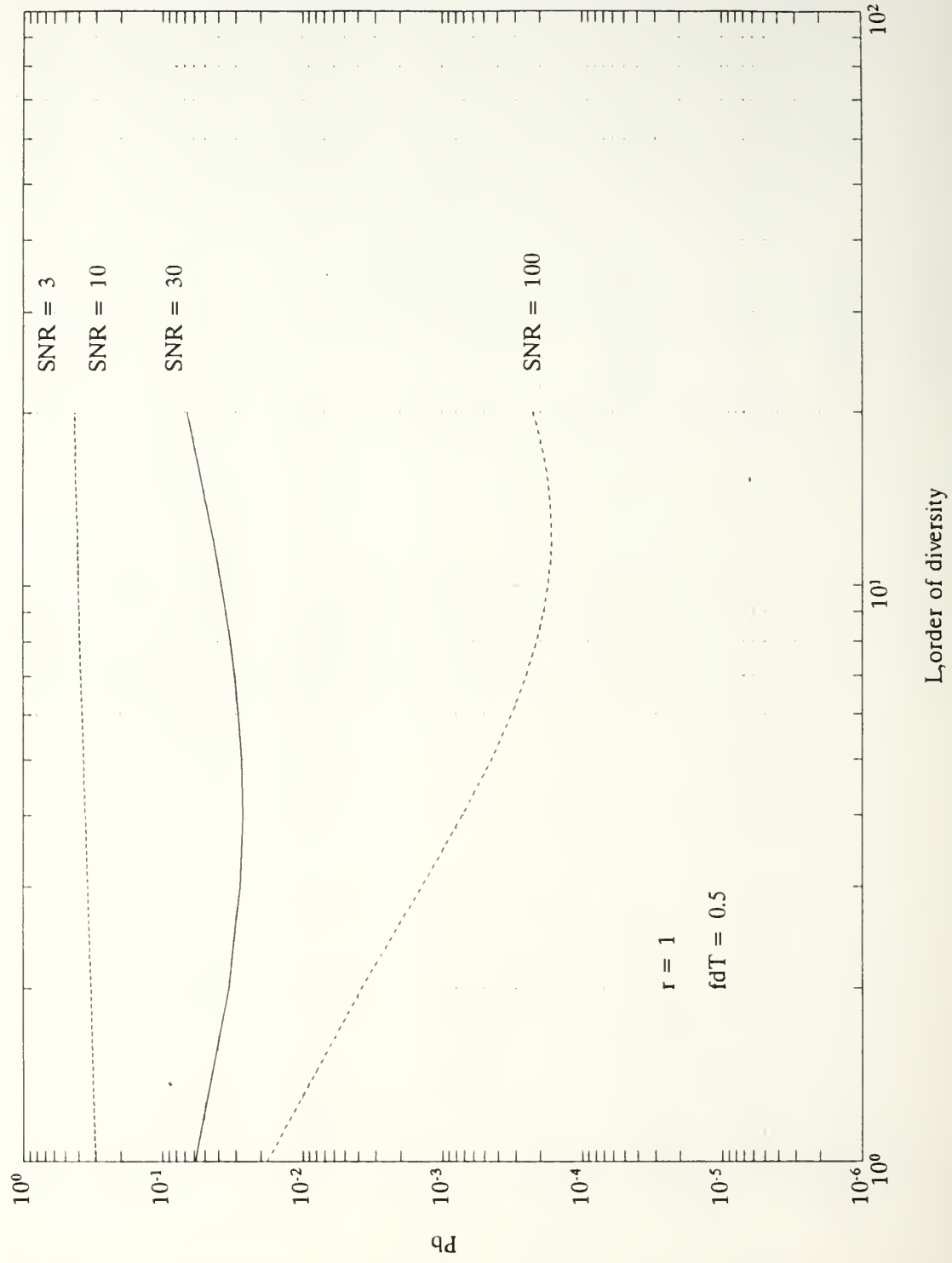


**Figure 7: Probability of bit error conditioned on the Doppler effect coefficient ($f_dT = 0.5$) in a Ricean fading channel ($r = 1$) as a function of the system diversity.**

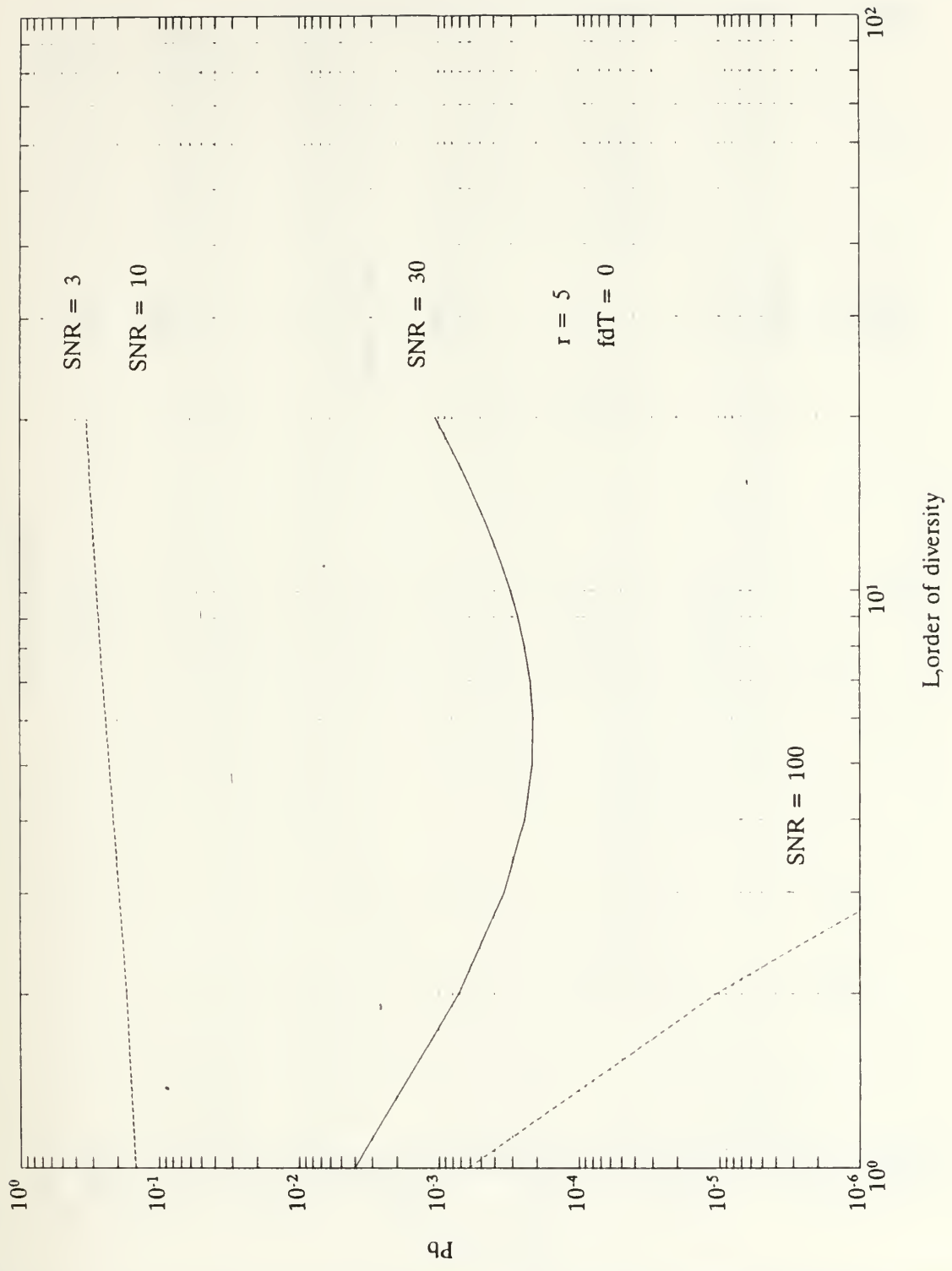


**Figure 8: Probability of bit error conditioned on the Doppler effect coefficient ($f_dT = 0$) in a Ricean fading channel ($r = 5$) as a function of the system diversity.**

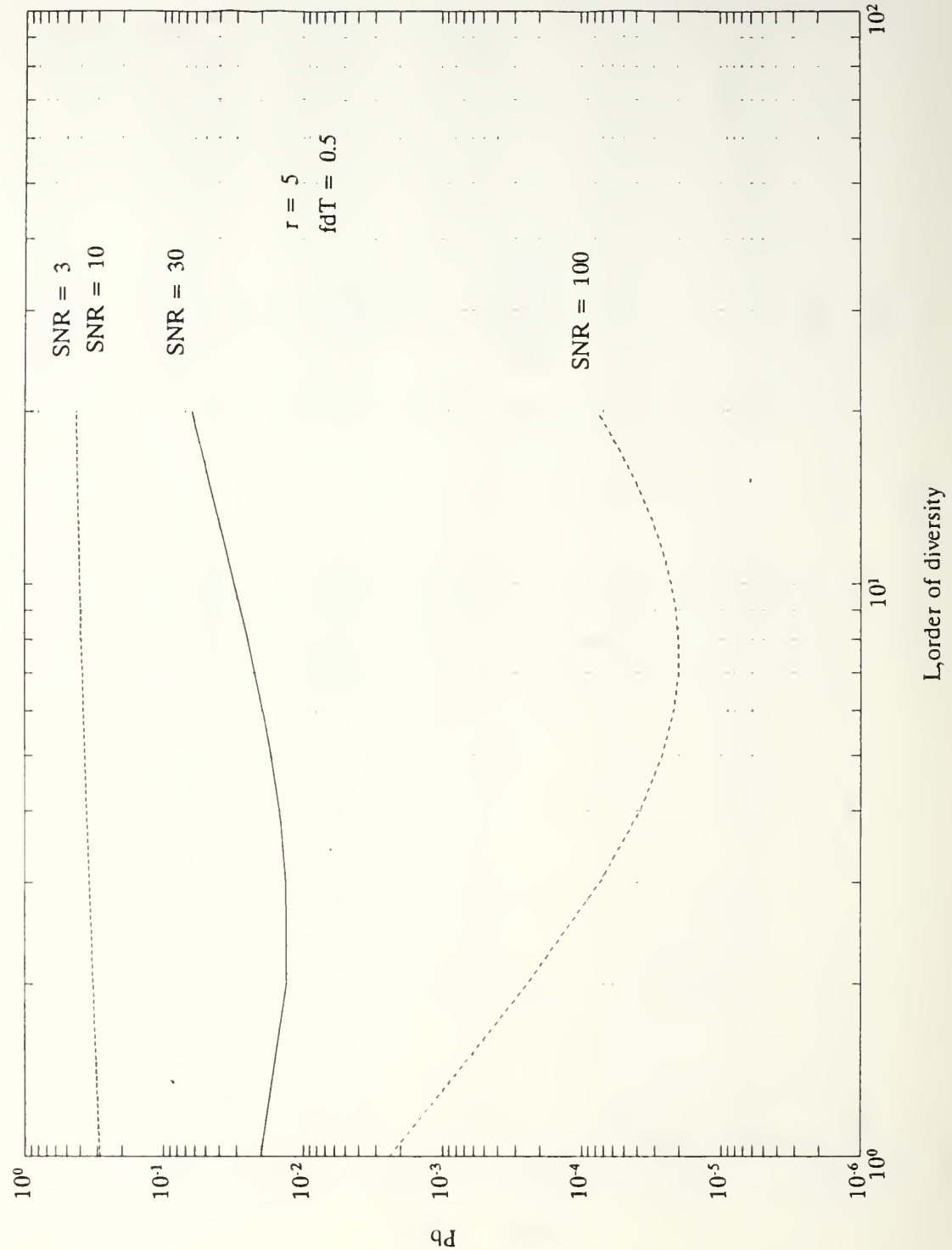


**Figure 9: Probability of bit error conditioned on the Doppler effect coefficient ($f_dT = 0.5$) in a Ricean fading channel ($r = 5$) as a function of the system diversity.**

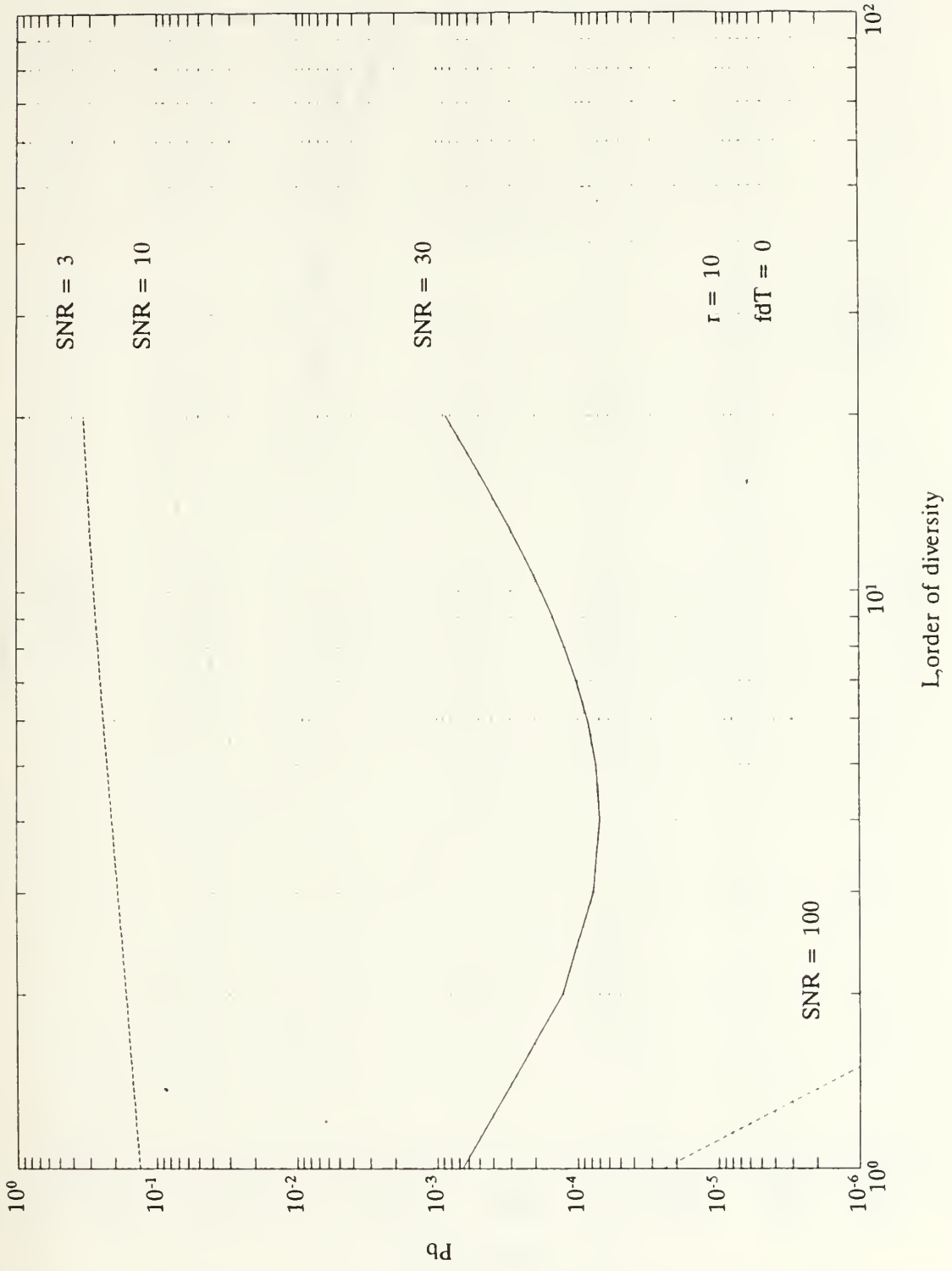


**Figure 10: Probability of bit error conditioned on the Doppler effect coefficient ($f_dT = 0$) in a Ricean fading channel ($r = 10$) as a function of the system diversity.**

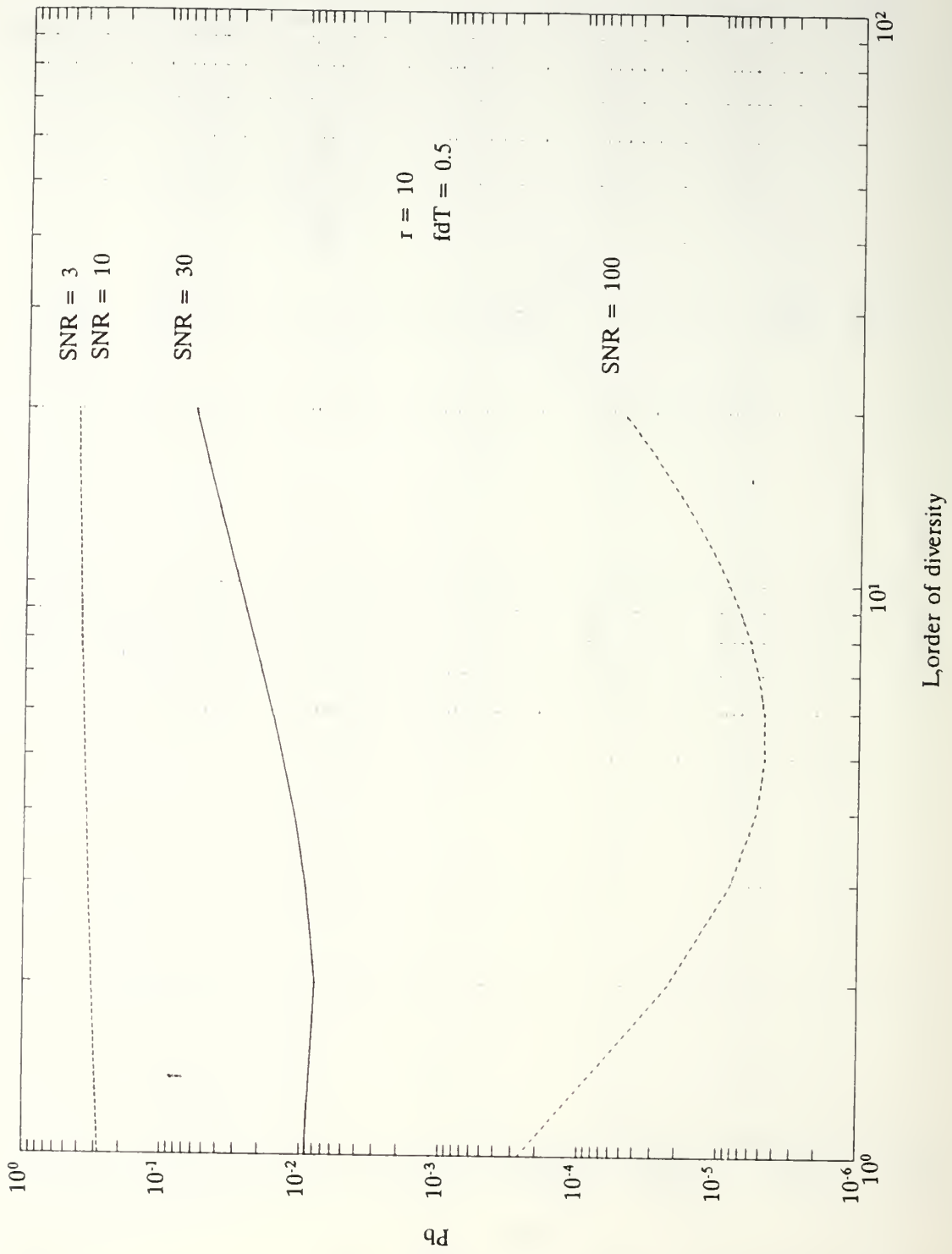


**Figure 11: Probability of bit error conditioned on the Doppler effect coefficient ($f_dT = 0.5$) in a Ricean fading channel ($r = 10$) as a function of the system diversity.**

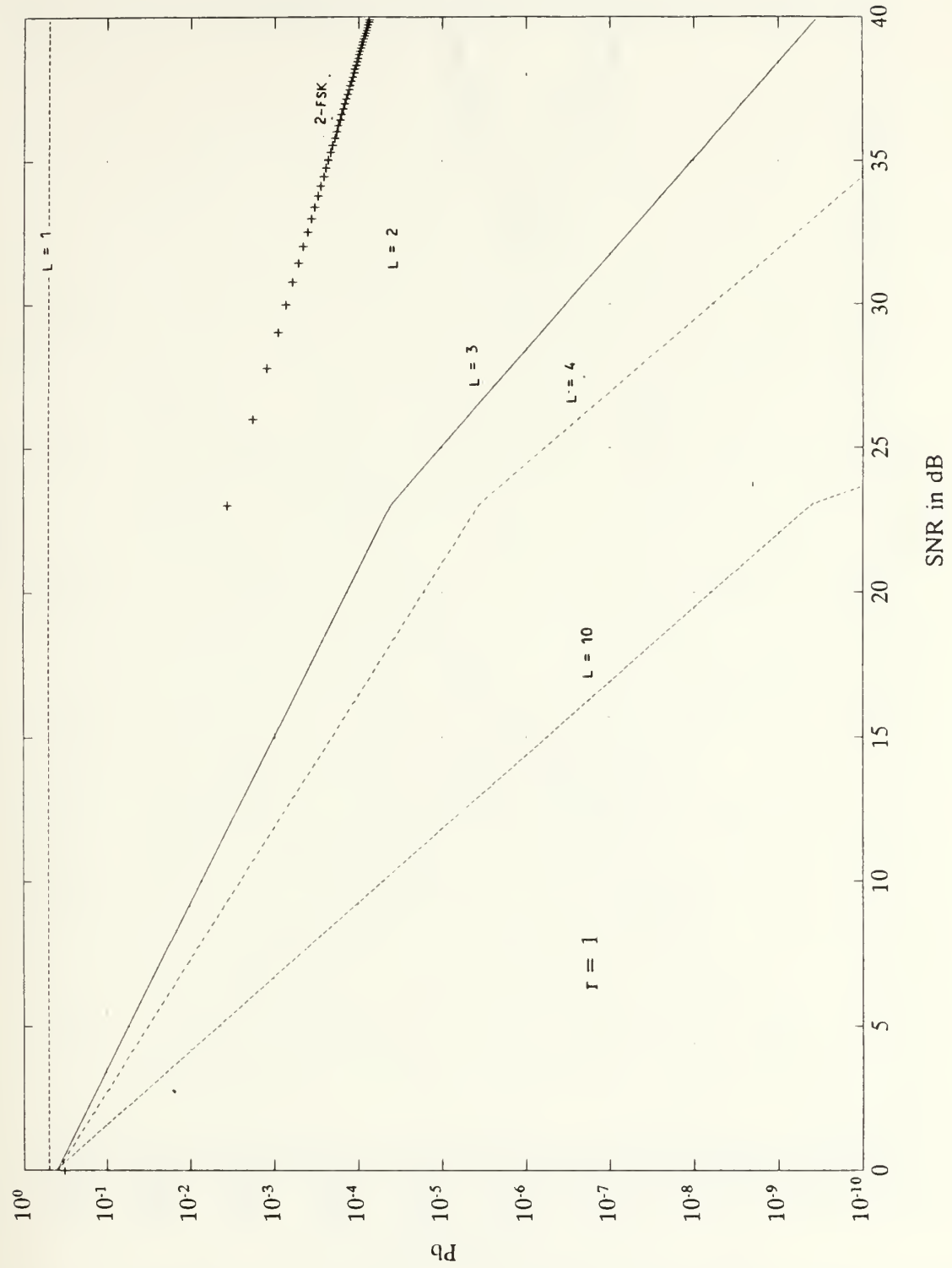


**Figure 12: Probability of bit error conditioned on the Doppler effect coefficient in a Ricean fading channel ($r = 1$) as a function of the system diversity.**

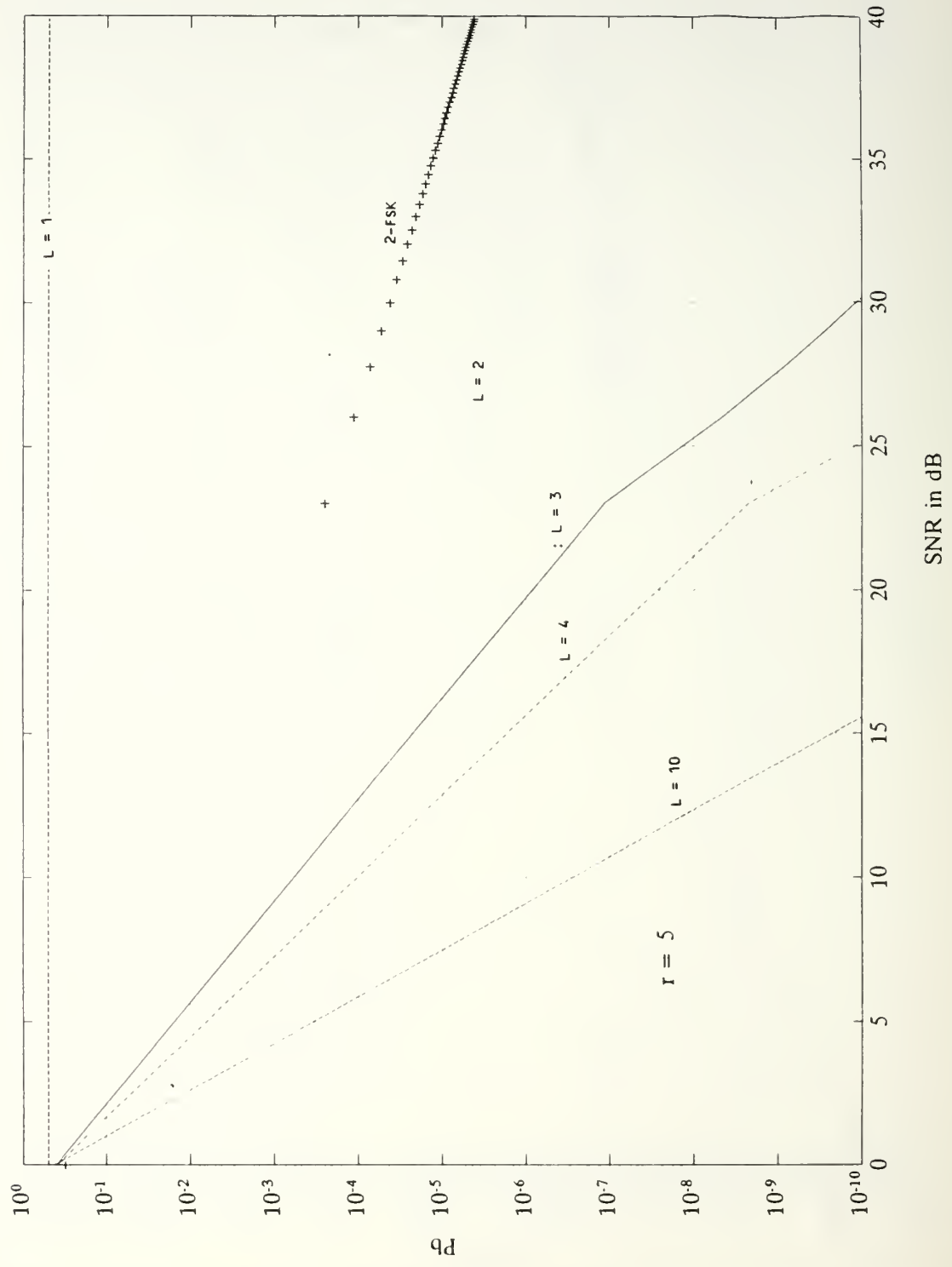


**Figure 13: Probability of bit error conditioned on the Doppler effect coefficient in a Ricean fading channel ($r = 5$) as a function of the system diversity.**

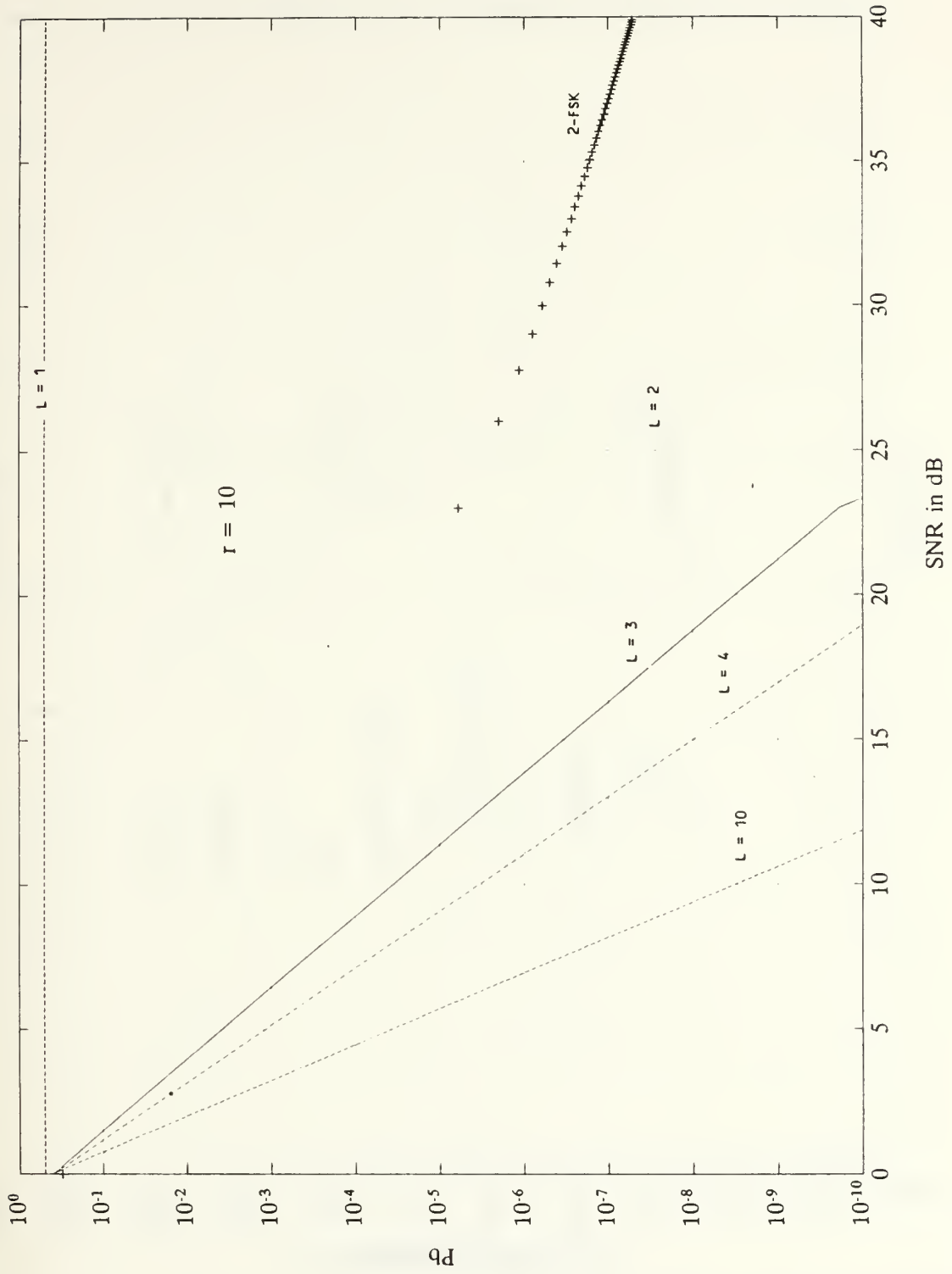


**Figure 14: Probability of bit error conditioned on the Doppler effect coefficient in a Ricean fading channel ($r = 10$) as a function of the system diversity.**

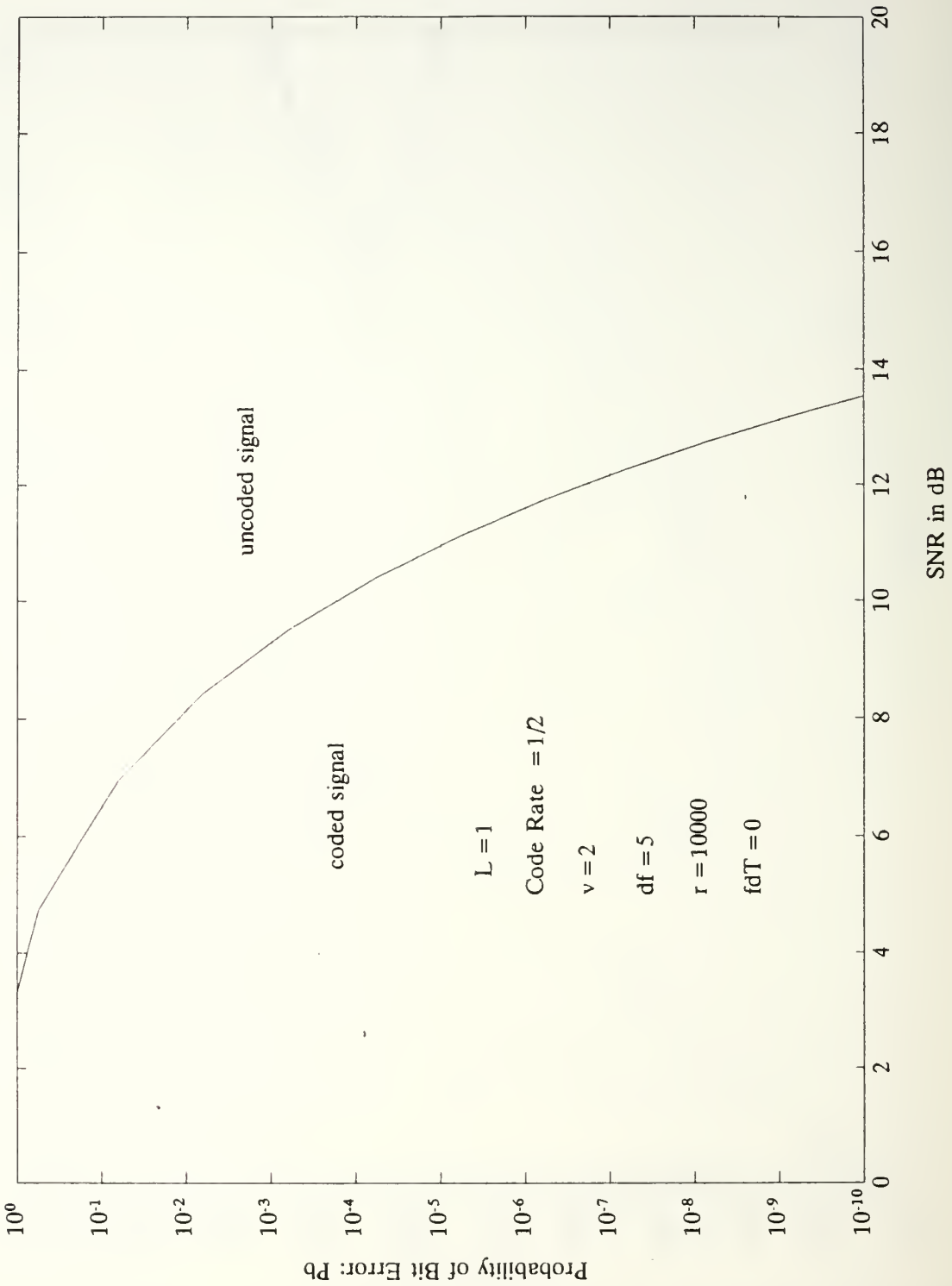


**Figure 15: Probability of bit error conditioned on the Doppler effect coefficient in an almost AWGN channel ($r = 10,000$) and no Doppler effect for a rate 1/2, $\nu = 2$ convolutional code and system diversity $L = 1$.**

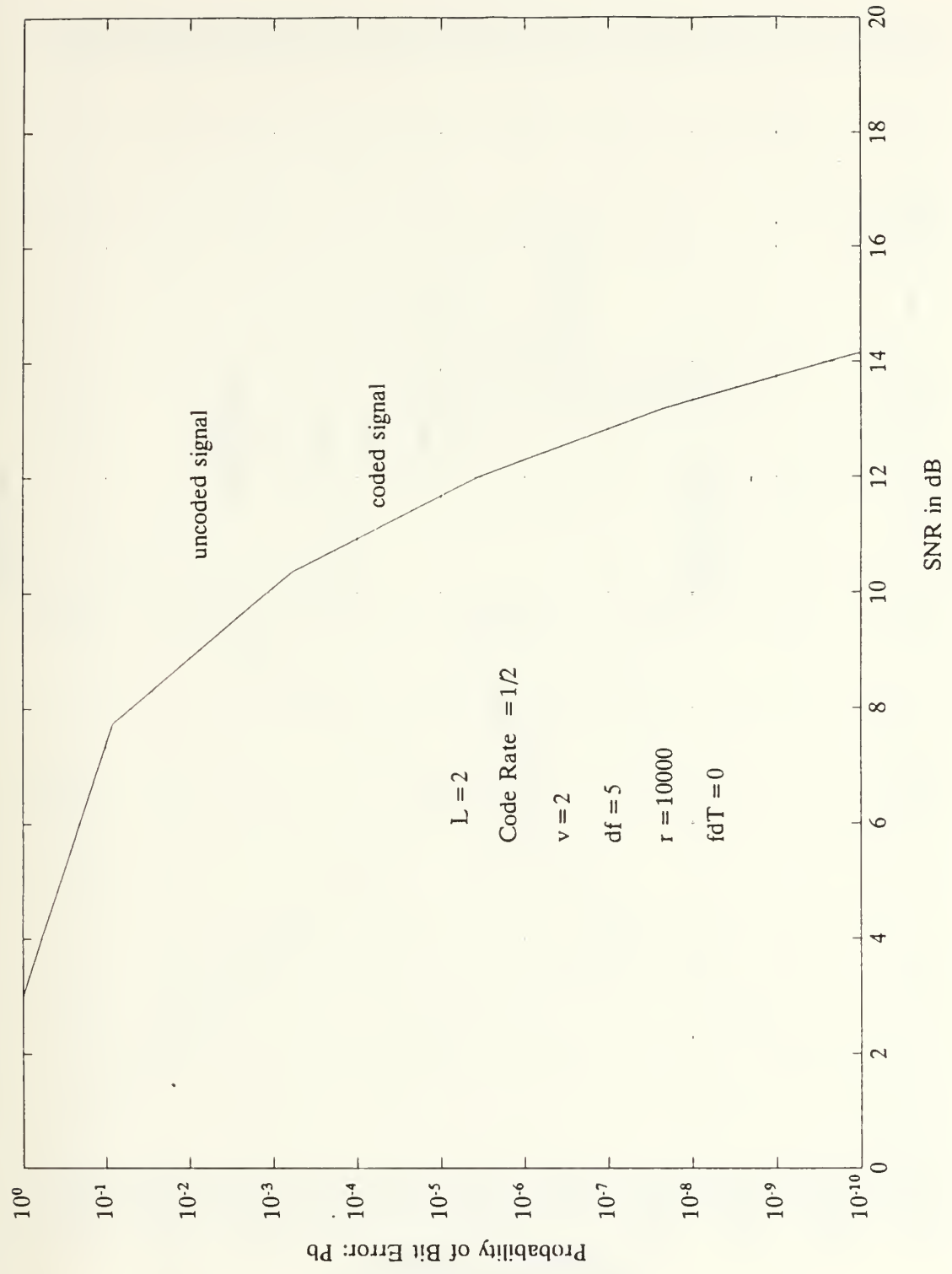


**Figure 16: Probability of bit error conditioned on the Doppler effect coefficient in an almost AWGN channel ($r = 10,000$) and no Doppler effect for a rate 1/2, $\nu = 2$ convolutional code and system diversity $L = 2$.**

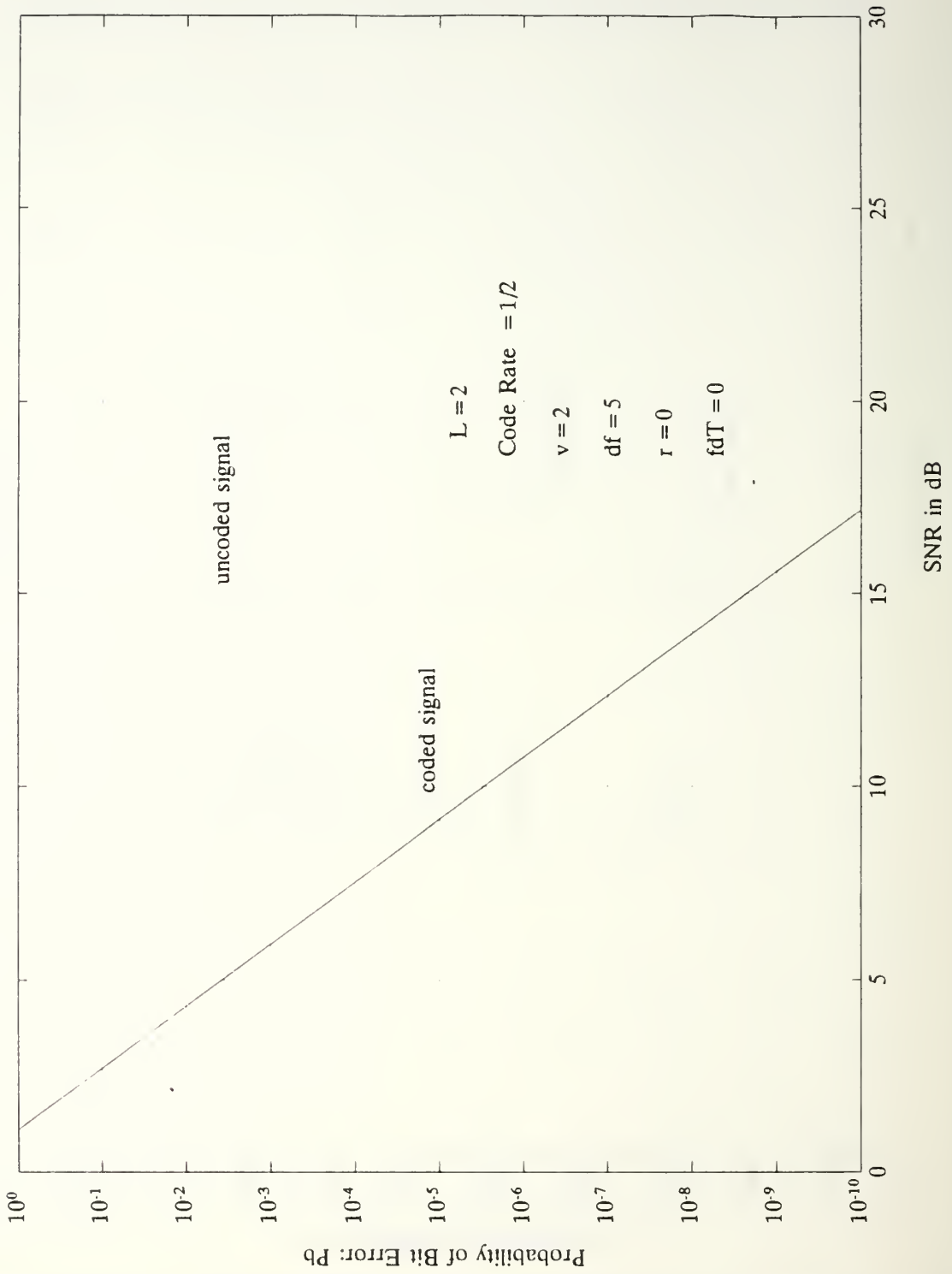


**Figure 17: Probability of bit error conditioned on the Doppler effect coefficient in a Rayleigh fading channel ($r = 0$) and no Doppler effect for a rate 1/2, $\nu = 2$ convolutional code and system diversity $L = 2$.**

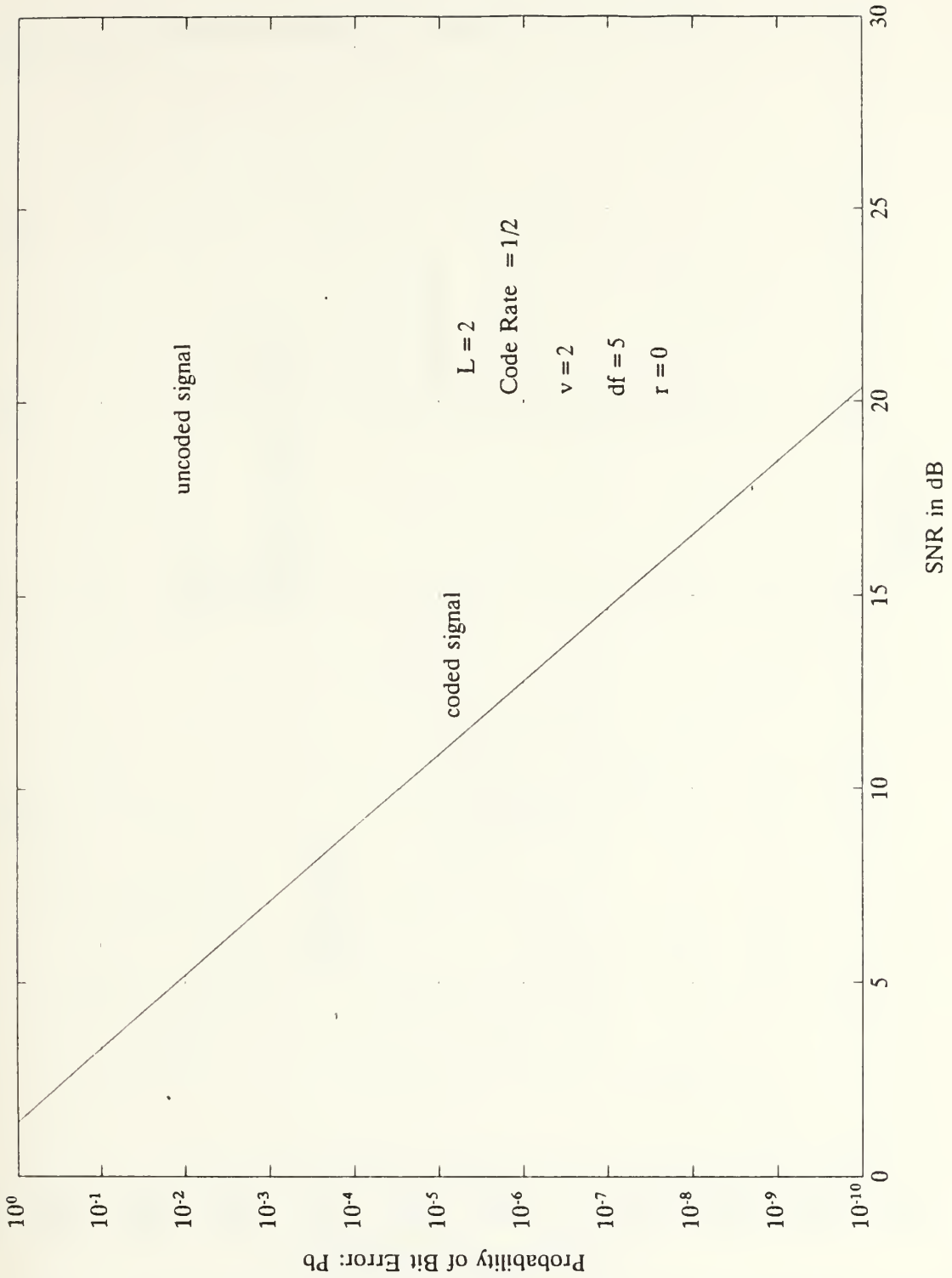


**Figure 18: Probability of bit error conditioned on the Doppler effect coefficient in a Rayleigh fading channel ($r = 0$) and maximum Doppler effect, i.e., minimal Doppler effect coefficient for a rate 1/2, $\nu = 2$ convolutional code and system diversity $L = 2$.**

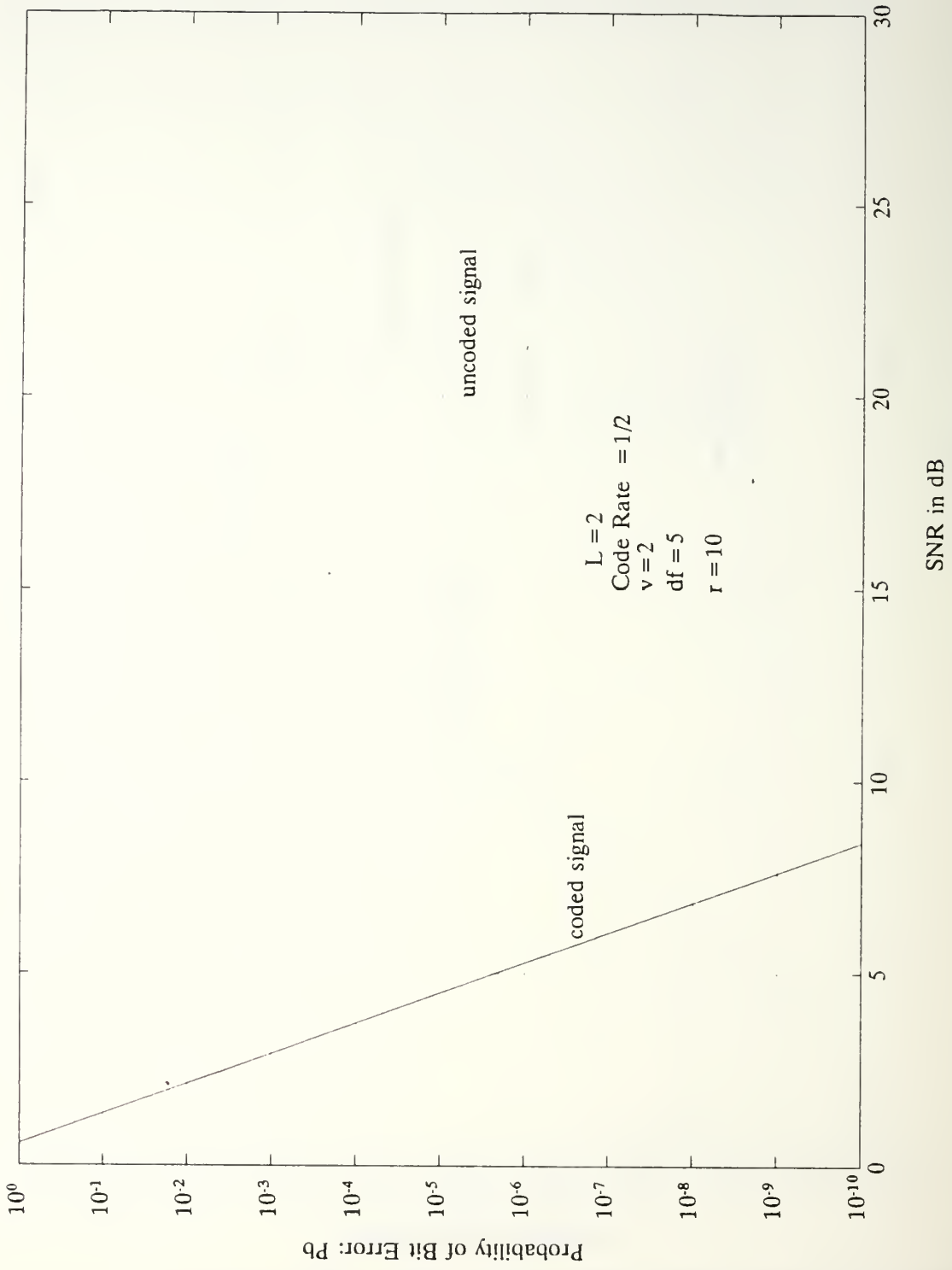


**Figure 19: Probability of bit error conditioned on the Doppler effect coefficient in a Ricean fading channel ($r = 10$) and maximum Doppler effect, i.e., minimal Doppler effect coefficient for a rate 1/2, $\nu = 2$ convolutional code and system diversity $L = 2$.**

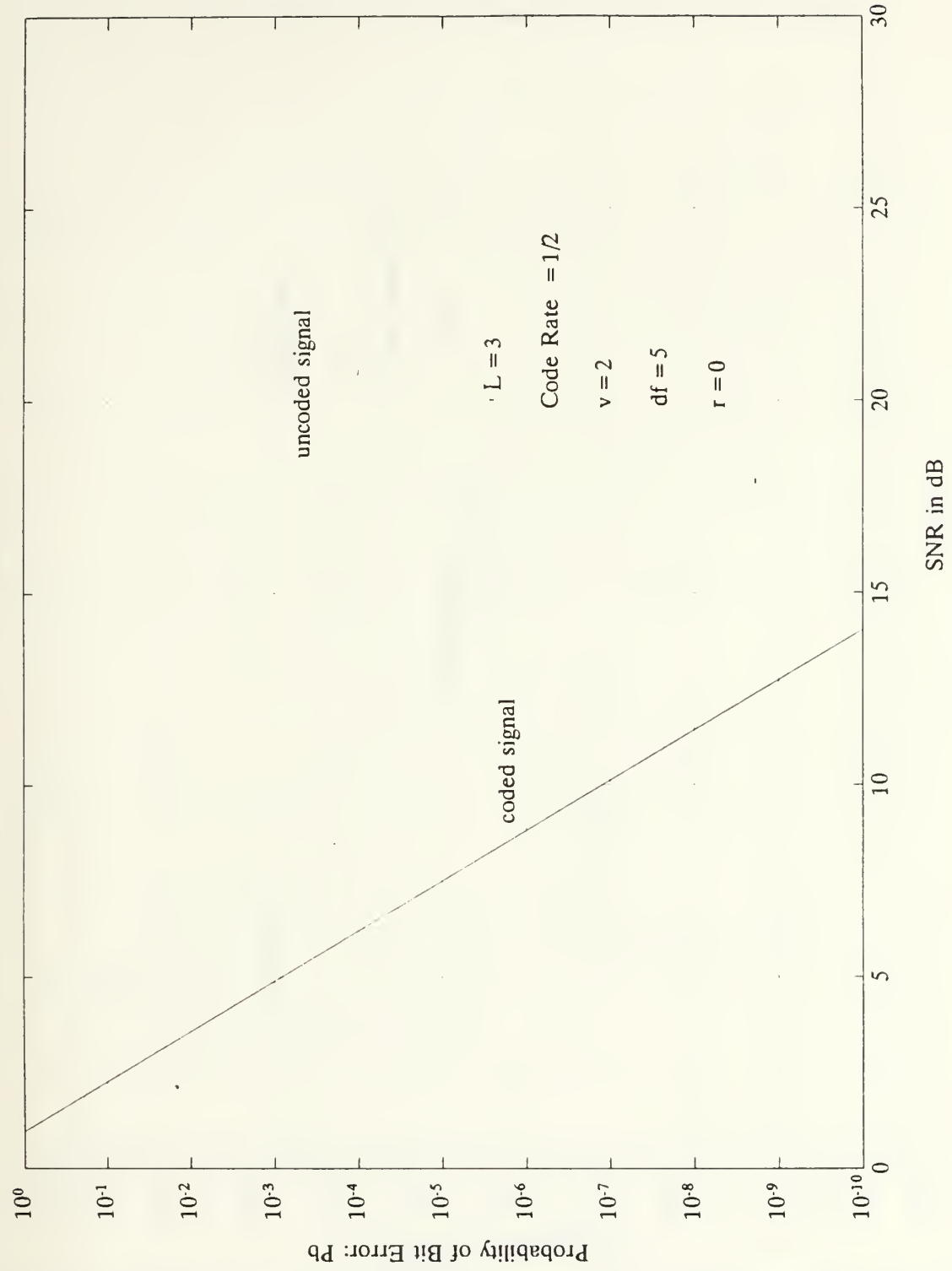


**Figure 20: Probability of bit error conditioned on the Doppler effect coefficient in a Rayleigh fading channel ($r = 0$) and maximum Doppler effect, i.e., minimal Doppler effect coefficient for a rate 1/2, $\nu = 2$ convolutional code and system diversity $L = 3$.**

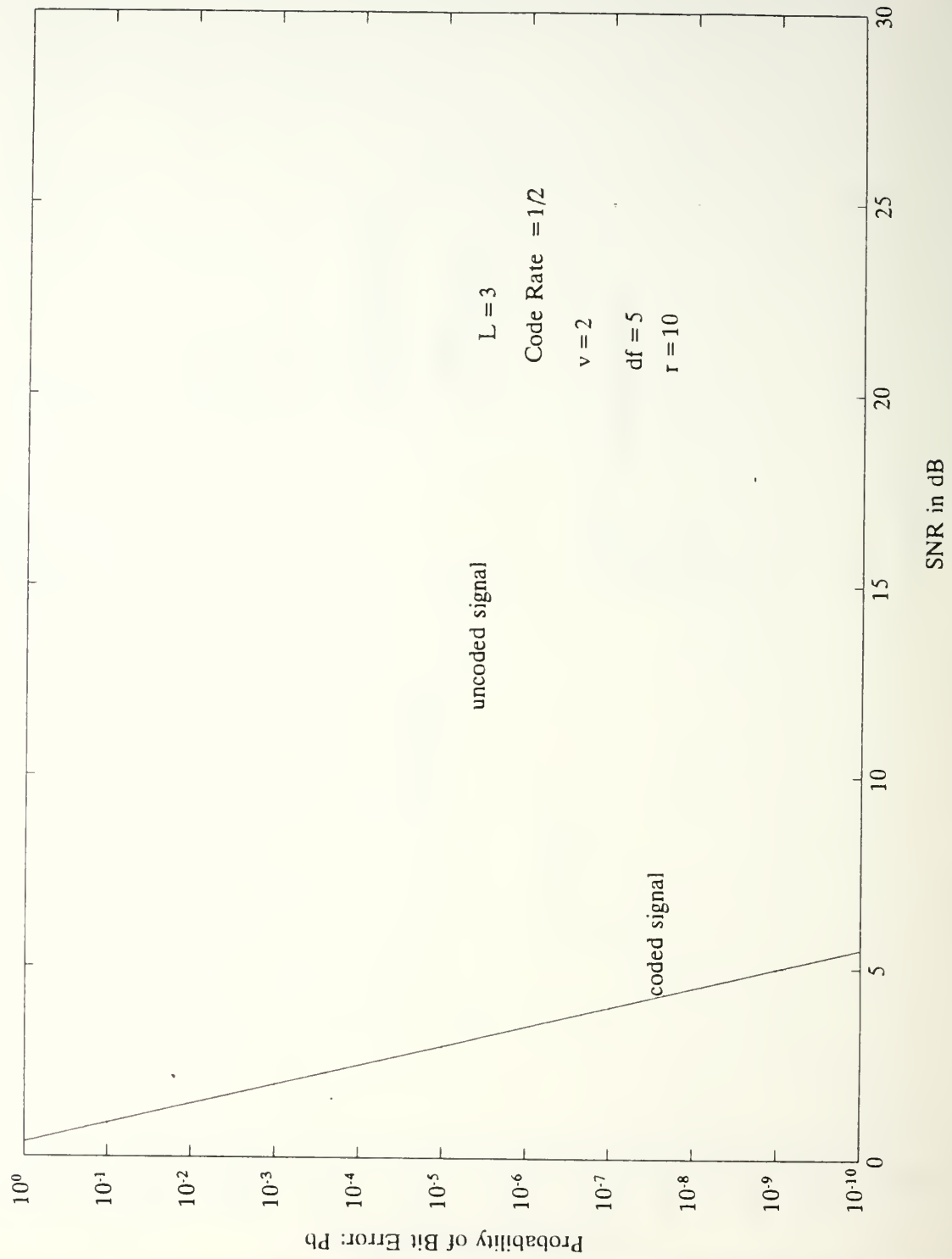


**Figure 21: Probability of bit error conditioned on the Doppler effect coefficient in a Ricean fading channel ($r = 10$) and maximum Doppler effect, i.e., minimal Doppler effect coefficient for a rate 1/2, $\nu = 2$ convolutional code and system diversity $L = 3$.**

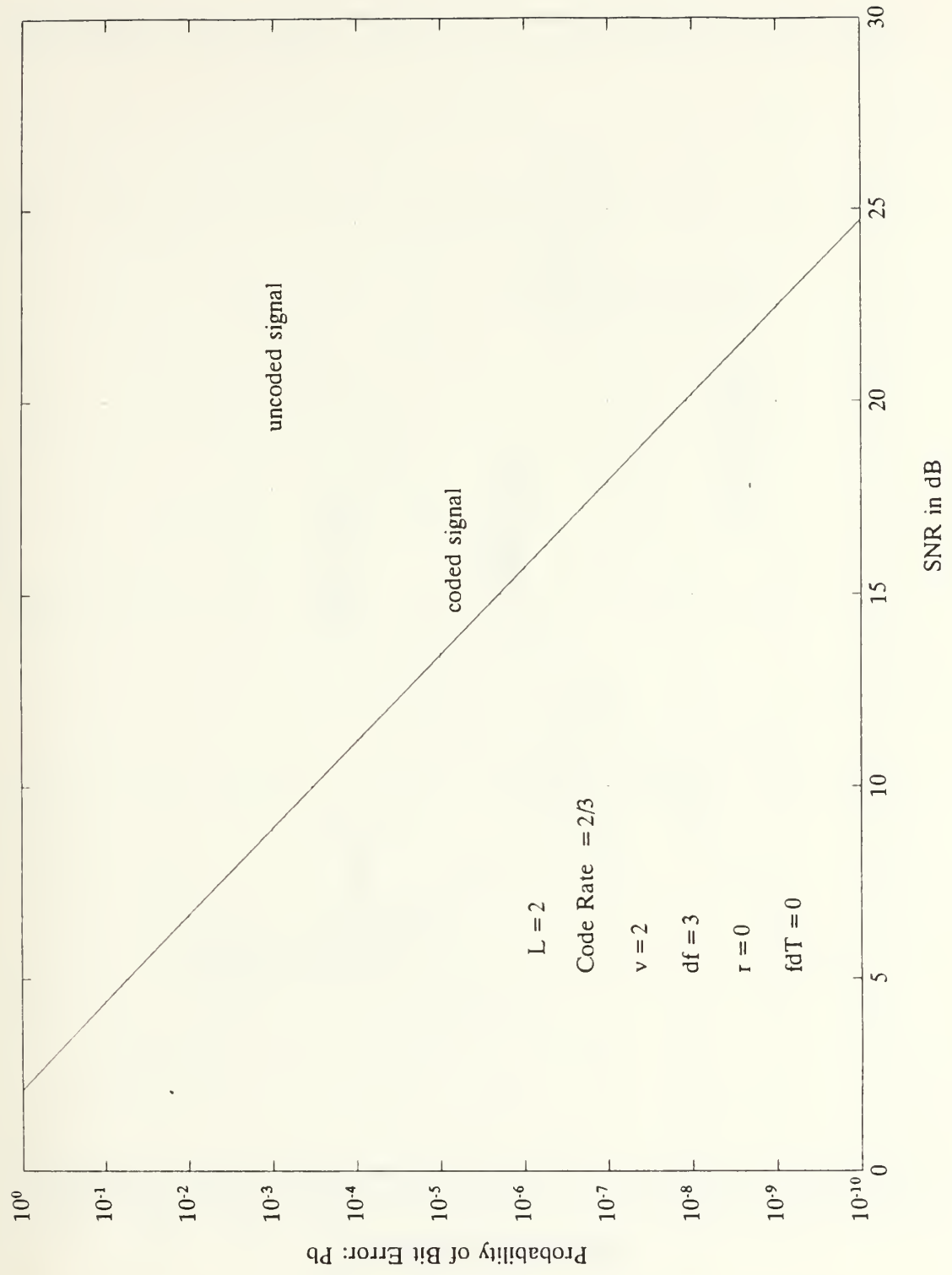


**Figure 22: Probability of bit error conditioned on the Doppler effect coefficient in a Rayleigh fading channel ($r = 0$) and no Doppler effect for a rate 2/3, $\nu = 2$ convolutional code and system diversity $L = 2$.**

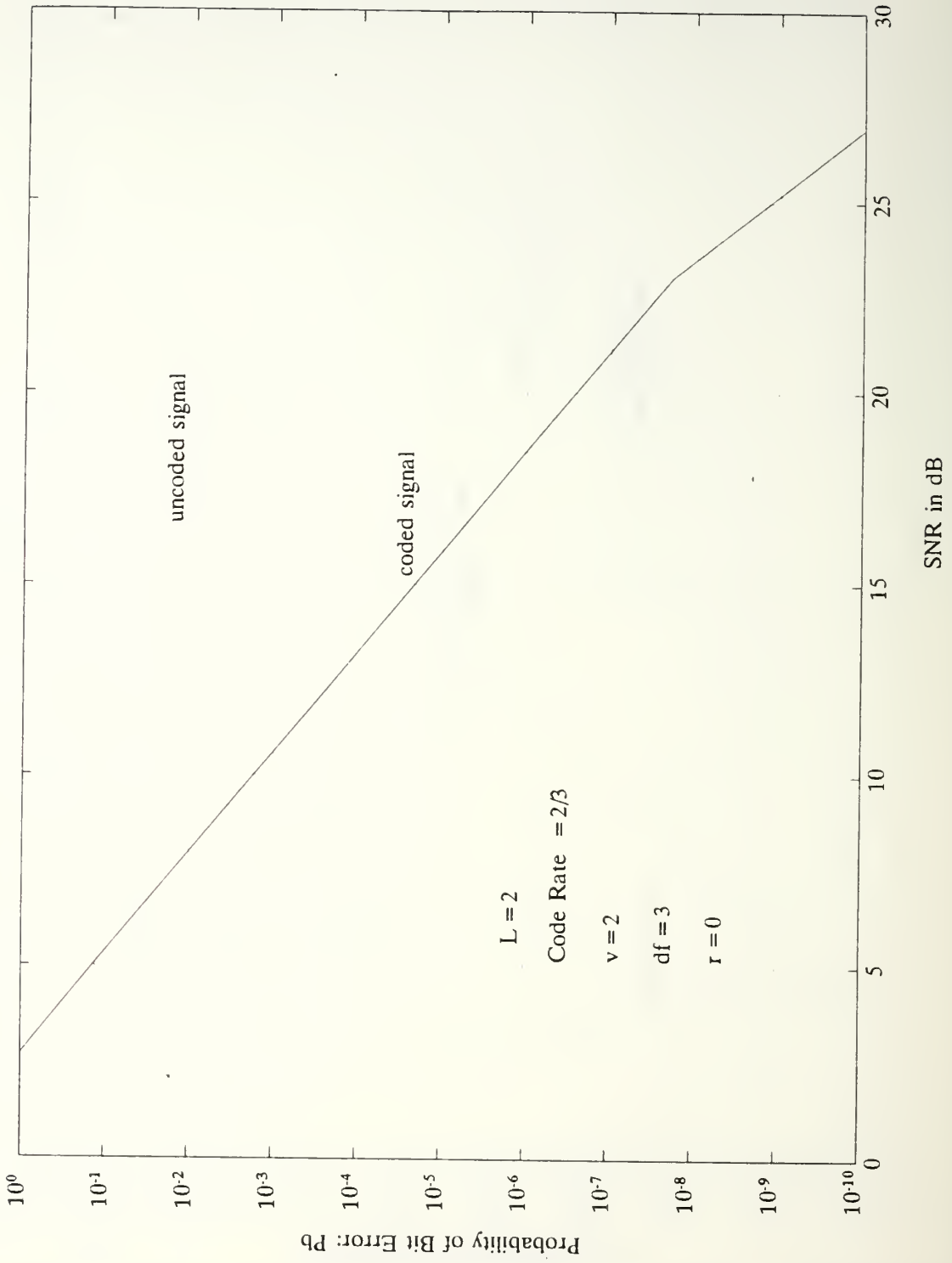


**Figure 23: Probability of bit error conditioned on the Doppler effect coefficient in a Rayleigh fading channel ($r = 0$) and maximum Doppler effect, i.e., minimal Doppler effect coefficient for a rate 2/3, $\nu = 2$ convolutional code and system diversity $L = 2$.**

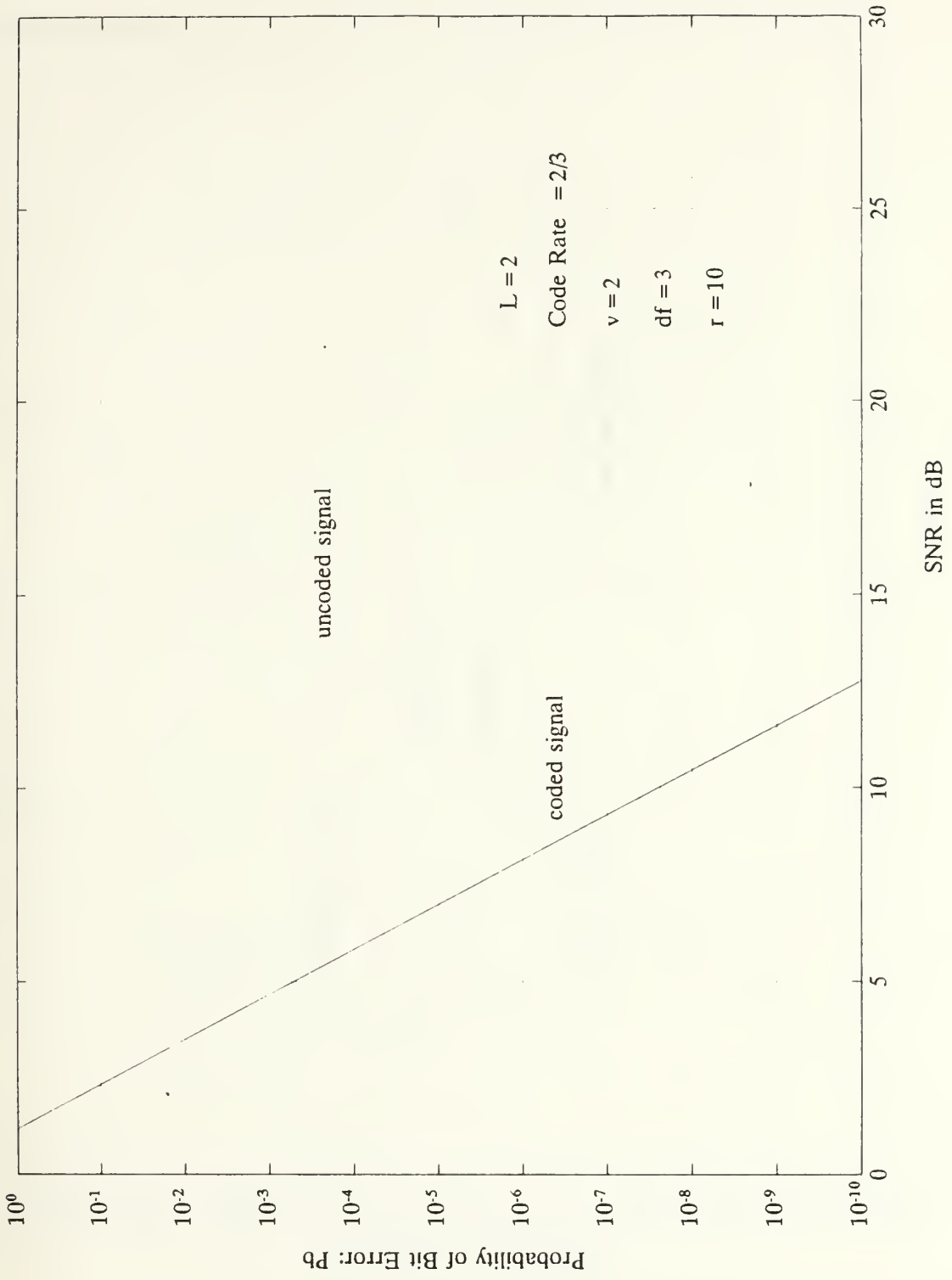


**Figure 24: Probability of bit error conditioned on the Doppler effect coefficient in a Ricean fading channel ($r = 10$) and maximum Doppler effect, i.e., minimal Doppler effect coefficient for a rate 2/3, $\nu = 2$ convolutional code and system diversity $L = 2$.**

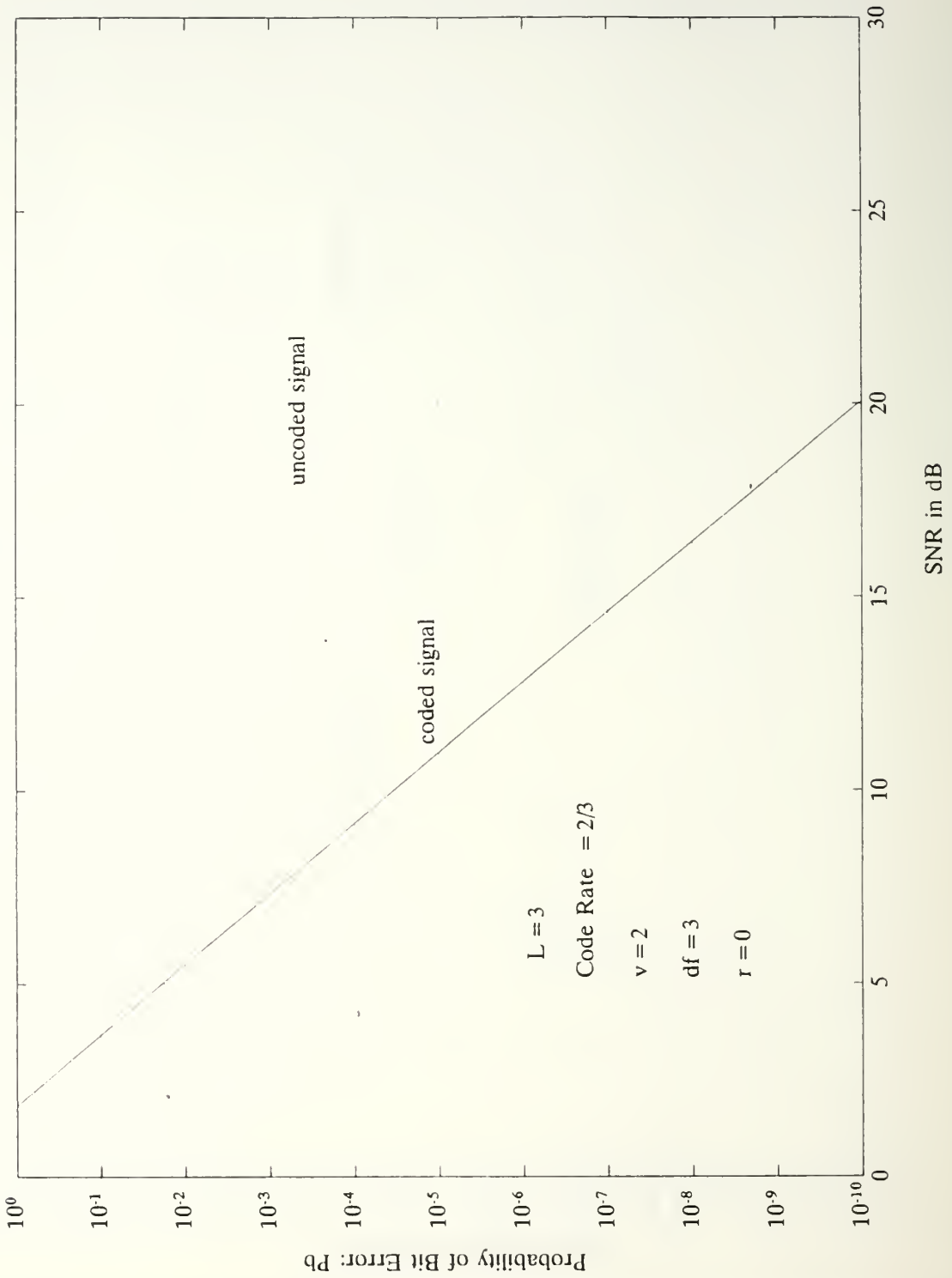


**Figure 25: Probability of bit error conditioned on the Doppler effect coefficient in a Rayleigh fading channel ($r = 0$) and maximum Doppler effect, i.e., minimal Doppler effect coefficient for a rate 2/3, $\nu = 2$ convolutional code and system diversity $L = 3$.**

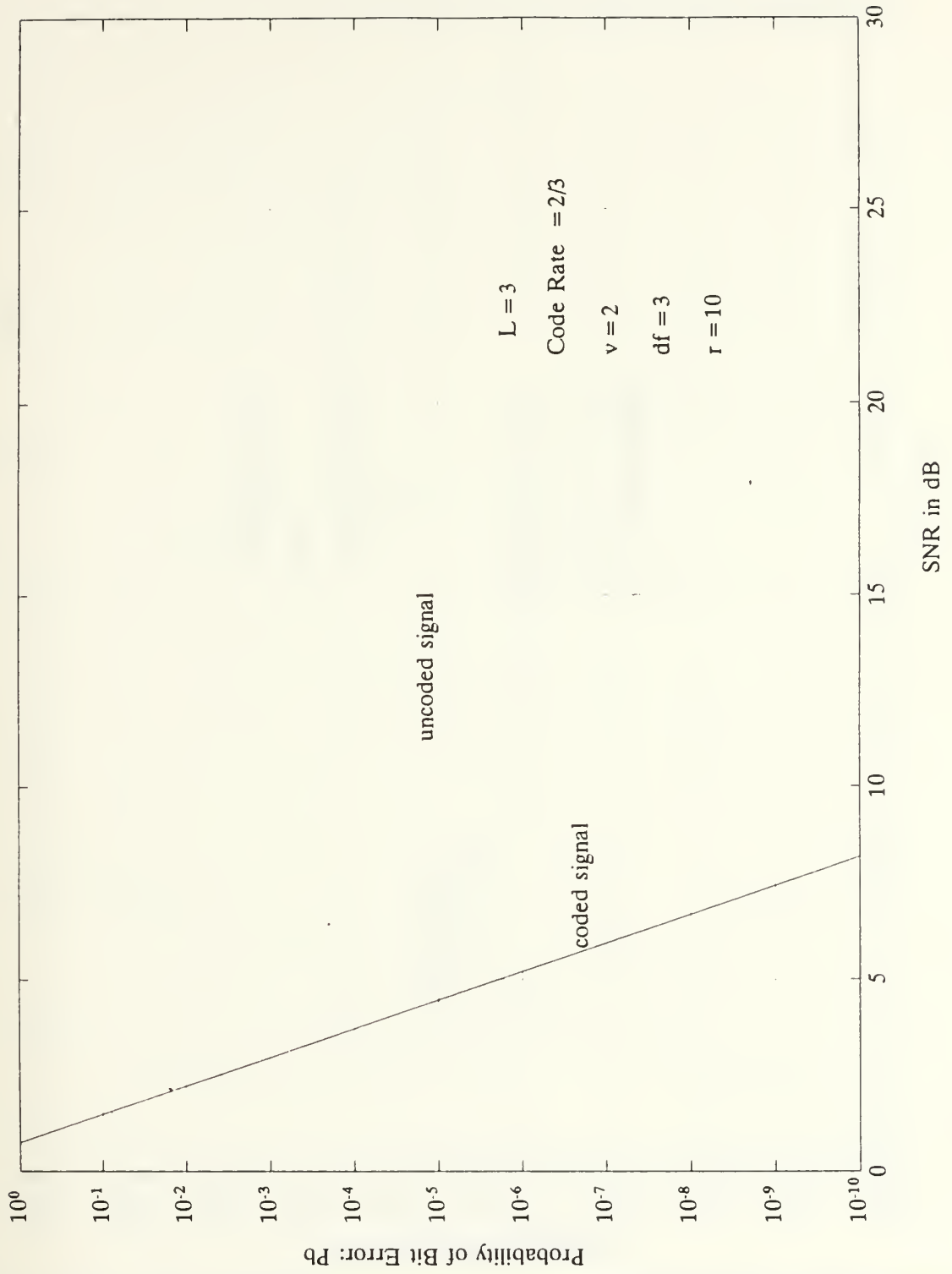


**Figure 26: Probability of bit error conditioned on the Doppler effect coefficient in a Ricean fading channel ($r = 10$) and maximum Doppler effect, i.e., minimal Doppler effect coefficient for a rate 2/3, $\nu = 2$ convolutional code and system diversity $L = 3$.**

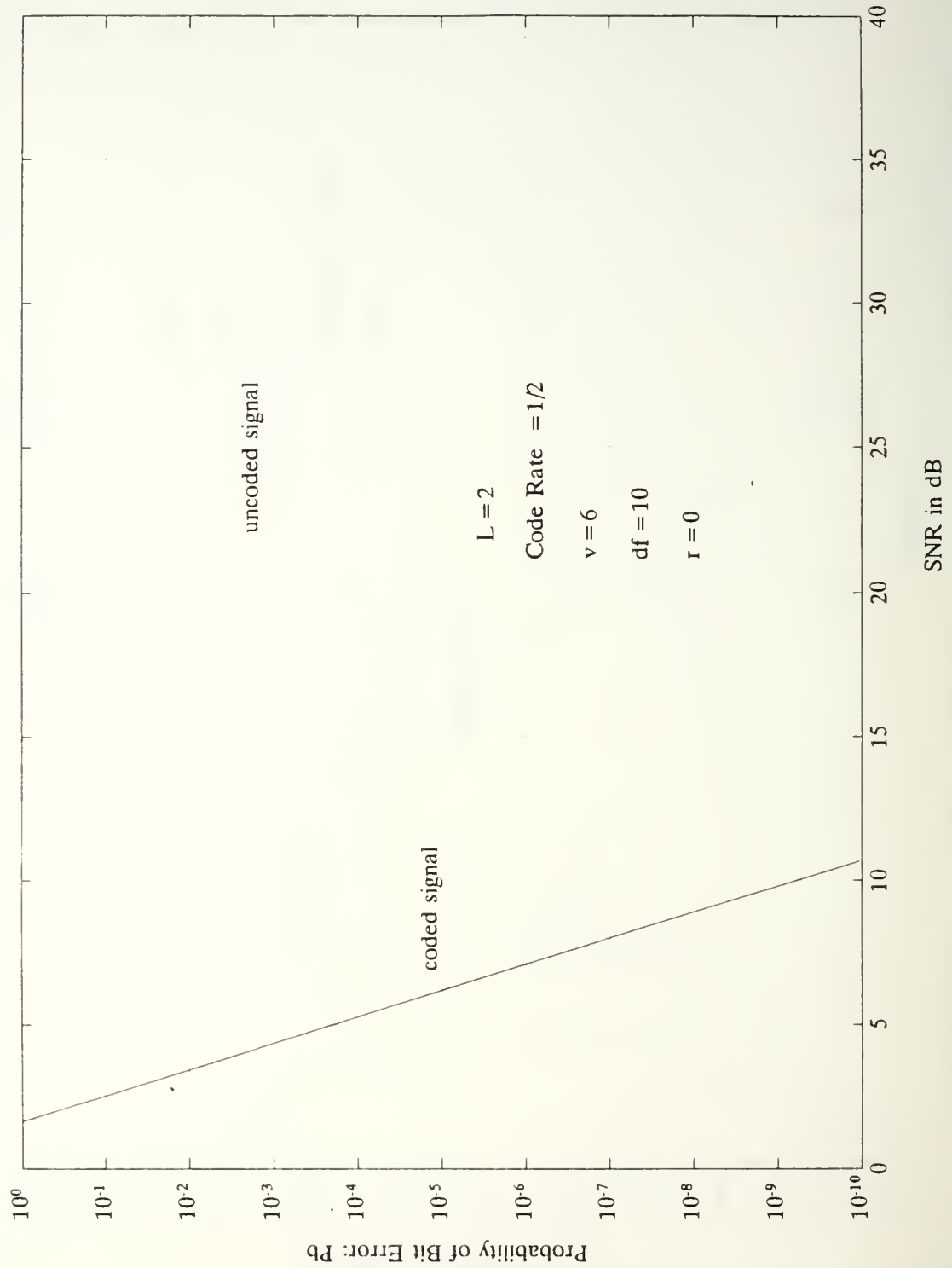


**Figure 27: Probability of bit error conditioned on the Doppler effect coefficient in a Rayleigh fading channel ($r = 0$) and maximum Doppler effect, i.e., minimal Doppler effect coefficient for a rate 1/2, $\nu = 6$ convolutional code and system diversity $L = 2$.**

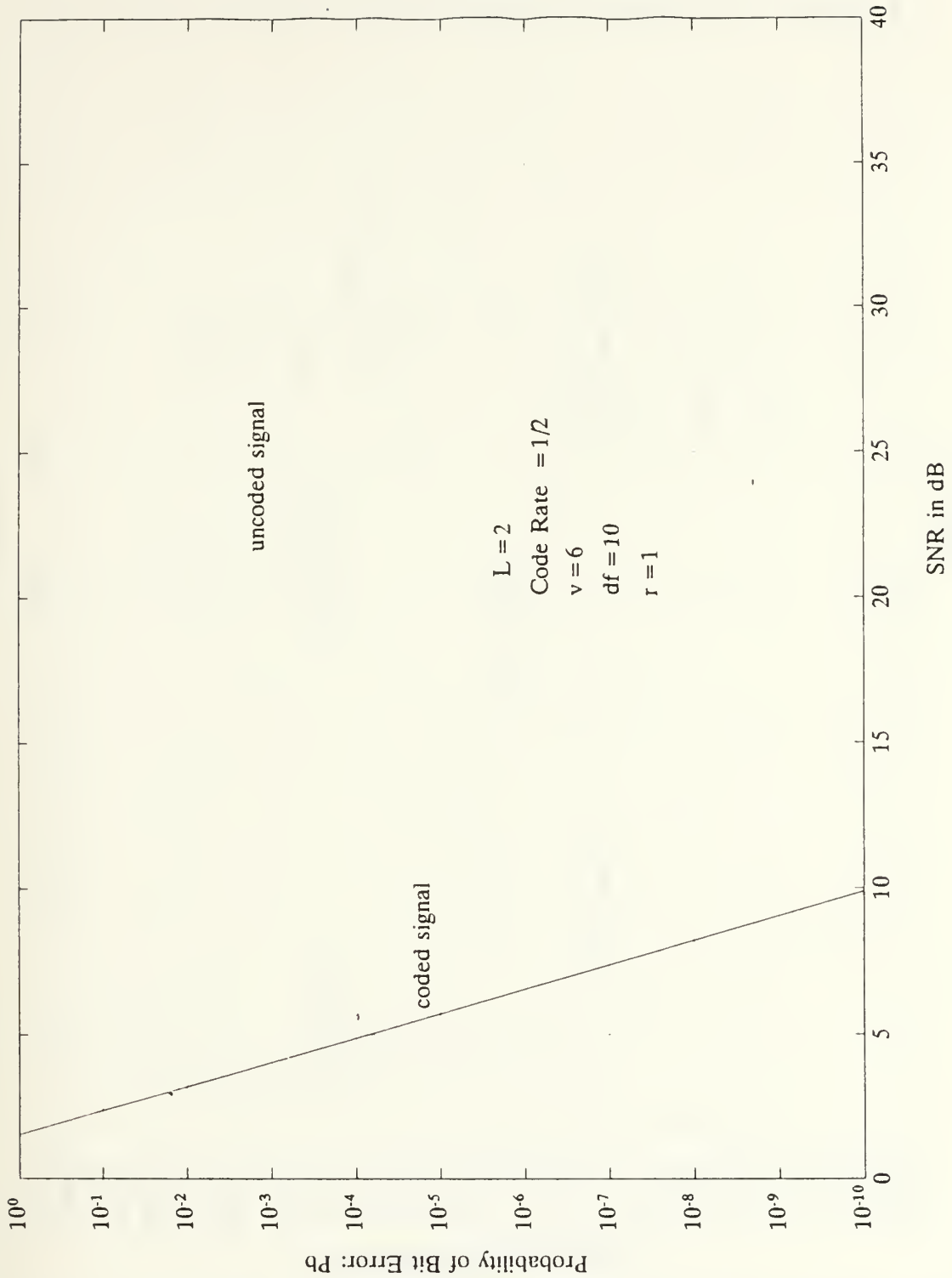


**Figure 28: Probability of bit error conditioned on the Doppler effect coefficient in a Ricean fading channel ($r = 1$) and maximum Doppler effect, i.e., minimal Doppler effect coefficient for a rate 1/2, $\nu = 6$ convolutional code and system diversity $L = 2$.**

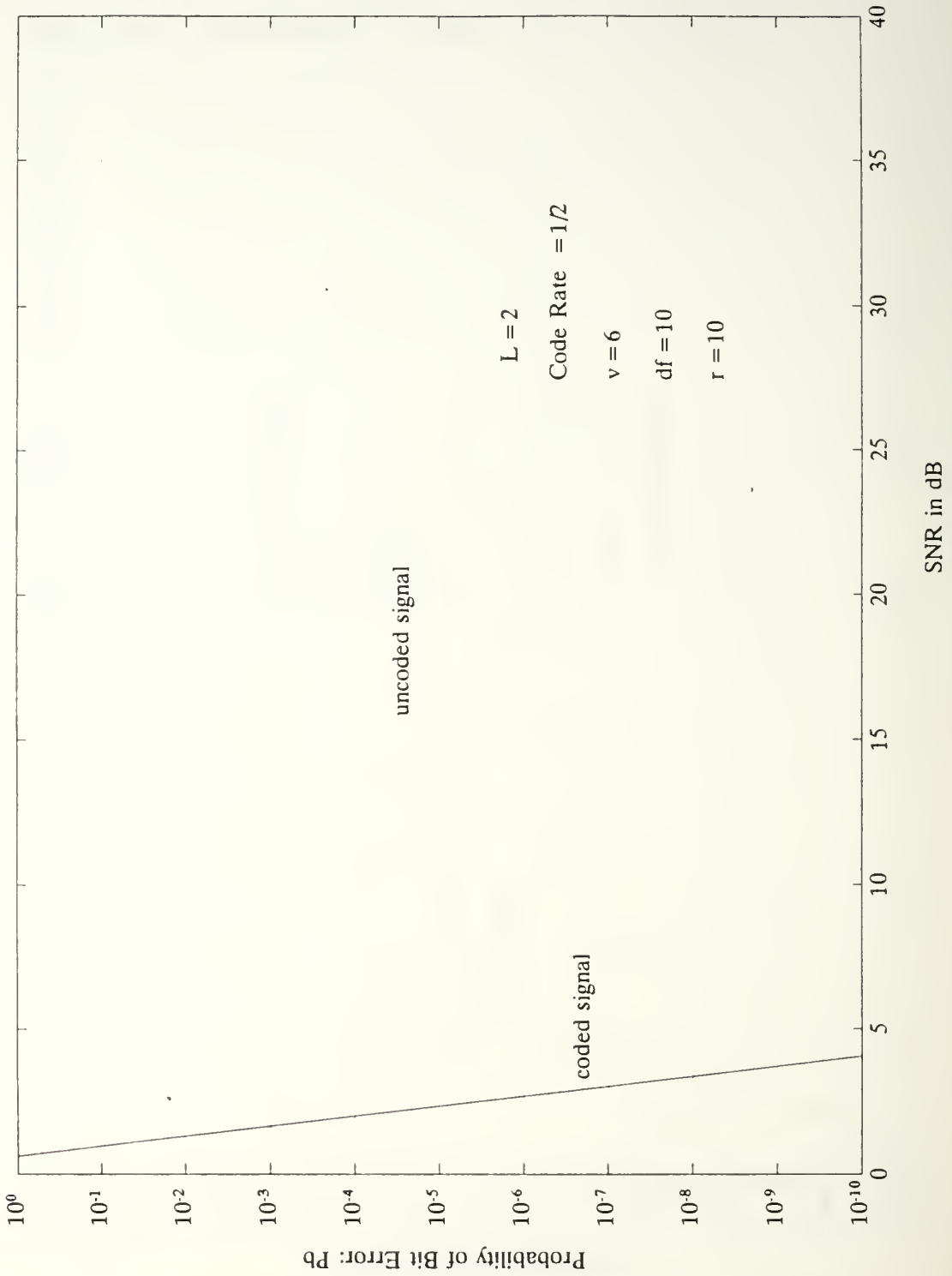


**Figure 29: Probability of bit error conditioned on the Doppler effect coefficient in a Ricean fading channel ($r = 10$) and maximum Doppler effect, i.e., minimal Doppler effect coefficient for a rate 1/2, $\nu = 6$ convolutional code and system diversity $L = 2$.**

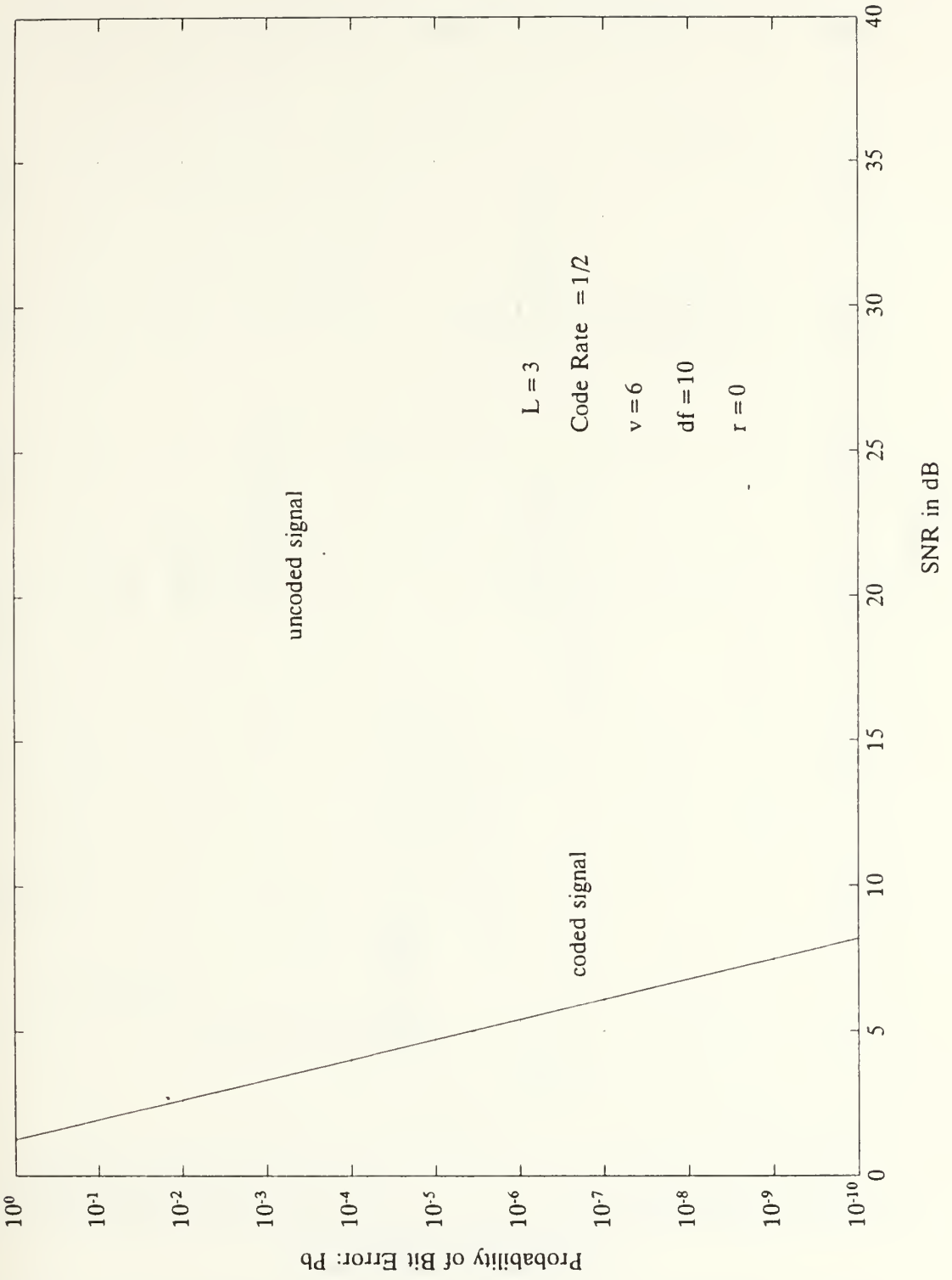


**Figure 30: Probability of bit error conditioned on the Doppler effect coefficient in a Rayleigh fading channel ($r = 0$) and maximum Doppler effect, i.e., minimal Doppler effect coefficient for a rate $1/2$, $\nu = 6$ convolutional code and system diversity $L = 3$.**

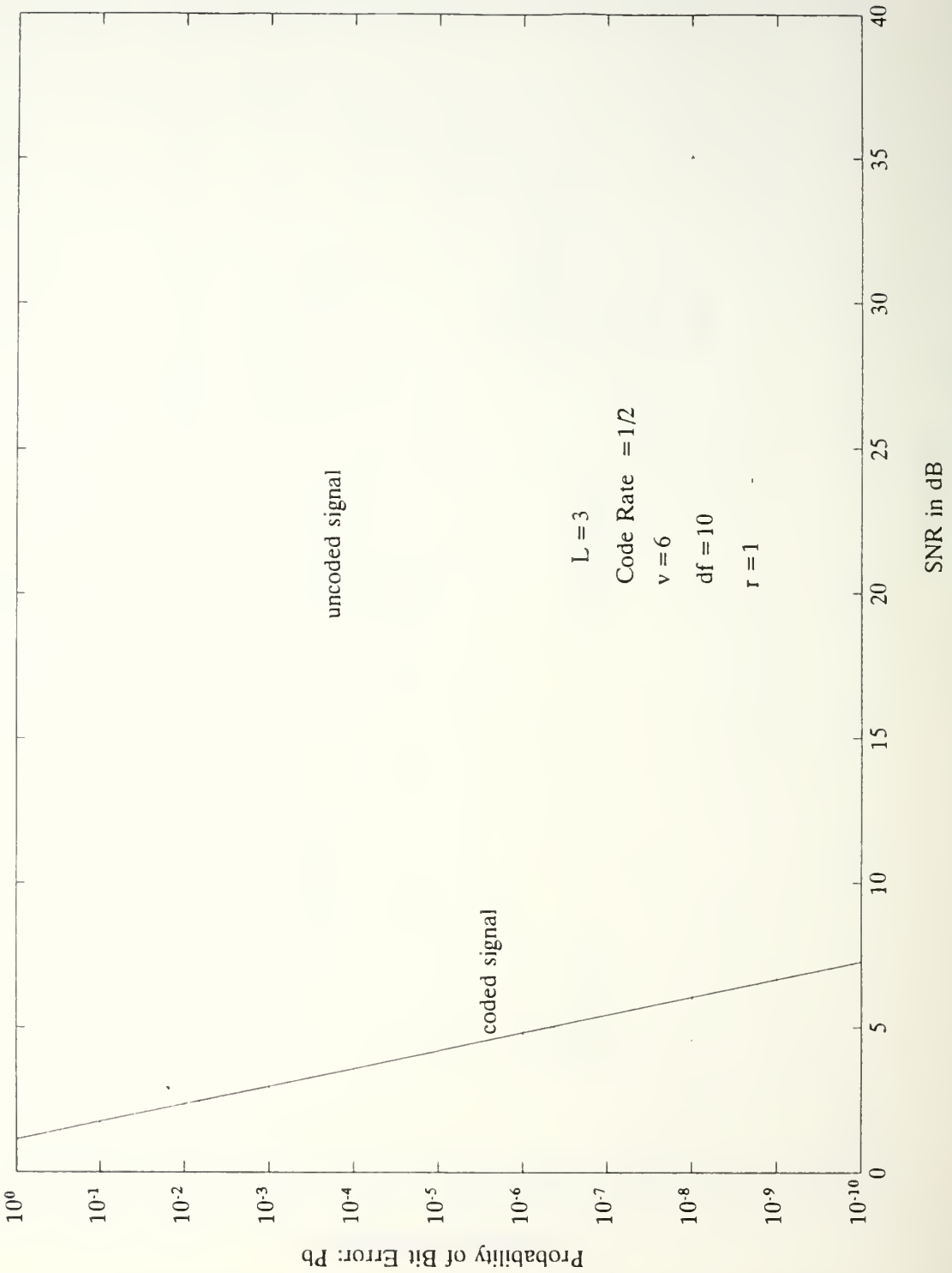


**Figure 31: Probability of bit error conditioned on the Doppler effect coefficient in a Ricean fading channel ($r = 1$) and maximum Doppler effect, i.e., minimal Doppler effect coefficient for a rate 1/2, $\nu = 6$ convolutional code and system diversity $L = 3$.**

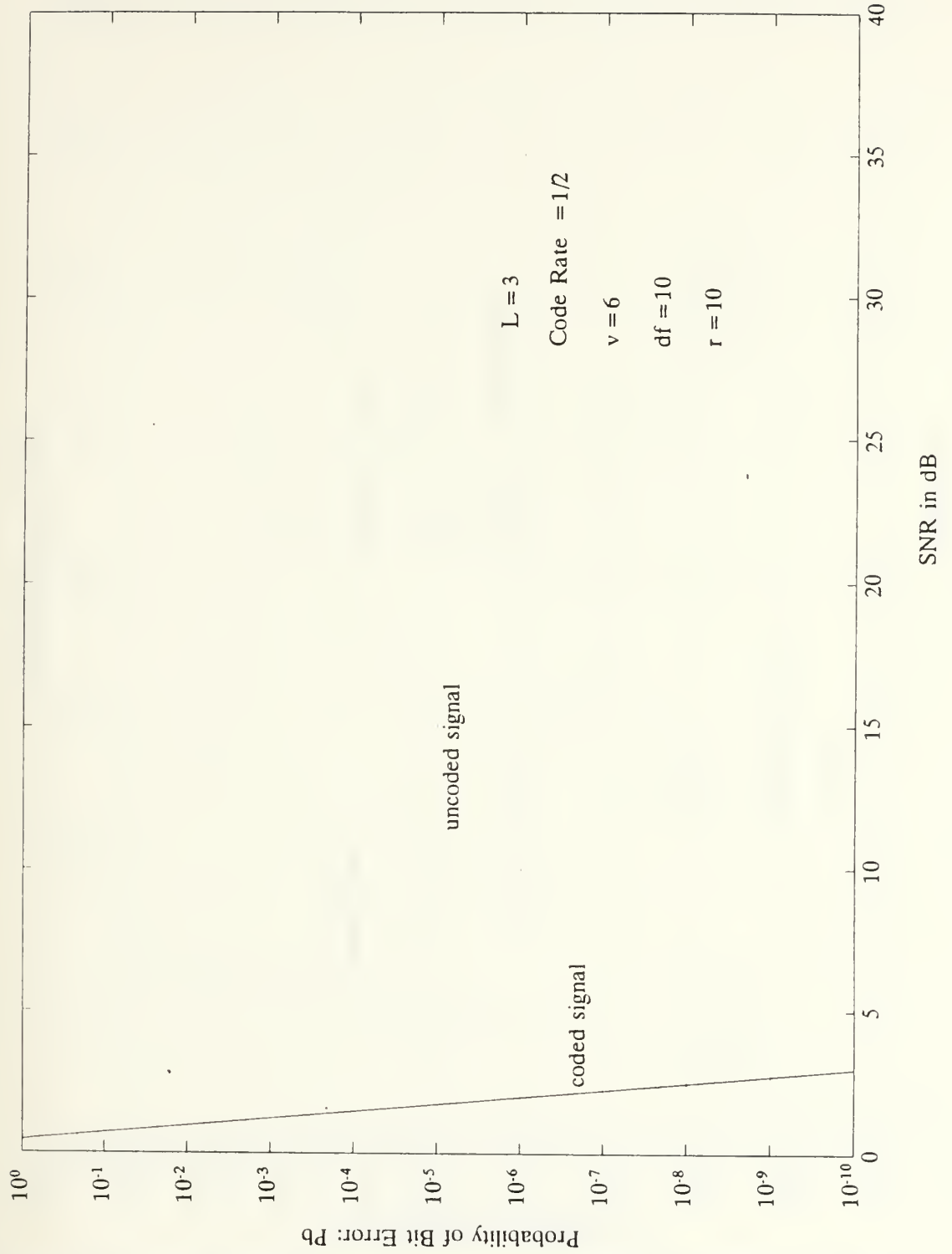


**Figure 32: Probability of bit error conditioned on the Doppler effect coefficient in a Ricean fading channel ($r = 10$) and maximum Doppler effect, i.e., minimal Doppler effect coefficient for a rate 1/2, $\nu = 6$ convolutional code and system diversity $L = 3$.**

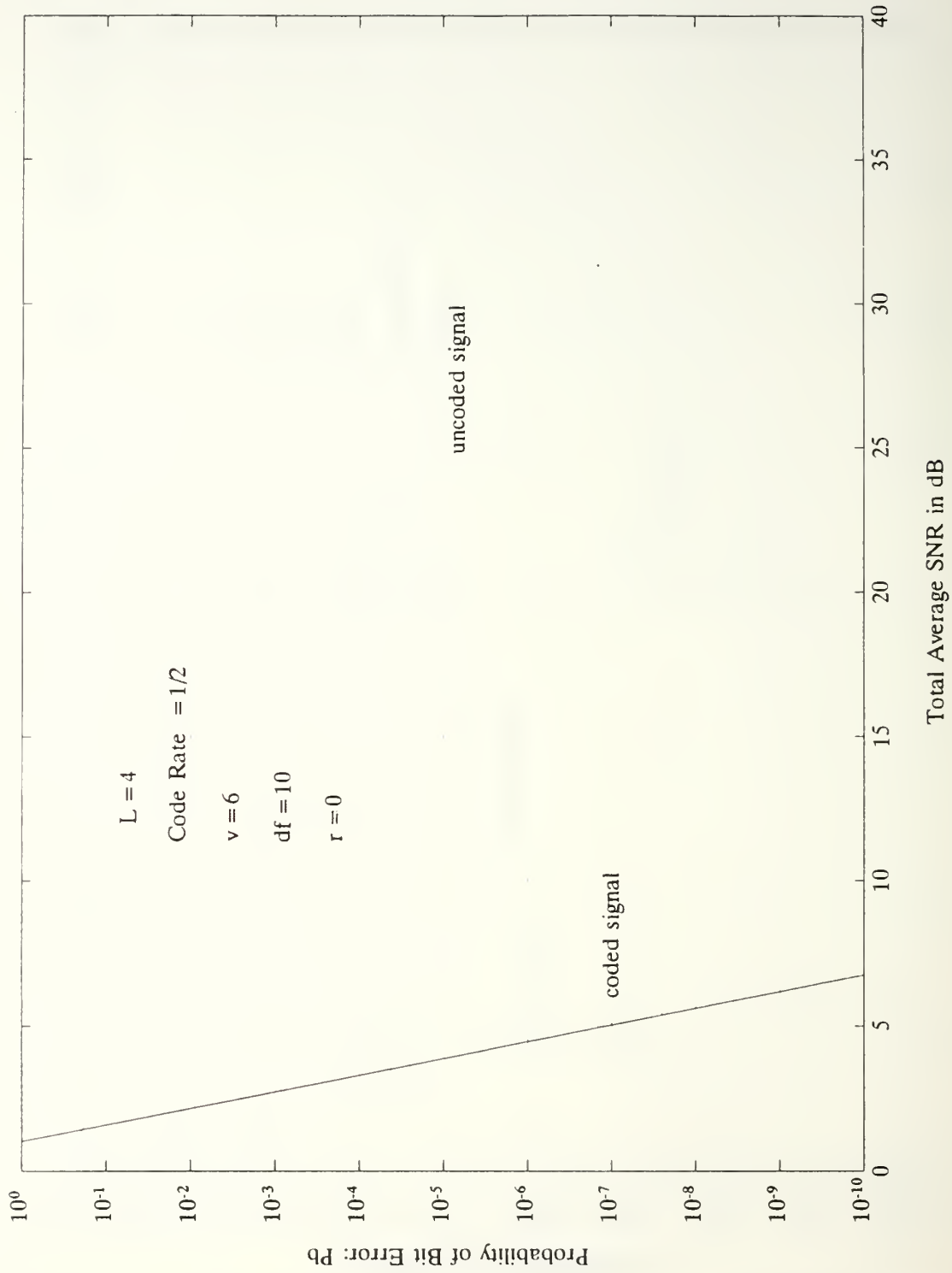


**Figure 33: Probability of bit error conditioned on the Doppler effect coefficient in a Rayleigh fading channel ($r = 0$) and maximum Doppler effect, i.e., minimal Doppler effect coefficient for a rate 1/2, $\nu = 6$ convolutional code and system diversity $L = 4$.**

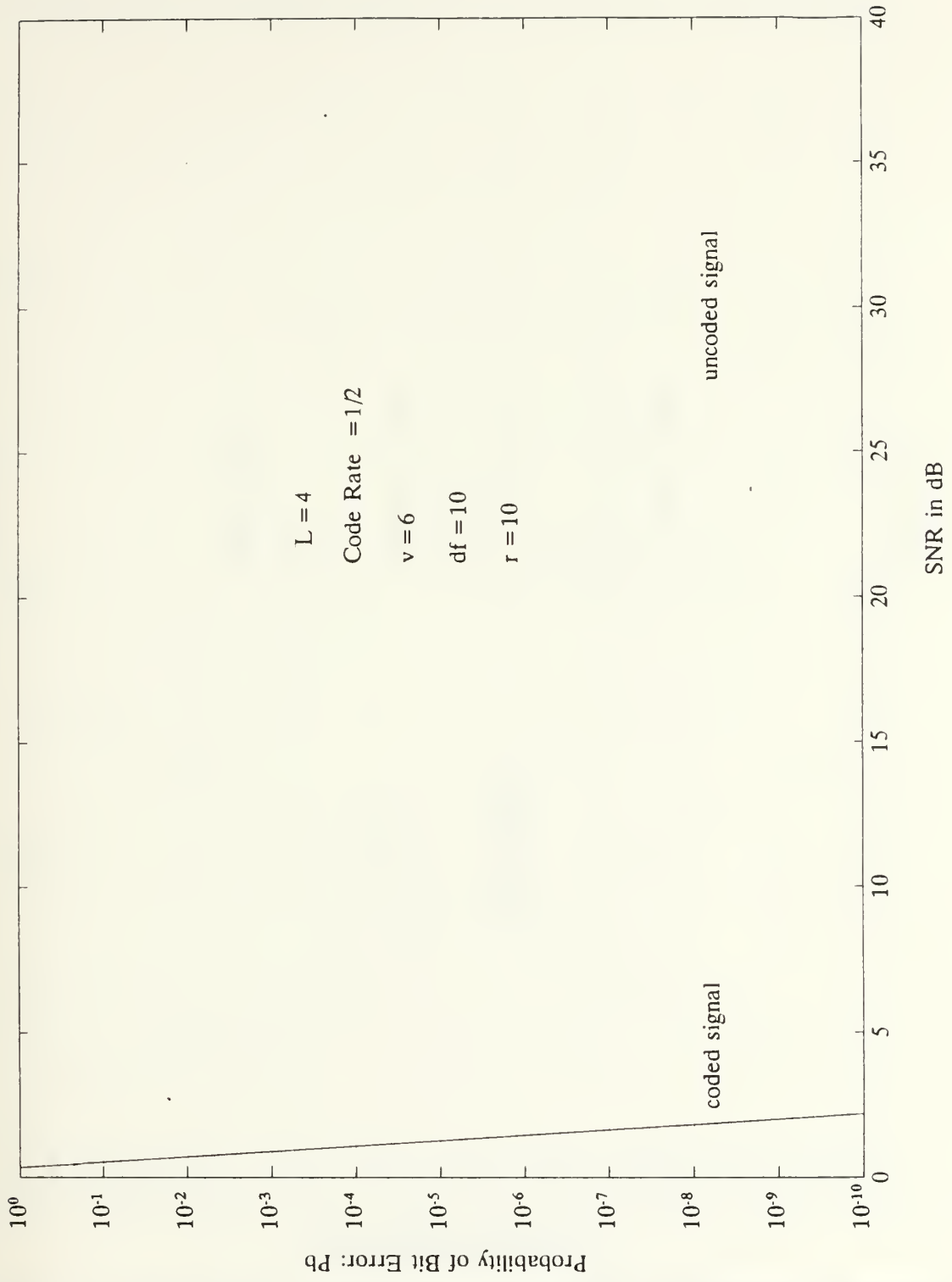


**Figure 34: Probability of bit error conditioned on the Doppler effect coefficient in a Ricean fading channel ($r = 10$) and maximum Doppler effect, i.e., minimal Doppler effect coefficient for a rate 1/2, $\nu = 6$ convolutional code and system diversity $L = 4$.**

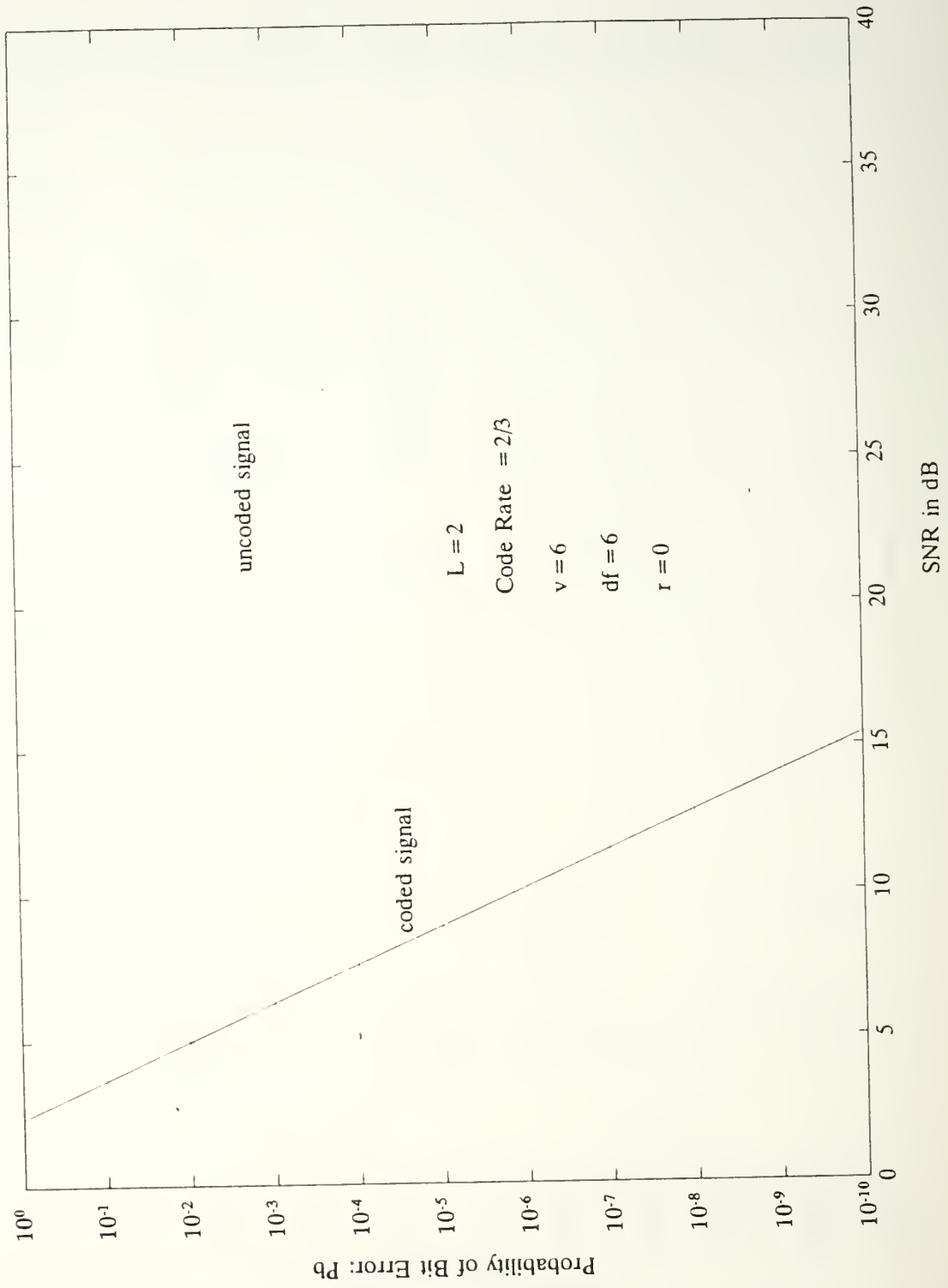


**Figure 35: Probability of bit error conditioned on the Doppler effect coefficient in a Rayleigh fading channel ($r = 0$) and maximum Doppler effect, i.e., minimal Doppler effect coefficient for a rate 2/3, $\nu = 6$ convolutional code and system diversity $L = 2$.**

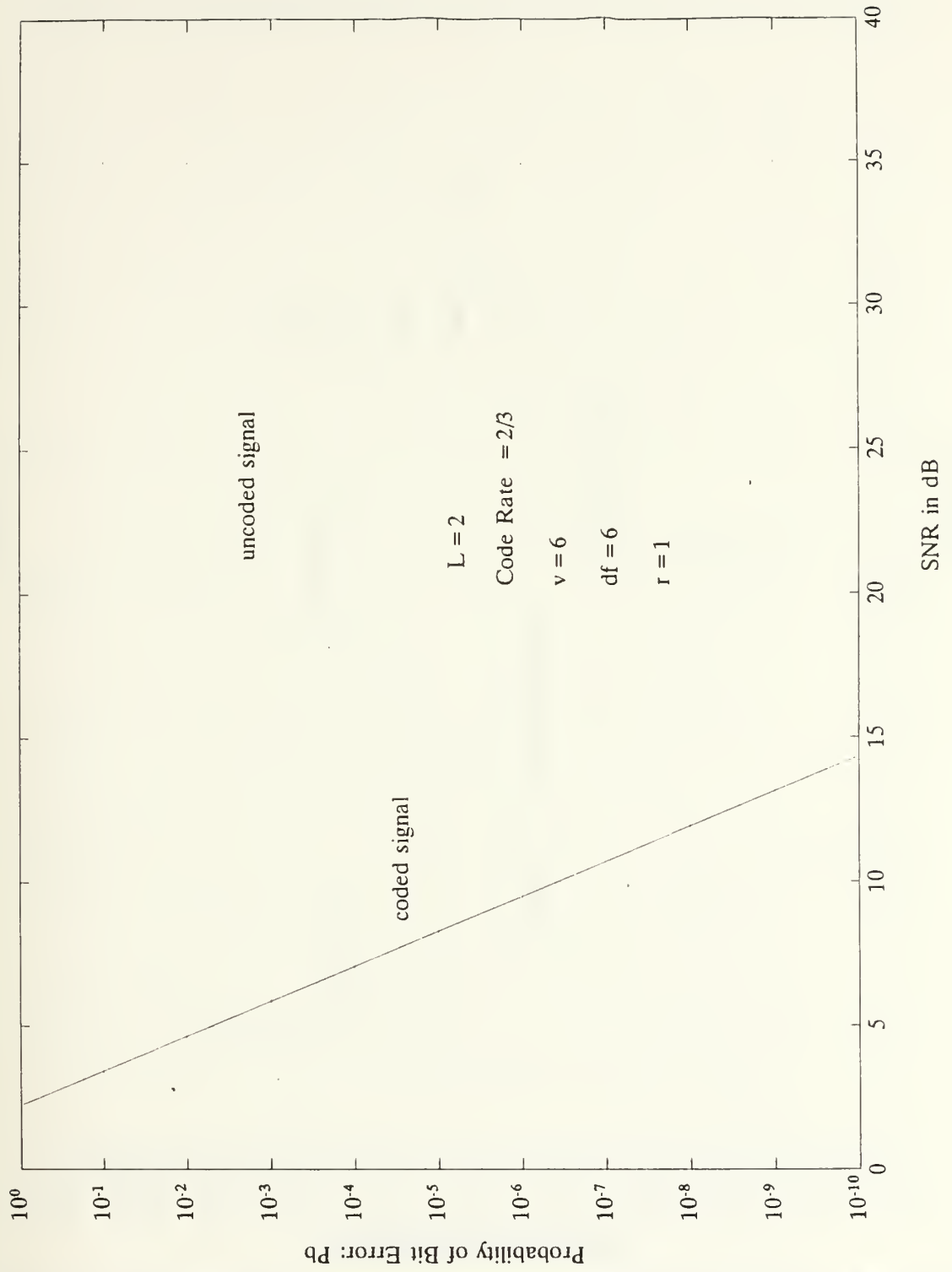


**Figure 36: Probability of bit error conditioned on the Doppler effect coefficient in a Ricean fading channel ($r = 1$) and maximum Doppler effect, i.e., minimal Doppler effect coefficient for a rate 2/3, $\nu = 6$ convolutional code and system diversity $L = 2$.**

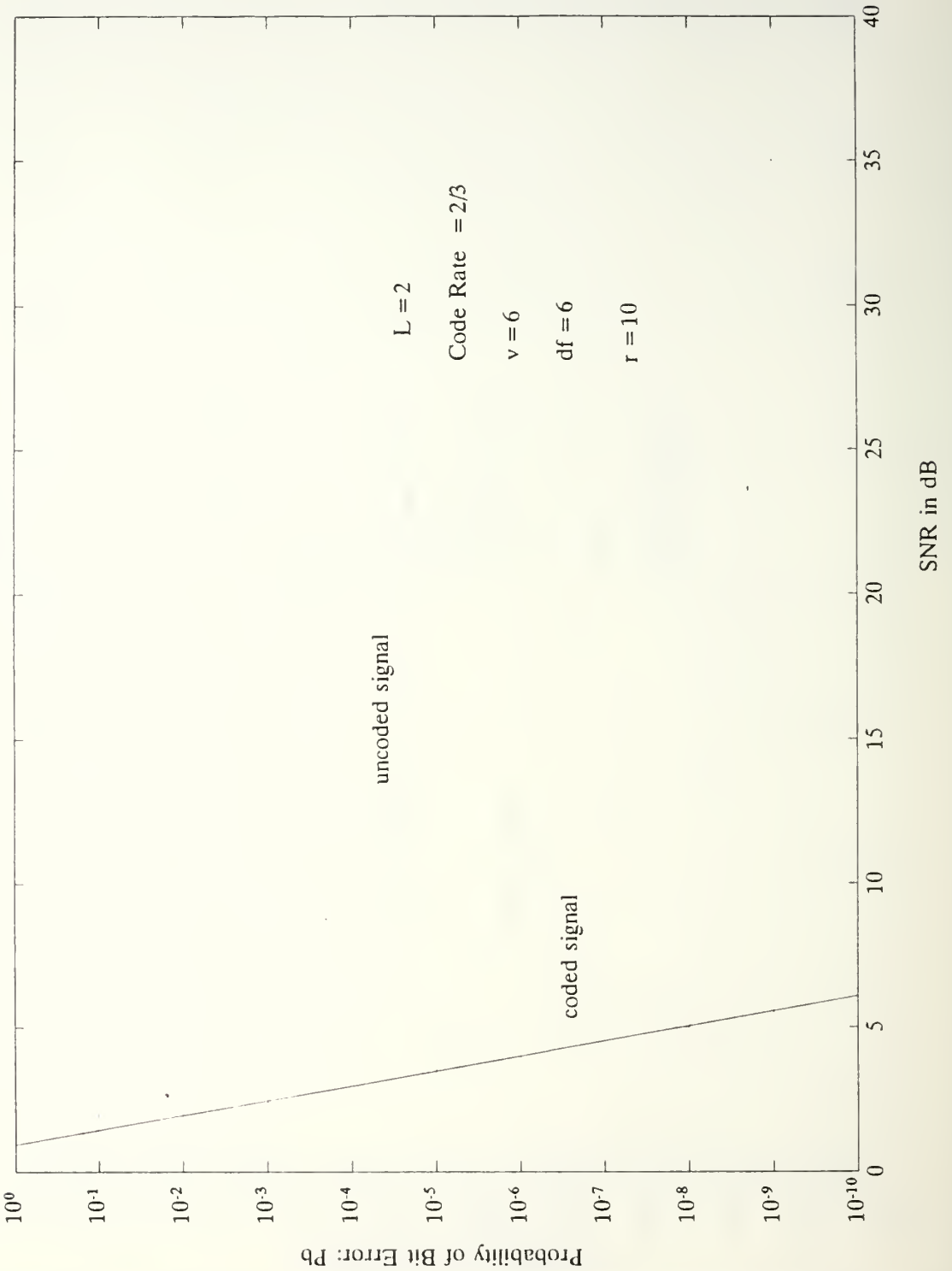


**Figure 37: Probability of bit error conditioned on the Doppler effect coefficient in a Ricean fading channel ($r = 10$) and maximum Doppler effect, i.e., minimal Doppler effect coefficient for a rate 2/3, $\nu = 6$ convolutional code and system diversity $L = 2$.**

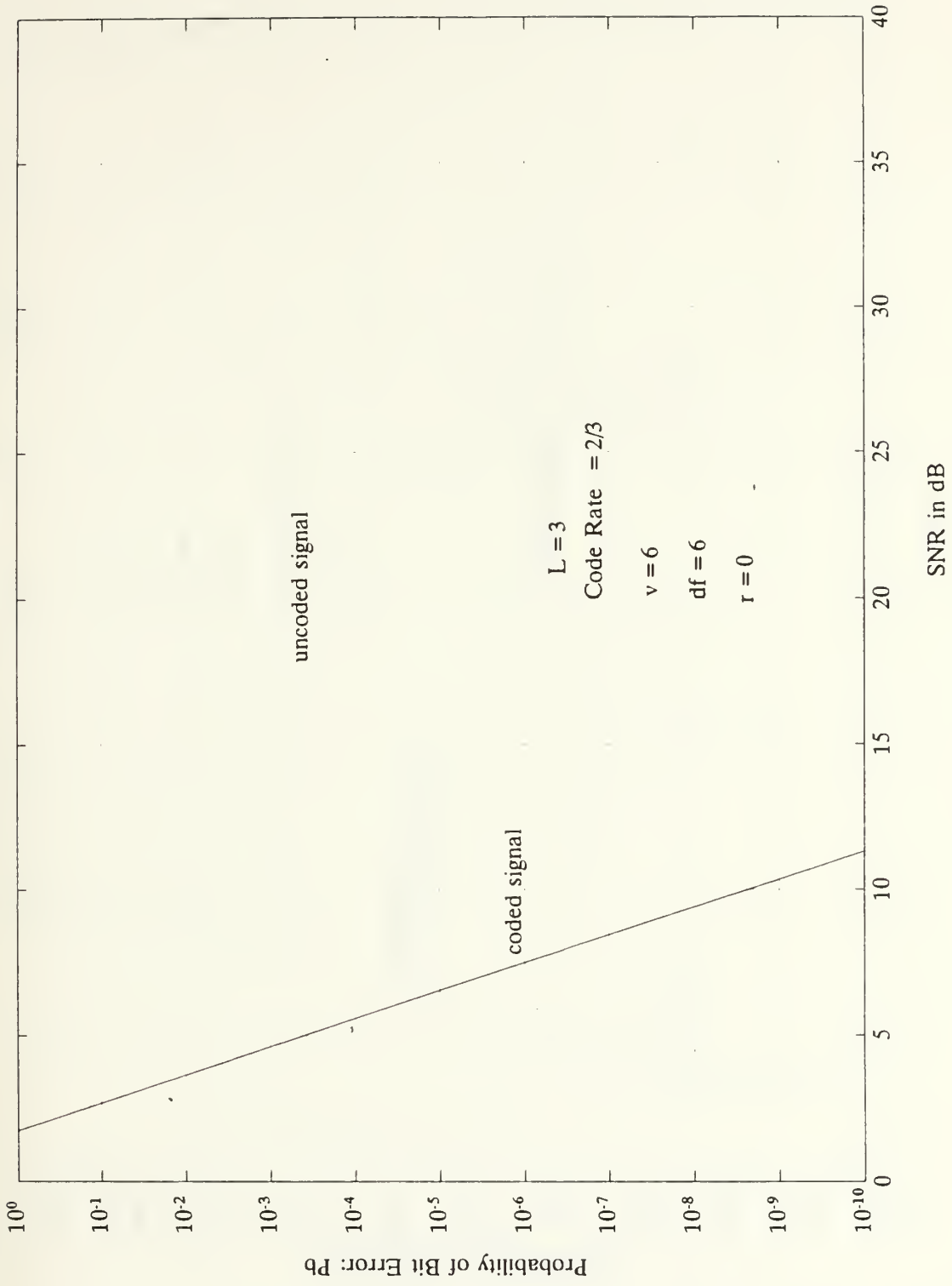


**Figure 38: Probability of bit error conditioned on the Doppler effect coefficient in a Rayleigh fading channel ($r = 0$) and maximum Doppler effect, i.e., minimal Doppler effect coefficient for a rate 2/3, $\nu = 6$ convolutional code and system diversity $L = 3$.**

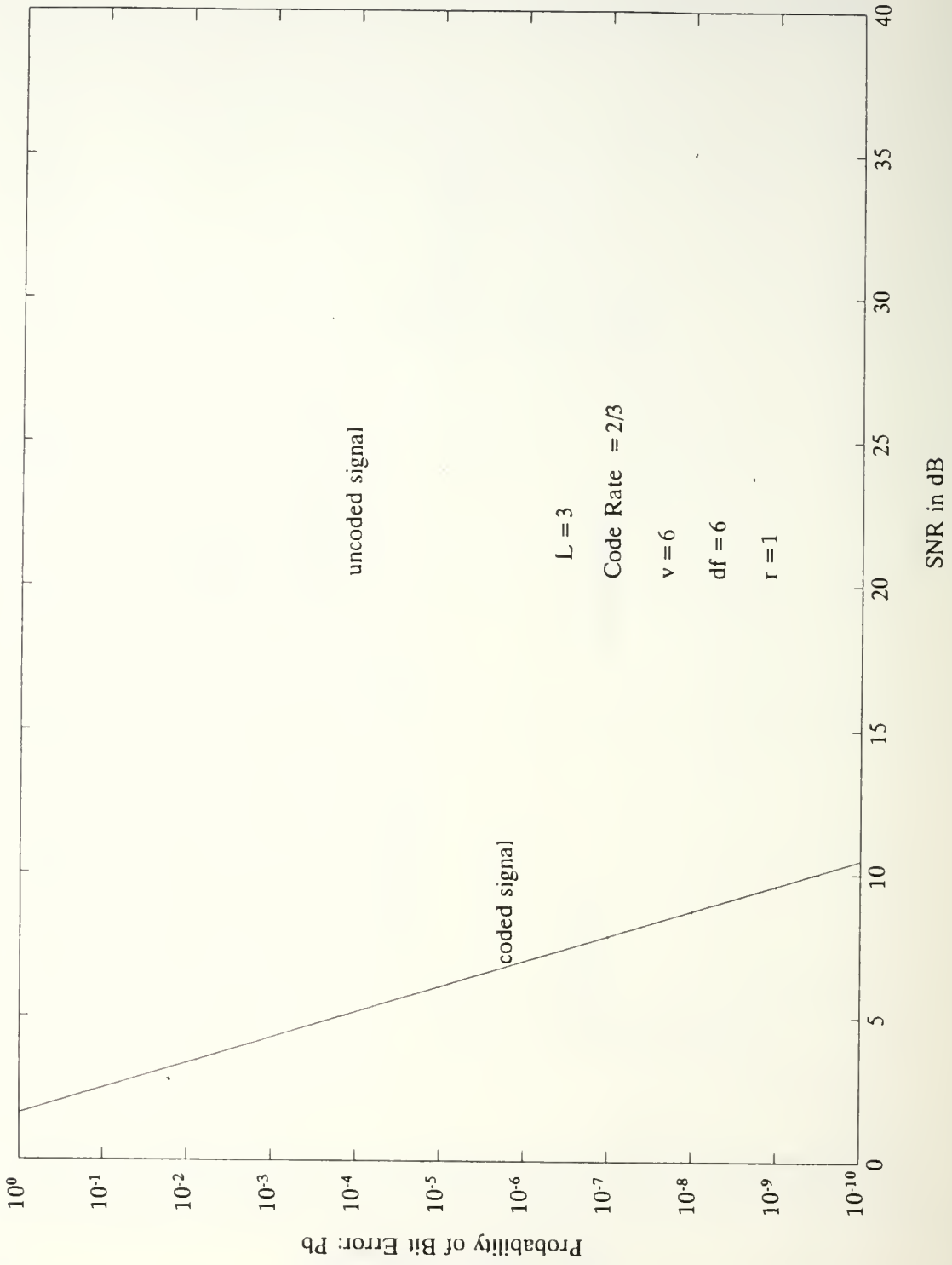


**Figure 39: Probability of bit error conditioned on the Doppler effect coefficient in a Ricean fading channel ($r = 1$) and maximum Doppler effect, i.e., minimal Doppler effect coefficient for a rate 2/3, $\nu = 6$ convolutional code and system diversity $L = 3$.**

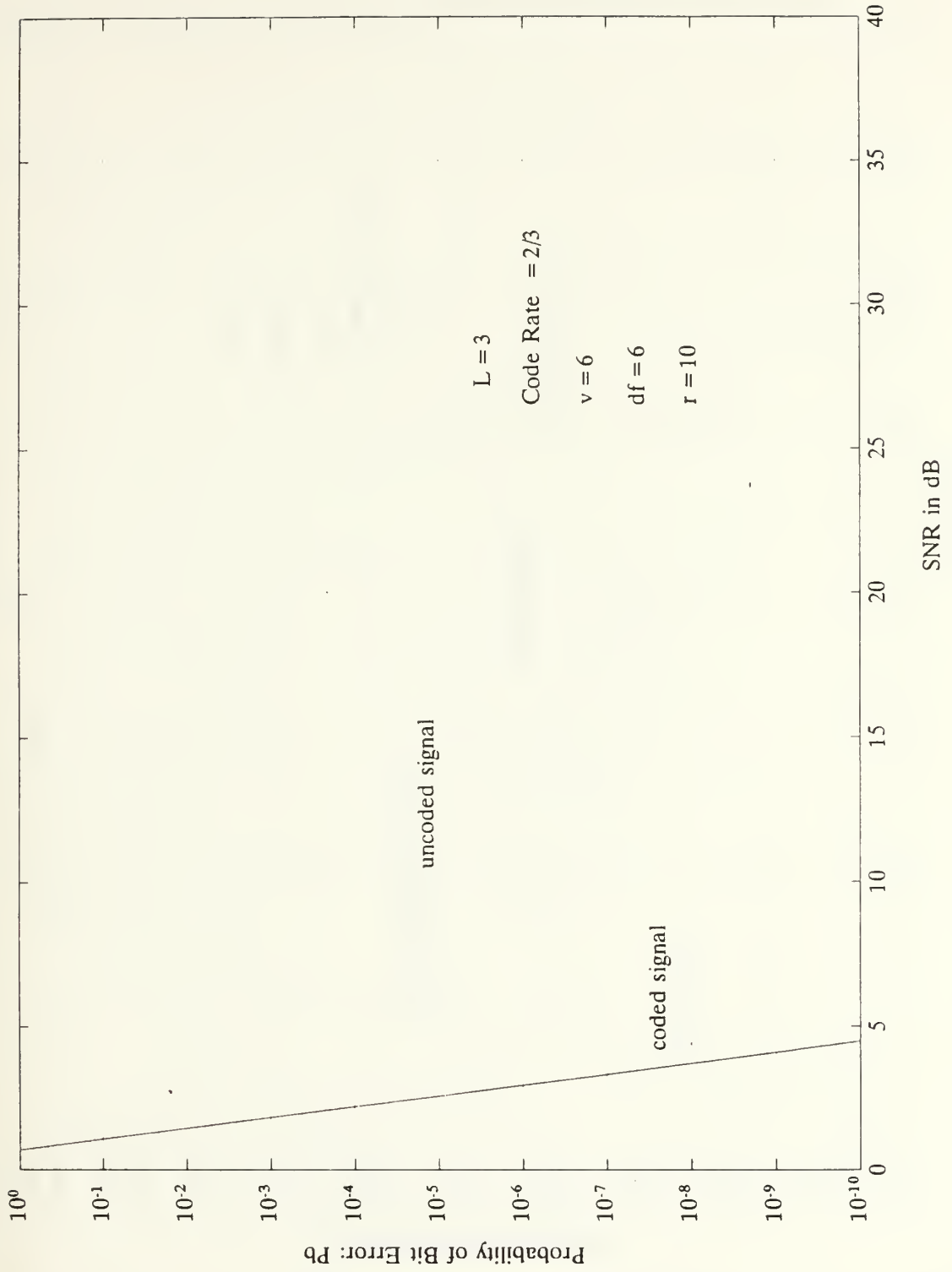


**Figure 40: Probability of bit error conditioned on the Doppler effect coefficient in a Ricean fading channel ($r = 10$) and maximum Doppler effect, i.e., minimal Doppler effect coefficient for a rate 2/3, $\nu = 6$ convolutional code and system diversity $L = 3$.**

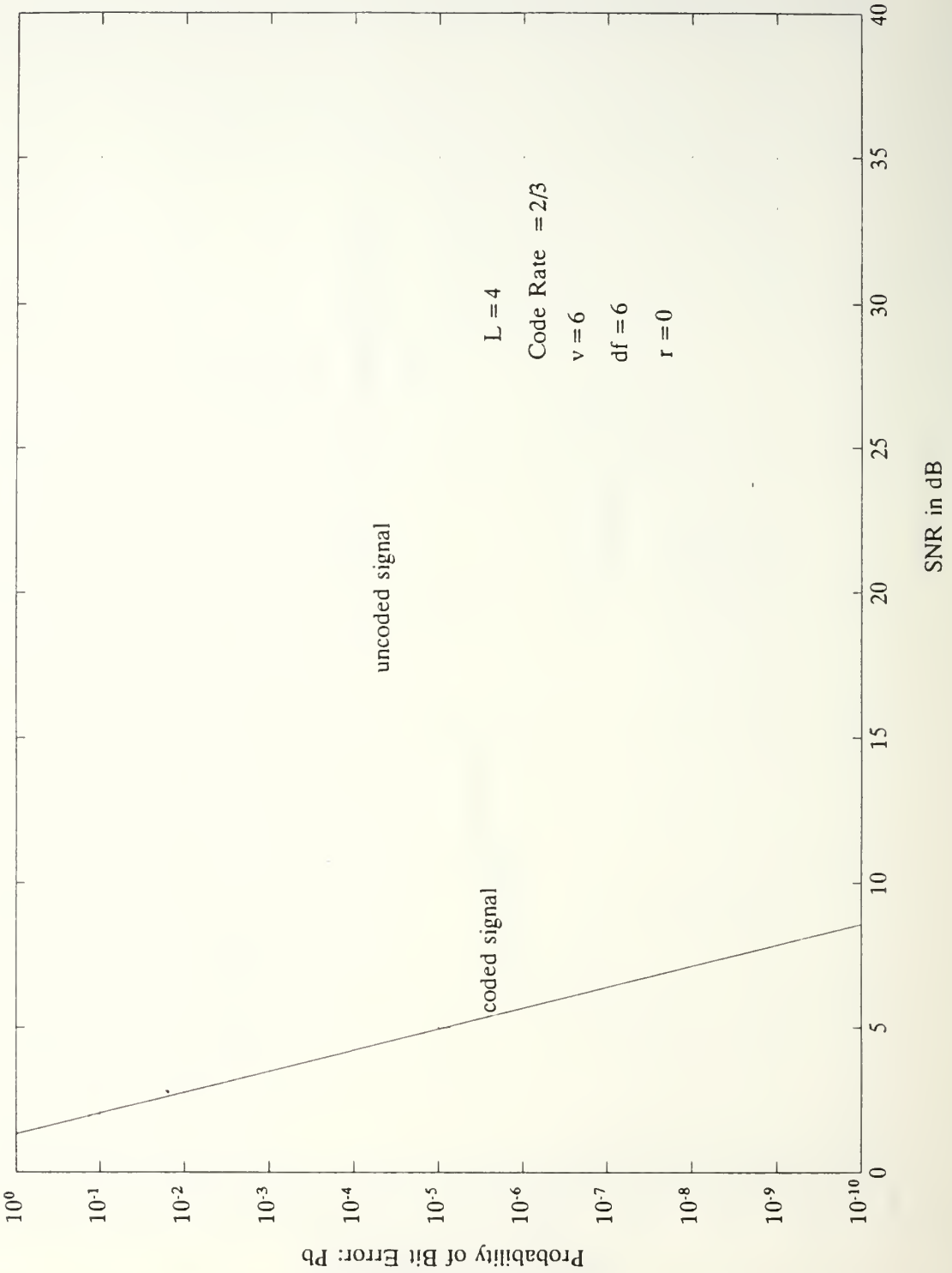


**Figure 41: Probability of bit error conditioned on the Doppler effect coefficient in a Rayleigh fading channel ($r = 0$) and maximum Doppler effect, i.e., minimal Doppler effect coefficient for a rate 2/3, $\nu = 6$ convolutional code and system diversity $L = 4$.**

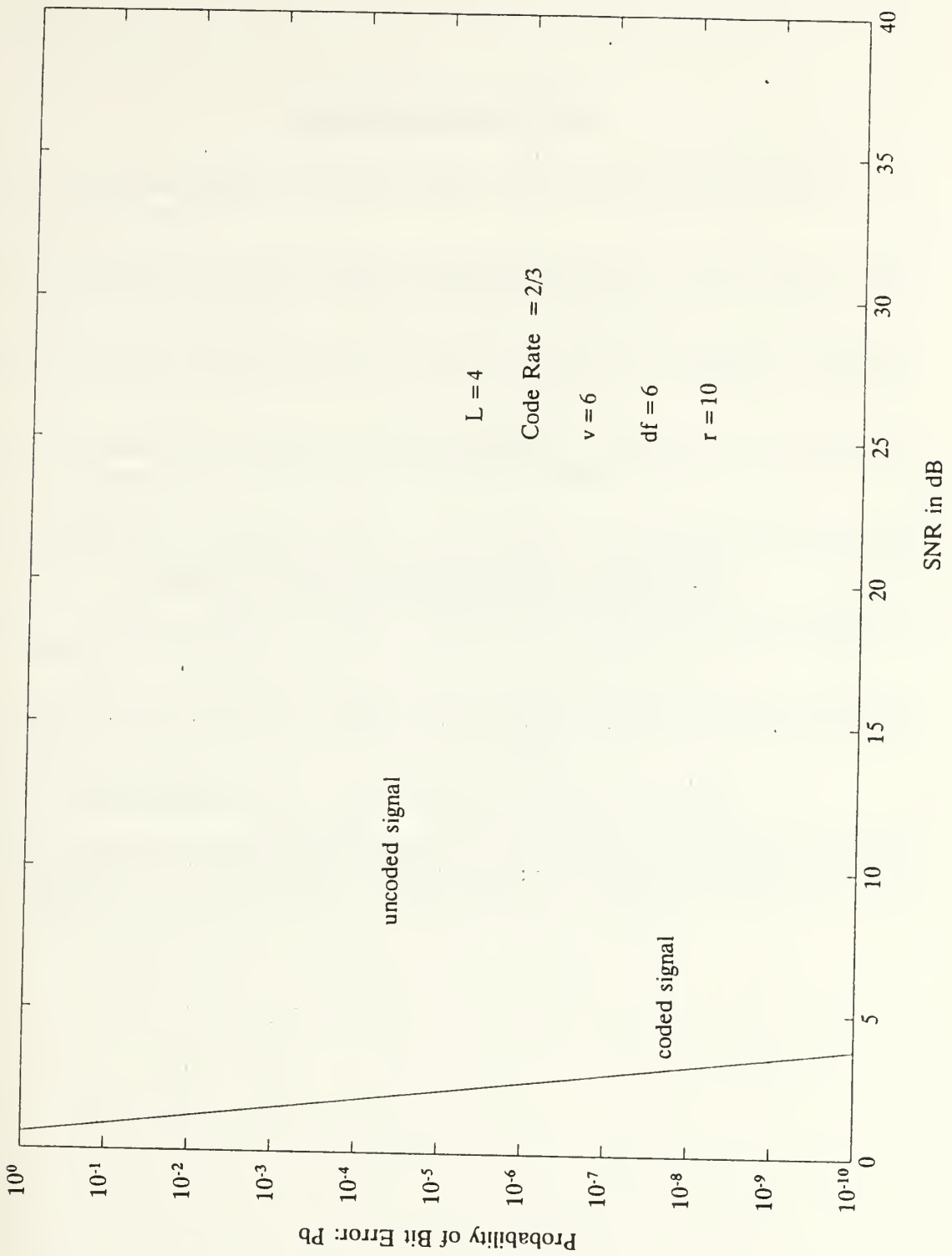


**Figure 42: Probability of bit error conditioned on the Doppler effect coefficient in a Ricean fading channel ($r = 10$) and maximum Doppler effect, i.e., minimal Doppler effect coefficient for a rate 2/3, $\nu = 6$ convolutional code and system diversity $L = 4$.**

[THIS PAGE INTENTIONALLY LEFT BLANK]

# REFERENCES


1. J. G. Proakis, *Digital Communications*, McGraw-Hill Book Company, New York, NY, 1989.

2. J. I. Marcum, "Statistical Theory of Target Detection by Pulsed Radar," *IEEE Trans. Inf. Theory*, Vol. IT-6, pp. 56–267, April 1960.

3. G. L. Turin, "Communication Through Noisy Random-Multipath Channels," *IRE Convention Record*, Part 4, pp. 159–166, 1956.

4. G. L. Turin, "On Optimal Diversity Reception," *IRE Trans. on Communications Systems*, Vol. CS-10, pp. 22-31, March 1962.

5. J. N. Pierce, "Theoretical Diversity Improvement in Frequency Shift Keying," *Proc. IRE*, Vol. 64, pp. 903–910, May, 1958.

6. A. J. Viterbi and J. K. Omura, *Principles of Digital Communication and Coding*, McGraw-Hill Book Company, New York, NY, 1979.

7. G. C. Clark, Jr. and J. R. Cain, *Error-Correction Coding for Digital Communications*, Plenum Press, New York, NY, 1981.

8. S. M. Ross, *Stochastic Processes*, Wiley, New York, NY, 1983.

9. W. C. Lindsey, "Error Probabilities for Ricean Fading Multichannel Reception of Binary and M-ary Signal," *IEEE Trans. Inf. Theory*, Vol. IT-10, pp. 339–350, October 1969.

[THIS PAGE INTENTIONALLY LEFT BLANK]

# INITIAL DISTRIBUTION LIST

| | | No. Copies |
|---|---|---|
| 1. | Defense Technical Information Center<br>Cameron Station<br>Alexandria, VA 22304-6145 | 2 |
| 2. | Library, Code 52<br>Naval Postgraduate School<br>Monterey, CA 93943-5002 | 2 |
| 3. | Chairman, Code EC<br>Department of Electrical and Computer Engineering<br>Naval Postgraduate School<br>Monterey, CA 93943-5000 | 1 |
| 4. | Professor Tri T. Ha, Code EC/Ha<br>Department of Electrical and Computer Engineering<br>Naval Postgraduate School<br>Monterey, CA 93943-5000 | 2 |
| 5. | Professor Ralph D. Hippenstiel, Code EC/Hi<br>Department of Electrical and Computer Engineering<br>Naval Postgraduate School<br>Monterey, CA 93943-5000 | 1 |
| 6. | Diretoria de Armamento e Comunicações da Marinha<br>Brazilian Naval Commission<br>4706 Wisconsin Avenue, NW<br>Washington, DC 20016 | 2 |
| 7. | Instituto de Pesquisas da Marinha<br>Brazilian Naval Commission<br>4706 Wisconsin Avenue, NW<br>Washington. DC 20016 | 2 |
| 8. | LCDR Abdon B. de Paula<br>R. Moraes E. Silva 25 AP 202<br>Tijuca Rio de Janeiro, RJ 20271, Brazil | 2 |